Doctoral thesis submitted for the degree of Doctor of Philosophy in Telecommunication Engineering

Postgraduate programme: Communication Technology

Dosimetric study of the radioelectric influence of humans into complex environments through determistic simulations and the implementation of a simplified model

Presented by:

Erik Aguirre Gallego

Supervised by:

Dr. Francisco Falcone Lanas and Dr. Luis Serrano Arriezu

Pamplona, 2014

Acknowledgements

Firstly, I would like to thank Dr. Francisco Falcone and Dr. Luis Serrano for supervising and helping me in the development of this work, especially to Francisco, whom I met by chance five years ago in one of his classes and who has been guiding and supporting me from my final project so far. I would also like to thank my team-mates, Leire and Peio, much of the work presented in this thesis would not have been possible without their help and a good teamwork.

I wish to express my gratitude to all our collaborators, thanks to the work and knowledge of Ana Alejos and the people from Carlos III, inter alia, we have been able to deepen in certain lines of work that otherwise would not have been possible.

Finally, it is a pleasure to acknowledge my family, girlfriend and friends, thanks to their support and teachings over the years, I have become who I am and I got to where I got.

Table of Contents

Introduction

This thesis describes the research work performed under the doctorate program "Communication Technology" from Public University of Navarra (UPNA), for the degree of Doctor of Philosophy (PhD) in Telecommunications Engineering. The guidance and supervision of this doctoral thesis has been conducted by Dr. Francisco Falcone Lanas from UPNA with the codirection of Dr. Luis Serrano Arriezu from UPNA. It has been entirely developed in UPNA.

Field of study and objectives

The research presented in this manuscript falls under the framework of dosimetry and deterministic estimations. A dosimetric study is carried out with the aid of a 3D Ray Launching simulation technique, by means of an in-house developed code at UPNA.

Dosimetry is defined as the calculation of the absorbed dose when a tissue is exposed to electromagnetic radiation, in this case, non-ionizing radiation. It has reached a great importance since a part of the society starts to show concern about the exposure of people to artificial exposures caused by mobile phones or Wi-Fi networks. In fact, some entities (administrations and health bodies) are involved in the regulation and the release of guidelines about this subject.

The objective of this thesis is to study dosimetry through 3D Ray Launching simulation technique, calibrating it by the implementation of several scenarios where the simulation tool is tested throughout the comparison of theoretical and measurement results. A simplified human body has been also developed with the aim of employing it in different scenarios, performing dosimetric estimations and providing insight on its influence in the electromagnetic power distribution inside an indoor scenario. Finally, obtained results are compared with different guideline thresholds giving an idea of the compliance of the law when usual wireless communication systems are emitting.

Structure of the thesis and personal contributions

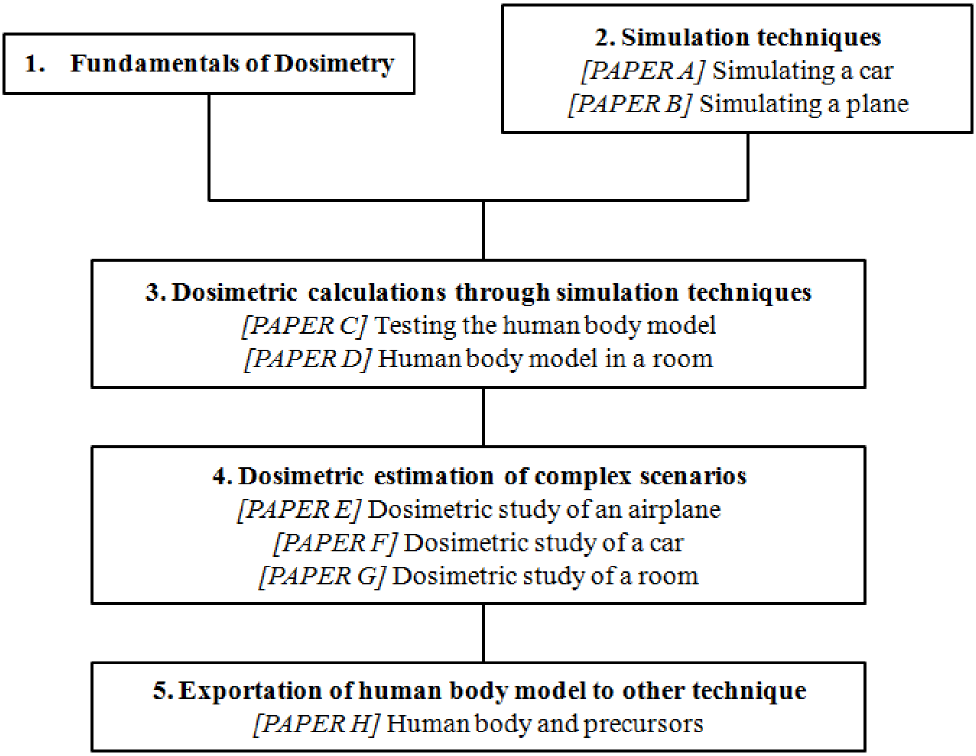

In this section the organization of the manuscript and the relation between the different works as well as the personal contribution of the author to all of them is highlighted. A schematic description of the thesis organization is provided in the upper graph. Starting from this *Introduction* where objectives and research line are defined the presented manuscript is divided in the next six chapters:

In *Chapter 1* the fundamentals of dosimetry are described to introduce the basic concepts for the rest of the thesis. Specific Absorption Rate (SAR) is defined as well as the fundamental concepts related with property of tissues and bio-heat equations. All legislation and guidelines around dosimetry are also presented and described in this chapter.

In *Chapter 2* most widely extended simulation methods are presented and not only their suitability as radioelectric simulation tool is described but also the reasons behind the choice of 3D Ray Launching method for the development of this work is explained. Two original contributions are presented where this tool is tested demonstrating all its potential by the introduction of two complex indoor scenarios.

- PAPER A: shows the consideration of vehicular environment as subject study introducing in the simulation tool a complete car. It allows a complete understanding of the electromagnetic waves behavior and validation of the accuracy of the tool through the comparison between simulations and measurements. This author took part in experimental measurements as well as in the processing of simulation results and wrote part of the paper.
- PAPER B: provides a more challenging scenario to study, being this a large commercial aircraft with all the related implications: a larger scenario with high number of obstacles, with large computational complexity. In this case a complete radioelectric study is done, employing also different frequencies. This author carried out simulation and processed and analyzed all the obtained results; and wrote part of the paper.

Chapter 3 describes the use of simulation tools for dosimetric purposes and presents a wide study of the human body models that are usually utilized with those techniques. From this study a simplified human body is selected and developed for its application with the chosen simulation technique. Two contributions are included where the simplified human body model is tested:

- PAPER C: presents a deep study of the different simulation techniques and human body models. The developed human body is utilized and described for the first time, calculating the power distribution inside it when it is placed into a complex scenario. This author did the theoretical study, performed simulations and measurements and wrote the paper.
- PAPER D: introduces the generated human body model inside a scenario and considers its influence when a WBAN system is working. In this work the influence of the human body is considered in a wide area instead of in a localized area. This author provides the simplified human body model that is used in the paper

In *Chapter 4* dosimetric estimations inside complex scenarios are obtained, both, theoretically and experimentally. Three original contributions are included in this part:

- PAPER E: shows the dosimetric estimation inside a commercial aircraft where e-field strength values are calculated. Those values are compared with different recommendations obtaining law compliance maps. This author carried out all simulations and processed the obtained results; and wrote a part of the paper.

- PAPER F: presents dosimetric estimations but utilizing a car as scenario. Electric field values are also calculated and in this case they are compared with real measures obtained with a dosimeter and a spectrum analyzer. This author carried out measurements, processed obtained results and compared both, theoretical and experimental results; and wrote a part of the paper.
- PAPER G: presents a scenario where human body is introduced and dosimetric calculations are done. In this work a Wi-Fi based communication system is tested getting its near and far field e-field strength as well as Specific Absorption Rate values obtained in the simplified human body model. All of them are compared with guideline thresholds. The influence caused by the introduction of a person inside a scenario is also demonstrated. This author carried out far field measurements and simulations, SAR estimations and the study of human body influence, also wrote a part of the paper.

Chapter 5 presents the exportation of simplified human body model to other simulation tool introducing an original contribution:

- PAPER H: shows the utilization of the human body interacting with electromagnetic precursors. This author provides the human body model and all the dielectric properties of the parts that compose it.

Finally, the main body of the thesis is closed with a *General discussion of results, current work and future lines* section where a summary of the thesis is presented and the work that is being developed as well the future steps are described.

At the end of the manuscript, all the *References* utilized throughout the work are presented, continuing with *Author's merits* where not only the presented publications [PAPER A]-[PAPER H] are given, but also conference proceedings and an unenclosed contribution are listed.

Chapter 1.

Fundamentals of Dosimetry

In this chapter the main dosimetry concepts are introduced with to put the thesis in its context. Specific Absorption Rate (SAR) and the basic concepts related with the human body tissues and their energy absorption process are presented which are directly related with their dielectric properties and therefore their electromagnetic behavior. Bio-heat equations which allow the estimation of the produced heat by tissues when radioelectric waves interact with them are also introduced as well as guidelines and legislation related with dosimetry are considered studying main standards and how the different governments legislate about it. Finally, the main wireless communication systems that have been used in the dosimetry study are presented.

1.1 Introduction to dosimetry

Humans have been exposed to natural electromagnetic (EM) waves caused by all the materials and especially by sun since the beginning of their existence. Their interactions with natural media as well as their potential use in communications have led to understand and control the transmission and propagation of these waves, starting from the Mawell's equations and the later development of radio communication system at the end of the 19th century. From this milestone the development of wireless communication systems and the coexistence of the human being with artificial radioelectric waves have steadily grown, especially since the first mobile phones appeared until now.

Nowadays millions of devices are able to communicate wirelessly producing large amounts of radioelectric waves causing concern within part of the population of the harmful effects that could cause the exposure to these waves. This situation reveals the relevance of studying dosimetry and the corresponding legislation behind it. Therefore, according to [SANC 09], the electromagnetic dosimetry establishes the relationship between an electromagnetic field distributed through the free space and the inducted fields into the biological tissues.

It must be taken into account that depending on the frequency of the transmitted electromagnetic wave, radiation will be ionizing or non-ionizing (figure1), ergo, the radiations of high frequency like X or gamma rays have the capacity to ionize matter. In this work only dosimetry when considering non-ionizing radiation are studied, those frequencies can transmit information to long distances and are usually employed in wireless communication systems. They also could be dangerous for people, considering that non-ionizing radiation are capable of heating tissues with which they interact if the transmit power is large enough. This phenomenon is produced when the electromagnetic energy is converted in heat due to dielectric losses. More than this, the higher the frequency is, the larger the amount of energy that is transmitted is and therefore, higher frequencies inside the non-ionizing frequencies group can heat tissues more easily than the lower ones.

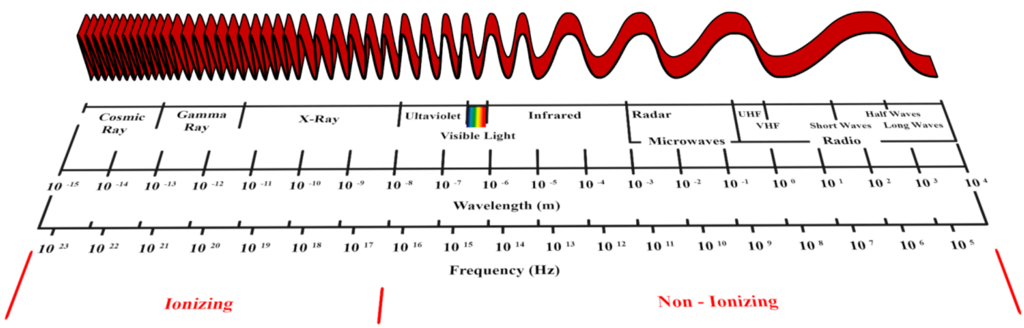

Figure 1.1 Radioelectric spectrum division considering systems, frequencies, wavelength and ionizing capacity

The main parameter that quantifies the electromagnetic absorption of the biological tissues in frequencies between 100 KHz and 10 GHz is known as SAR (Specific Absorption Rate) and according to [SANC 09] it is described as follows:

"SAR is defined as the time rate at which energy is deposited in any kind of material per unit of mass; that is, the power absorbed by the tissue per unit of mass. Thus, SAR is the parameter employed to quantify the electromagnetic absorption inside biological tissues like human body. It is also defined as the ratio between the infinitesimal amount of radiofrequency power absorbed in the infinitesimal mass of

tissue surrounding a specific point. In other terms, SAR can be seen as the velocity at which the human body absorbs the electromagnetic energy."

More definitions of SAR can be found in the literature [IEEE 99], nevertheless all of them agree in the concept of quantity of power absorbed by the tissues per unit of mass and in an interval of time.

It is accepted as the standard indicator of dosimetry [WANG 11] and it is used to evaluate the hazards of a radioelectric transmission calculating it through the following formula [SANC 09]:

$$AR = \frac{\sigma}{\rho}\left|\vec{E}\right|^2 \tag{1.1}$$

As it can be seen, SAR [W/Kg] is strongly related to the received rms electric field value ($\vec{\mathrm{E}}$) and to the characteristics of the exposed tissue, taking into account its density ρ [Kg/ m3] and conductivity σ [S/m].

By performing the time integral of SAR, Specific Absorption (SA) is obtained which is evaluated as the relationship between electromagnetic field energy (dW) and a differential mass element (dm) that absorbs it [SANC 09]:

$$SA = \frac{dW}{dm} \tag{1.2}$$

According to [WANG 08] two approached can be defined for the SA calculation, the first one in the time domain:

$$SA = \int_0^T J(t)E(t)/\rho \cdot dt \tag{1.3}$$

where $J(t)$ is the current density and the second one in the frequency domain:

$$SA = \int_{-\infty}^{\infty} \sigma(\omega)|E(\omega)|^2/\rho \cdot df \tag{1.4}$$

where $\sigma(\omega)$ is the conductivity and $E(\omega)$ is the Fourier transform of $E(t)$. SA is therefore a valid approach to obtain an effective exposure for multi-frequency signals, such as UMTS, that SAR is not able to consider since it only takes into account the time variation of sinusoidal signals.

Since the exposure to electromagnetic field is defined in terms of electric field, magnetic field and incident power density in the range of 3KHz to 300 GHz this parameter must be understood. In near field absorption is complex and therefore it is not definable as a vector. However in far field the frequency, polarization and dimensions of the material are fundamental and the calculation of the incident power density can be done utilizing the following formula [SANC 09]:

$$\vec{P} = \frac{1}{2}\vec{E} x \vec{H}^* \tag{1.5}$$

where $\vec{P}$ is the incident power density in W/m^2 and $\vec{H}^*$ is the complex conjugate of the magnetic field intensity.

1.2 Properties of tissues

Some concepts must be internalized when talking dosimetry and to understand what happen when a non-ionizing radiation interact with a biological tissue or any material [SANC 09]. Both, **electric permittivity** and **magnetic permeability** are essential when an electromagnetic problem is analyzed. In fact, they complete Maxwell equations introducing the material electromagnetic properties in the calculation:

$$\nabla \times \vec{E} = -\frac{\partial \vec{B}}{\partial t} \tag{1.6}$$

$$\nabla \times \vec{H} = \vec{J} + \frac{\partial \vec{D}}{\partial t} \tag{1.7}$$

$$\nabla \cdot \vec{D} = \rho \tag{1.8}$$

$$\nabla \cdot \vec{B} = 0 \tag{1.9}$$

$$\vec{D} = \varepsilon \vec{E} \tag{1.10}$$

$$\vec{B} = \mu \vec{H} \tag{1.11}$$

where $\vec{E}$ is the electric field, $\vec{B}$ is the magnetic field, $\vec{J}$ is the surface density, ρ is the volumetric density, $\vec{D}$ is the electric flux and $\vec{B}$ is the magnetic flux. The first four formulas complete the classical Maxwell equations, nevertheless, electric permittivity ε (F/m) gives a description of the interaction between the electric field intensity and the dielectric material, while magnetic permeability μ (H/m) provides the interaction of the material with the magnetic field.

Electric permittivity can be defined as follows:

$$\varepsilon = \varepsilon_0(\varepsilon' - j\varepsilon'') \tag{1.12}$$

where ε_0 is the electric permittivity of the vacuum, ε' is the dielectric constant and ε'' is the loss factor. Dielectric constant represents the facility of the exposed material to preserve electric energy and according to [SANC 09] relative electric permittivity (ε_r) is also used:

$$_r = \frac{\varepsilon}{\varepsilon_0} = \quad ' - j\varepsilon'' = \quad '(1 - jtan\delta) \tag{1.13}$$

From this expression the **dielectric loss tangent** ($tan\delta$) is extracted and as the loss factor it is defined as the dissipated energy due to the polarization mechanism inside the dielectric. Finally the electric **conductivity** $\boldsymbol{\sigma}$ (S/m) is defined as the capacity of a material to let the electric current pass through.

$$\sigma = \frac{J}{E} \tag{1.14}$$

When the human body is characterized the dielectric constant and conductivity of the different tissues that are considered should be utilized. These variables are obtained from the permittivity of the dielectric materials, however, obtaining this value is not a trivial task when the material under study is a biological tissue. Therefore, for this purpose two different techniques are proposed, so-called In Vivo and In Vitro.

In Vivo method involves the appliance of the probe directly inside the tissue, hence, sedation or surgery may be required and this is the reason why this kind of methods are usually used in animals and not in humans [WARS 74].

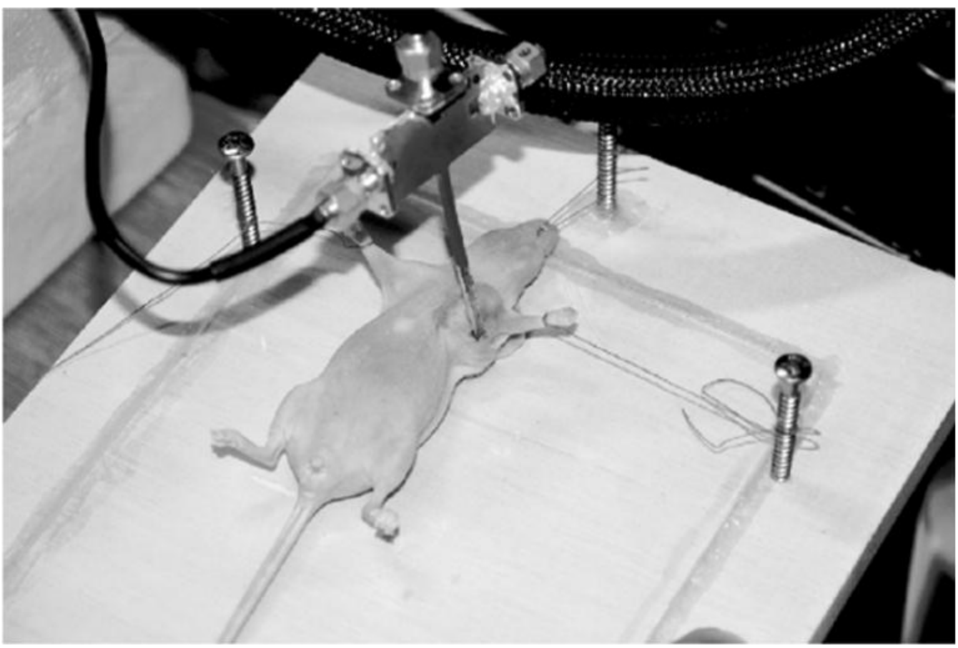

Figure 1.2 Example of in vivo measurement inserting the probe in a mouse[KWON 06]

By contrast, In Vitro techniques require the organ to be completely removed and placed in a suitable container for the measurements of the dielectric properties. These methods could cause errors considering that the conditions of the tissues are changed, because the temperature and the content of the sample are varied. The measurement will strongly depend on the origin and handling of the sample since a part of the water content of the biological tissues are evaporated in the time elapsed between the donor is deceased and the study is carried out, decreasing in this period the conductivity and permittivity caused by the decrease of the dipolar nature of the material.

In [SANC 09] an extensive literature where the dielectric properties of different human body tissues are obtained in a wide range of frequencies is shown, introducing also the pattern [GABR 96] that allows their calculation. Due to the complexity of their structure and composition, biological materials do not describe a lineal relationship between their dielectric characteristics and frequency, showing different "relaxation zones". A Cole-Cole expression lets user make a calculation for a range of hertz to gigahertz presenting four different dispersion regions.

$$\varepsilon(\omega) = \varepsilon_\infty + \sum_{m=1}^{4} \frac{\Delta\varepsilon_m}{1+(j\omega\tau_m)^{1-\alpha_m}} + \sigma_i/(j\omega\varepsilon_0) \qquad (1.15)$$

where ε is the permittivity, σ_i is the ionic conductivity, τm is the relaxation time and Δεm is the downfall of the permittivity for the frequency range $\omega\tau$<<1 to $\omega\tau$>>1. As aforementioned the needed dielectric properties are obtained from permittivity, being dielectric constant the real part of ε(ω) and conductivity its imaginary part. In Table 1.1 the parameters that allow the modeling of the frequency dependence of the dielectric properties for different biological materials is shown, depicting in Figure 1.3 the result for various tissues.

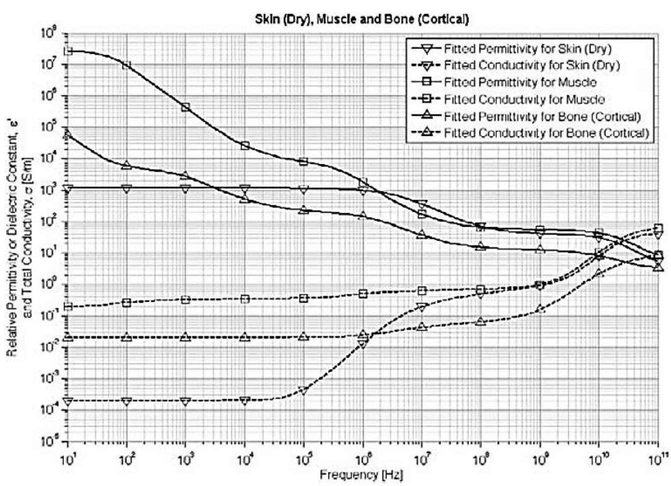

Figure 1.3 Conductivity and dielectric constant vs frequency for different types of biological tissues.

Tissue Type \ Parameter	ε	$\Delta\varepsilon_1$	τ_1[ps]	α_1	$\Delta\varepsilon_2$	τ_2[ns]	α_2	$\Delta\varepsilon_3$	τ_3[µs]	α_3	$\Delta\varepsilon_4$	τ_4[ms]	α_4	σ_1
Aorta	4	40	8,842	0,1	50	3183	0,1	100000	159155000	0,2	10000000	1592000000	0	0,25
Bladder	2,5	16	8,842	0,1	400	159,155	0,1	100000	159,155	0,2	10000000	15,915	0	0,2
Blood	4	56	8,377	0,1	5200	132,629	0,1	0	159,155	0,2	0	15,915	0	0,7
Bone (Canlellous)	2,5	18	13,263	0,22	300	79,577	0,25	20000	159,155	0,2	20000000	15,915	0	0,07
Bone (Cortical)	2,5	10	13,263	0,2	180	79,577	0,2	5000	159,155	0,2	100000	15,915	0	0,02
Bone Marrow (Infiltrated)	2,5	9	14,469	0,2	80	15,915	0,1	10000	1591,549	0,1	2000000	15,915	0,1	0,1
Bone Marrow (Not Infiltrated)	2,5	3	7,958	0,2	25	15,915	0,1	5000	1591,549	0,1	2000000	15,915	0,1	0,001
Brain (Grey Matter)	4	45	7,958	0,1	400	15,915	0,15	200000	106,103	0,22	45000000	5,303	0	0,02
Brain (White Matter)	4	32	7,958	0,1	100	7,958	0,1	40000	53,052	0,3	35000000	7,958	0,2	0,02
Breast fat	2,5	3	17,68	0,1	15	63,66	0,1	50000	454,7	0,1	20000000	13,26	0	0,01
Cartilage	4	38	13,263	0,15	2500	144,686	0,15	100000	318,31	0,1	40000000	15,915	0	0,15
Cerebellum	4	40	7,958	0,1	700	15,915	0,15	200000	106,103	0,22	45000000	5,305	0	0,04
Cerebro Spinal Fluid	4	65	7,958	0,1	40	1,592	0	0	159,155	0	0	15,915	0	2
Cervix	4	45	7,958	0,1	200	15,915	0,1	150000	106,103	0,18	40000000	1,592	0	0,3
Colon	4	50	7,958	0,1	3000	159,155	0,2	100000	159,155	0,2	40000000	1,592	0	0,01
Cornea	4	48	7,958	0,1	4000	159,155	0,05	100000	15,915	0,2	40000000	15,915	0	0,4
Dura	4	50	7,958	0,15	200	7,958	0,1	10000	159,155	0,2	1000000	15,915	0	0,5
Eye Tissues (Solera)	4	50	7,958	0,1	4000	159,155	0,1	100000	159,155	0,2	5000000	15,915	0	0,5
Fat (Average Infiltrated)	2,5	9	7,958	0,2	35	15,915	0,1	33000	159,155	0,05	10000000	15,915	0,01	0,035
Fat (Not Infiltrated)	2,5	3	7,958	0,2	15	15,915	0,1	33000	159,155	0,05	10000000	7,958	0,01	0,01
Gall Bladder	4	55	7,579	0,05	40	1,592	0	1000	159,155	0,2	10000	15,915	0	0,9
Gall Bladder Bile	4	66	7,579	0,05	50	1,592	0	0	159,155	0,2	0	15,915	0,2	1,4
Heart	4	50	7,958	0,1	1200	159,155	0,05	450000	72,343	0,22	25000000	4,547	0	0,05
Kidney	4	47	7,958	0,1	3500	198,944	0,22	250000	79,577	0,22	30000000	4,547	0	0,05
Lens Cortex	4	42	7,958	0,1	1500	79,577	0,1	200000	159,155	0,1	40000000	15,915	0	0,3
Lens Nucleus	3	32	8,842	0,1	100	10,61	0,2	1000	15,915	0,2	5000	15,915	0	0,2
Liver	4	39	8,842	0,1	6000	530,516	0,2	50000	22,736	0,2	30000000	15,915	0,05	0,02
Lung (Deflated)	4	45	7,958	0,1	1000	159,155	0,1	500000	159,155	0,2	10000000	15,915	0	0,2
Lung (Inflated)	2,5	18	7,958	0,1	500	63,662	0,1	250000	159,155	0,2	40000000	7,958	0	0,03
Muscle	4	50	7,234	0,1	7000	353,678	0,1	1200000	318,31	0,1	25000000	2,274	0	0,2
Nerve	4	26	7,958	0,1	500	106,103	0,15	70000	15,915	0,2	40000000	15,915	0	0,006
Ovary	4	40	8,842	0,15	400	15,915	0,25	100000	159,155	0,27	40000000	15,915	0	0,3
Skin (Dry)	4	32	7,234	0	1100	32,481	0,2	0	159,155	0,2	0	15,915	0,2	0,0002
Skin (Wet)	4	39	7,958	0,1	280	79,577	0	30000	1,592	0,16	30000	1,592	0,2	0,0004
Small Intestine	4	50	7,958	0,1	10000	159,155	0,1	500000	159,155	0,2	40000000	15,915	0	0,5
Spleen	4	48	7,958	0,1	2500	63,662	0,15	200000	265,258	0,25	50000000	6,366	0	0,03
Stomach	4	60	7,958	0,1	2000	79,577	0,1	100000	159,155	0,2	40000000	15,915	0	0,5

Table 1.1 Summary of all variables utilized for the calculation of dielectric properties of different biological tissues by Cole-Cole expression [SANC 09]

1.3 Bioheat equation

Temperature increase produced when electric field penetrates inside biological tissues as a result of the dielectric losses caused when electromagnetic energy turns into heat, is a complex process where more than one mechanism of the human body takes part. This means that there is not a direct relationship between the arrived electric field and the produced heat and it is influenced by thermal migration, blood perfusion or convection. The following equation is the first bioheat equation which was proposed by Pennes [SANC 09], [PENN 48]:

$$C\rho \frac{\partial T}{\partial t} = K \cdot \nabla^2 T + h_m + h_b \tag{1.16}$$

where C[J/kg·K] is the specific heat, ρ [kg/m3] is the tissue density, K[J/(s·m·K) is the thermal conductivity, T[K] is the tissue temperature, h_m[J/(s·m3)] is the rate of tissue heat production and h_b[J/(s·m3)] is the rate of heat transfer from blood to tissue.

This equation has evolved over the time with the aim of considering more natural mechanisms that human body utilizes to generate or disperse heat and to correct fundamental errors of the original equation. Thus, including the effect of blood perfusion and the volumetric metabolic heat generation [SANC 09], [ZHOU 09], [XIE 10], [HU 11]:

$$C\rho \frac{\partial T}{\partial t} = K\nabla^2 T + \omega_b C_b (T_a - T) + q_m \tag{1.17}$$

where ω_b [Kg/(m3·s)] is the volumetric blood perfusion rate, C_b [J/(kg·K)] is the specific heat of blood T_a[K] is the temperature of arterial blood and q_m[J/(s·m3)] is the volumetric metabolic heat generation rate.

The bioheat equation is modified to the following version where absorbed microwave power is considered. [SANC 09], [YANG 07]:

$$C\rho \frac{\partial T}{\partial t} = K\nabla^2 T + A_0 + Q_v - B(T - T_b) \tag{1.18}$$

where A_0 [J/(s·m3)] is the metabolic heat generation, Q_v [J/(s·m3)] is the heat deposition as a consequence of the absorbed microwave power and B[J/(s·m3)] is the heat exchange mechanism due to blood perfusion.

Finally SAR distribution is introduced to calculate induced heating profile [SANC 09], [CARL 13], [ALMO 10], [HIRA 00]:

$$C\rho \frac{\partial T}{\partial t} = K\nabla^2 T - \rho\rho_b C_b m_b T + \rho SAR \tag{1.19}$$

where ρb is the blood density and m_b[m3/(kg·s)] is the volumetric perfusion rate of blood.

In more recent approaches, previously showed bioheat equations are combined with different simulation techniques [SHAG 09], [BOTT 12], [SHOS 06] providing a powerful tool to calculate the generated heat when electromagnetic waves interact with biological tissues.

1.4 Recommendations and guidelines

All countries have independence when legislating about dosimetry and permitted maximum exposure levels, but those legislations are usually based on ICNIRP (International Commission on Non-Ionizing Radiation Protection) guidelines, an organization that has the approval of WHO (World Health Organization) [WHO 14].

These guidelines of the entity are based on the modern scientific knowledge, however, with the aim of being prudential they are usually far away from the real threshold that the science has considered as hazardous for human being, according to [BUE 06] the safety margin set guidelines ten times lower than the real threshold. ICNIRP only takes into account the elevated temperatures induced inside tissues due to short time exposures, since the potential carcinogenic effects produced by long exposures have not been proved enough to consider them as a cause to consider restrictions.

According to [ICNI 98] the following dosimetric quantities are considered in the different frequency ranges.

- Until 10 MHz → Current density **J**
- Until 110 MHz → Current **I**
- 100 KHz - 10 GHz → SAR
- 300 MHz - 10 GHz → SA
- 10 GHz - 300 GHz → Power density **S**

In the following tables the accepted reference levels by ICNIRP for occupational and general public are shown. Evidently, the occupational reference levels are higher because a worker will be more exposed to radiations produced by an antenna when he get close to it, to repair or test the antenna.

Frequency range	E-field strength (V m^{-1})	H-field strength (A m^{-1})	B-field (μT)	Equivalent plane wave power density S_{eq} (W m^{-2})
up to 1 Hz	—	1.63×10^5	2×10^5	—
1–8 Hz	20,000	$1.63 \times 10^5/f^2$	$2 \times 10^5/f^2$	—
8–25 Hz	20,000	$2 \times 10^4/f$	$2.5 \times 10^4/f$	—
0.025–0.82 kHz	$500/f$	$20/f$	$25/f$	—
0.82–65 kHz	610	24.4	30.7	—
0.065–1 MHz	610	$1.6/f$	$2.0/f$	—
1–10 MHz	$610/f$	$1.6/f$	$2.0/f$	—
10–400 MHz	61	0.16	0.2	10
400–2,000 MHz	$3f^{1/2}$	$0.008f^{1/2}$	$0.01f^{1/2}$	$f/40$
2–300 GHz	137	0.36	0.45	50

Table 1.2 Reference levels for occupational exposure to variant in time magnetic and electric fields [ICNI 98].

Frequency range	E-field strength (V m^{-1})	H-field strength (A m^{-1})	B-field (μT)	Equivalent plane wave power density S_{eq} (W m^{-2})
up to 1 Hz	—	3.2×10^4	4×10^4	—
1–8 Hz	10,000	$3.2 \times 10^4/f^2$	$4 \times 10^4/f^2$	—
8–25 Hz	10,000	$4{,}000/f$	$5{,}000/f$	—
0.025–0.8 kHz	$250/f$	$4/f$	$5/f$	—
0.8–3 kHz	$250/f$	5	6.25	—
3–150 kHz	87	5	6.25	—
0.15–1 MHz	87	$0.73/f$	$0.92/f$	—
1–10 MHz	$87/f^{1/2}$	$0.73/f$	$0.92/f$	—
10–400 MHz	28	0.073	0.092	2
400–2,000 MHz	$1.375f^{1/2}$	$0.0037f^{1/2}$	$0.0046f^{1/2}$	$f/200$
2–300 GHz	61	0.16	0.20	10

Table 1.3 Reference levels for general public exposure to variant in time magnetic and electric fields [ICNI 98].

Of these tables it follows that for 2.4 GHz (the most commonly used Industrial Scientific Medical, ISM, frequency) the maximum power density that a worker could be exposed is of 50 W/m2 and the general public could be exposed to 10 W/m2. Utilizing E-field strength, one of the most widely used indicators when dosimetry is studied, it can be seen that the occupational level is of 137 V/m and a common person could be exposed to 61 V/m. In Figure 1.4 the evolution of the reference E-field strength threshold considering all the spectra is depicted.

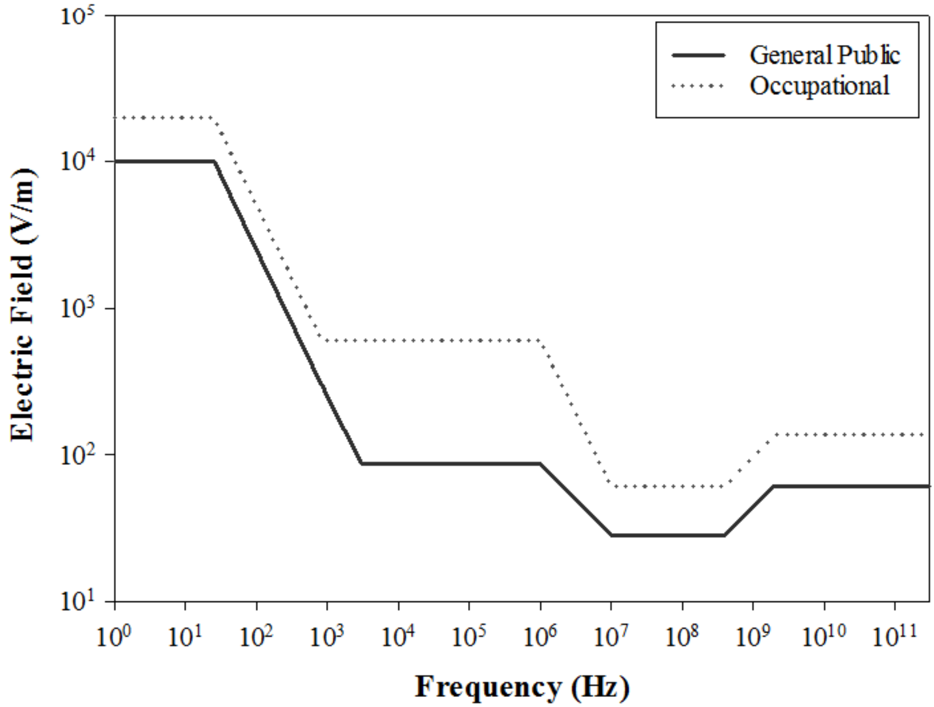

Figure 1.4 Evolution of E-field strength level with the frequency for general public and workers [ICNI 98].

As aforementioned, ICNIRP only does the recommendations and each government is in charge of doing their country legislation, e.g. Spain applies ICNIRP recommendations through the "Real Decreto 1066/2001" that are based on European Union 1999/519/CE [BUEN 06] recommendation that have followed ICNIRP recommendations. In fact, this procedure is common in most countries of the European Union with few exceptions. In Figure 1.3 a map with the different legislations that are established in the countries of European Union is depicted with information extracted from [STAM 11].

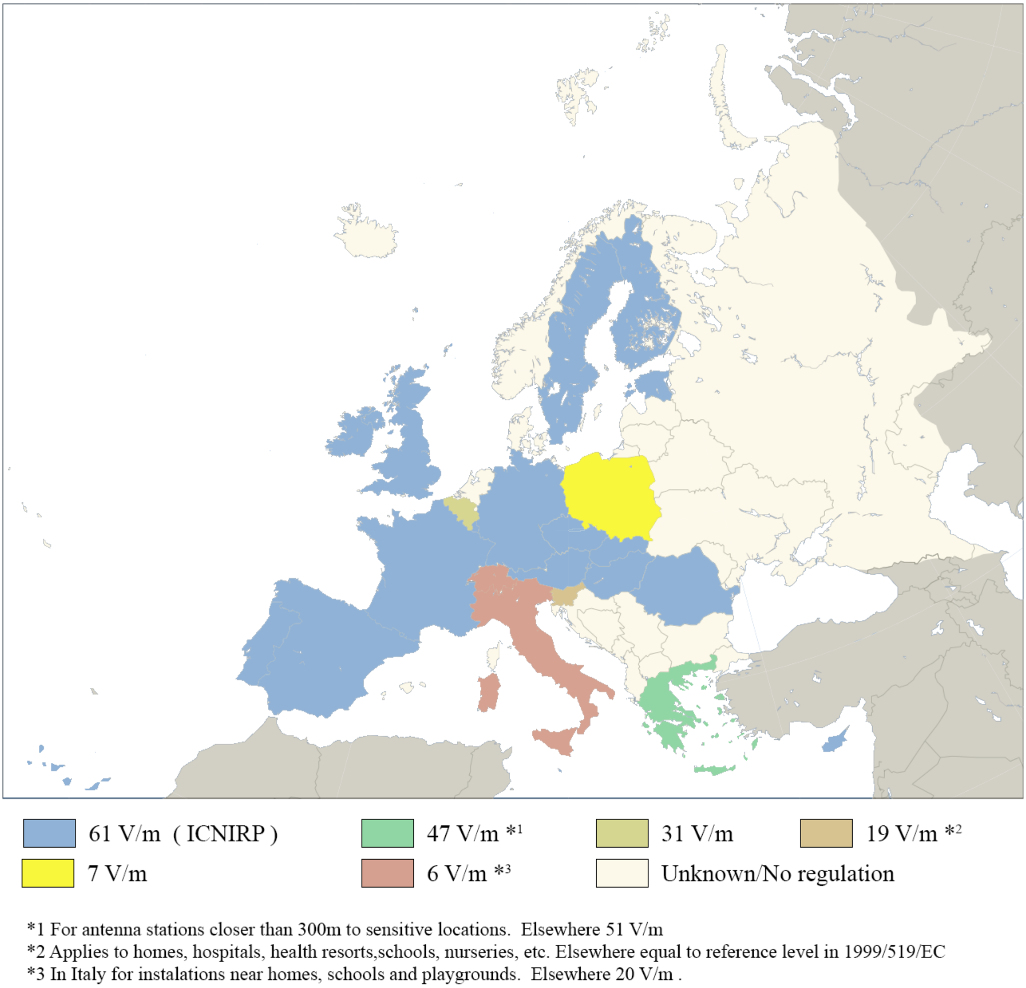

Figure 1.5 Map of maximum electric field exposure levels imposed in all European Union countries [STAM 11].

The Institute of Electronic and Electronics Engineers (IEEE) has developed another internationally well recognized standard, the IEEE C95.1 [IEEE 99] . The approach is similar to that seen in ICNIRP guidelines with some differences in thresholds. As it happens with ICNIRP recommendations, C95.1 has been adopted by some countries, in fact, U.S. Federal Communications Commission and Canada have issued their own laws based on these recommendations. It is used in the frequency range 3 KHz-300 GHz and two different environments are distinguished, controlled (occupational) and uncontrolled (generic public).

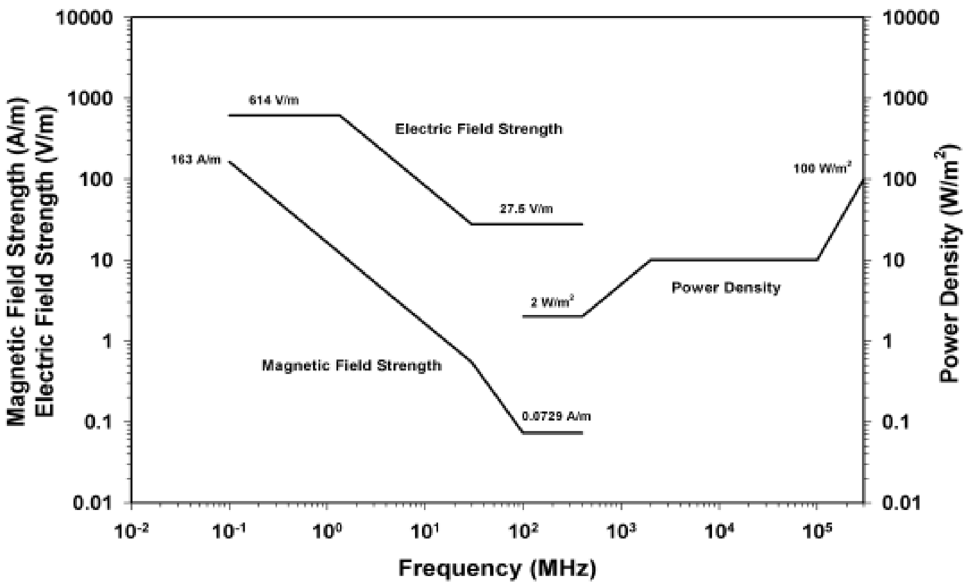

Figure 1.6 Power density, electric and magnetic field strength thresholds established by IEEE C95.1 standard for generic public.

Recommendations not only deal with SAR limits, but also some of them try to specify the protocols that should be followed when SAR measurements are done. IEEE SCC34 [GROU 14] standard describes, inter alia, measurement techniques, calibration techniques or phantom models. On the other hand, 3GPP TR 25.914 [3GPP 05] standard describes the way in which the measurements should be done for 3G user equipment and CTIA standard [CTIA 13] defines general requirements for laboratory tests as equipment configurations or laboratory techniques

1.5 Systems under consideration.

The need for dosimetry and its regulation is a consequence of the high spread of different wireless systems in the last twenty years. The biggest revolution in this sense is the introduction of mobile technologies, thus becoming the mobile phone into an indispensable device in the life of millions of people all over the world. This fast growth of a new technology arises doubts in relation to their safety and the introduction of new technologies as Wi-Fi increase population concern level.

Moreover, since wireless technologies are becoming cheaper and more accessible a great number of new applications where numerous devices interact among each other are being developed nowadays, giving rise to the concept of Internet of Things (IoT) [COET11], [BARI 13], [ATZO 14], [HUAN 10]. IoT congregates the most extended wireless communication standards working together to provide a service where the user can interact transparently with a huge amount of objects [BELL 13]. It is supported by Wireless Sensor Networks (WSN) which are responsible for capturing and sending information about different aspects depending on the purpose of the system [BENK 14], [DIAO 10], [ALAL 05], [ALEM 07], [GAO 14]. In Figure 1.7 a schema of IoT with the most usual technologies employed is shown.

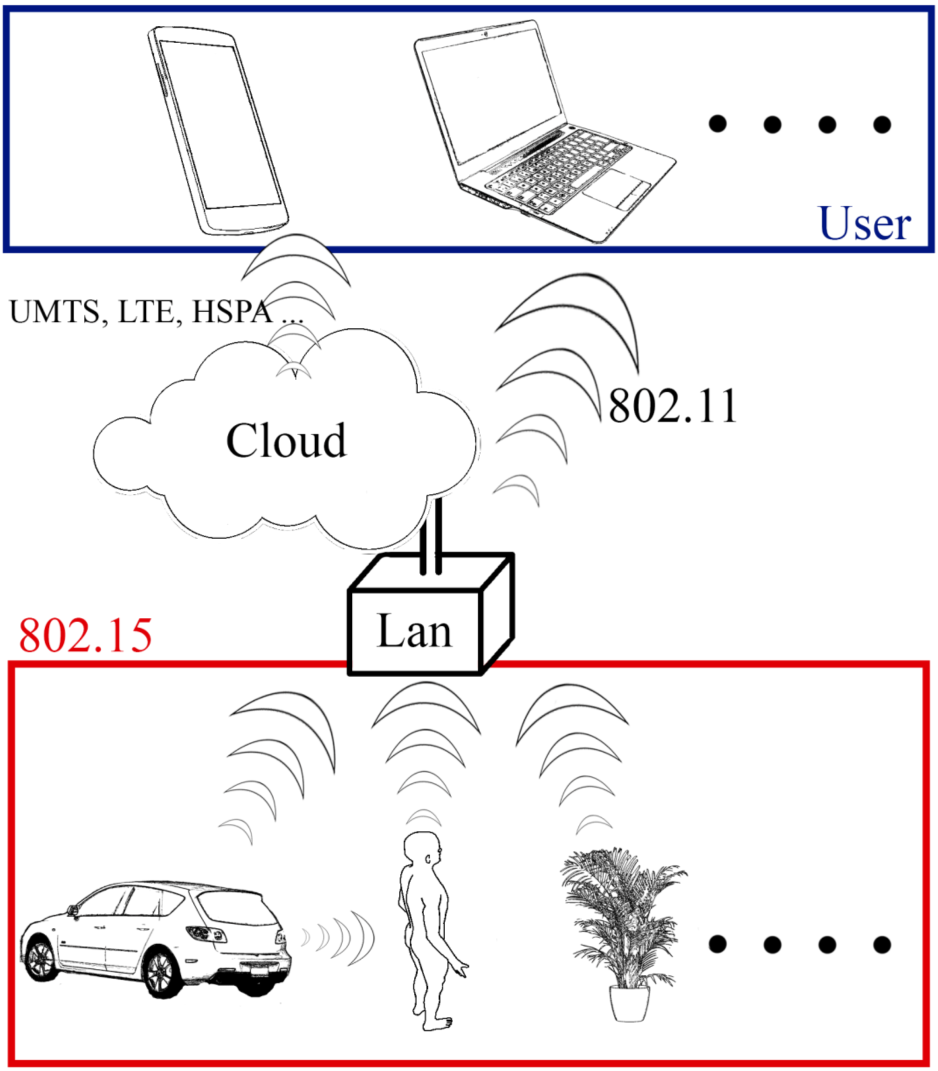

Figure 1.7 IoT functioning schema.

Examples of WSN systems that nowadays are under development and that could become commonplace in the future are electronic health (e-Health) systems [CAST 13], [COVA 09] and Intelligent Transport Systems (ITS) [ZENG 10], [DILE 09], [SELV 08]. E-Health allows the implementation of real time patient monitoring systems that can help to increase the efficiency of medical staff since emergencies can be detected faster [PODZ 12], [SHIN 04], [FRUH 11]. It can also accelerate the diagnose process giving to the family doctor a great record of different vital constants as well as allow distance diagnosis or telemedicine [NOIM 11], [BOBA 07], [ZEEB 10], [MWES 13], [LIU 13], [HASS 13a], [PAPA 13].

On the other hand ITS have the potential to increment not only the driver and passenger comfort, but also the security of road trips. Nowadays two kinds of communications are distinguished based on Vehicular Ad-hoc NETworking (VANET), Vehicle to Vehicle (V2V) [WANG 13a], [KAVI 09], [BAZZ 11] and Vehicle to Infrastructure (V2I) systems [HUAN 13], [IDE 12], [MILA 12], [MA 12], [HASS 13b], where the vehicle is connected to sensors situated in other vehicles or in the infrastructure of the road such as traffic signals or streetlights.

Considering not only current wireless communication systems, but also future trends, some wireless technologies have been taken under consideration in the different experiments carried out in this thesis.

IEEE 802.15

IEEE 802.15 workgroup is responsible of the release of standards related with Wireless Personal Area Networks (WPAN), being the most extended technologies Bluetooth, RFID and ZigBee. Seven task groups are defined under this standard, placing Bluetooth in 802.15.1 and ZigBee and RFID in 802.15.4.

According to the standard [IEEE 05], WPAN allow the connection among a private group of participants covering short distances and without a direct connection to an outside network as Internet. Taking into account this definition, inexpensive and power efficient solutions can be implemented.

Since Bluetooth comes as standard in mobile phones, it has become the most widely utilized WPAN technology. A high number of applications have been developed basing on this standard, starting from popular hand-free car systems [HEHU 12], to more complex tools that are being developed nowadays [HUNG 14], [LIU 14], [SANG 14].

Bluetooth works in 2.4 GHz ISM (Industrial, Scientific and Medical) band reaching ranges from 10m to 100m emitting with 1mW, 2.5mW or 100mW power. It is capable of supporting 7 users simultaneously and a maximum bit rate of 720Kbit/s.

On the other hand low rate WPANs as ZigBee or RFID are defined by IEEE 802.15.4 [IEEE 11]. The utilization of a lower rate is the result of searching a less complex and energy saving technology. In spite of the fact that the starting point is the same, the operation and objectives of these two technologies are completely different.

In RFID system a passive or active tag is interrogated by a reader and information is sent. The energy saving nature of RFID is especially true since passive tags are powered by the electromagnetic wave generated by the reader. As a consequence of the low price of these tags, RFID has been widely utilized as anti-thief system and as personal identification system [FLORE 08], [BERZ 12]. The standard defines different frequency bands that will be chosen depending on the purpose of the system. Evidently bit rate and consequently power consumption will change as a function of the employed frequency.

On the other hand, ZigBee systems are focused on WSN, allowing networks formed by 240 devices. It also operates in the 2.4GHz frequency band and reaches a maximum data rate of 250 kb/s, typically sufficient for WSN applications. The original idea behind ZigBee was its use in home automation [NEDE 09], [DOMI 12], developing wireless devices as switches or thermostats with long autonomy and easy installation. Nevertheless, a high number of new devices and applications are being developed based on this technology as a consequence of its flexibility [GUO 10], [SHIY 14], [BEDF 12].

Finally, IEEE 802.15.6 standard deals with Wireless Body Area Networks (WBAN), defined as a standard for the vicinity or inside a human body [IEEE 12a]. As a consequence of a very low transmit power, battery life is increased and SAR is minimized. Strong security is also provided for the case that sensitive information is transmitted. Evidently, the main field of application of this standard is e-health and medical environment [IVAN 12], [BARU 11]

IEEE 802.11

IEEE 802.11 specifies the use of Media Access Control (MAC) and physical layer (PHY) for Wireless Local Area Networks (WLAN) [IEEE 12b]. They are commonly known as Wi-Fi and allow the connection of a computer or other devices to a computer network in a local area, such as a home. The use of this technology has grown in the last decade thanks to the success of laptops and the usual policy of telephone companies of giving a router with each Internet connection contract. Wi-Fi systems have been controversial in the last years, especially for their installation in schools and the consequent exposure of children to electromagnetic waves.

Over time, the standard has evolved introducing different modulations, frequencies, higher data rates and other characteristics. Originally the IEEE 802.11 standard released in 1997 allows connections of 2Mb/s reaching 100 m distances. Nowadays, IEEE 802.11n [IEEE 12] standard defines the use of 5GHz frequency and can communicate with a data rate of 150 Mb/s reaching maximum distances of 250m.

Besides, four different frequencies are considered in the standards, 2.4GHz, 3.6GHz, 5GHz and 60GHz.

Since Wi-Fi is one of the most extended wireless communication systems, a large number of works have been published dealing with problems [JANE 07], [YOON 12] and offering different applications based on it [DOBI 11], [HERS 10]. This widespread adoption and the constant evolution of the standard shows that this technology will be used for a long time.

3GPP

With no doubt mobile technologies have become one of the biggest revolutions in the last decade. However, the necessary installation of base stations to allow correct system operation, especially in urban areas, has led to the rejection by a sector of the population to these communication systems.

The 3rd Generation Partnership Project (3GPP) is responsible for standards relating to mobile communication technologies. Originally the aim of this group consisted in developing the third generation mobile phone system based on Global System for Mobile Communications (GSM), however the scope was extended and nowadays they develop virtually all standards behind mobile communications.

Nowadays three standards are working together to offer data transmission to users, Universal Mobile Telecommunication System(UMTS), High Speed Packet Access (HSPA) and more recently Long Term Evolution (LTE). UMTS is known as 3G and it was defined firstly in Release 99. This system works in 2100 MHz and 900 MHz band in Europe and can reach data rates of 348 kbps [3GPP 00].

HSPA appeared by the first time in Release 5 allowing to communicate with a maximum data rate of 7.5Mbps, however, in Release 7 HSPA+ was presented and theoretical 42 Mbps data rate is supported. The main difference between HSPA and UMTs is modulation and reduction in Time to Transmit Intervals, since UMTS utilizes QPSK modulation and HPSA 16/64 QAM [3GPP 02], [3GPP 07].

Finally LTE was presented in Release 8 and improved in Release 10 with LTE advanced. Thanks to the use of a larger spectrum and a higher spectral efficiency LTE is able to offer a maximum bit rate of 300 Mb/s [3GPP 08], however LTE advanced is able to reach 1Gb/s bit rate [3GPP 11] thanks to, among other things, the implementation of MIMO and higher order Coding and Modulation schemes.

When these systems are studied, the behavior of the mobile phone must be considered since depending on the distance between the mobile phone and base station, the transmission power would change and therefore maximum and minimum thresholds should be taken under consideration.

Chapter 2.

Simulation techniques

In this chapter a variety of electromagnetic simulation techniques are introduced and described, presenting their main characteristics, advantages and disadvantages. Based on this study the most suitable simulation technique is chosen for this work and a complete description of its operation is presented. Two original contributions are presented: (i) the study of a vehicular scenario where the simulation technique is tested, (ii) the introduction of an aircraft inside the simulation tool as an example of a complex indoor scenario.

2.1 Description of simulation techniques

Thanks to simulation techniques the real world can be studied and understood with the only aid of a computer. The behavior of different systems in different environments can be emulated without any of them even existing. As an example, an architect can know how a building in project is going to withstand winds, earthquakes or any other natural effect to make major structural changes and minimize risks [ARCH 14].

When electromagnetic waves are simulated, how they propagated in an area or the way they interact with different materials can be determined. One of the most common ways to use those powerful tools is performing coverage calculations of wireless systems to determine the best locations to place access points or base stations [SKID 96], [BRAG 14], [CHRY 10], [HOU 11], [PAPK 08]. However, the validity of these results will strongly depend on the accuracy of the utilized simulation method which is the result of the correct consideration of the phenomena that occurs in the reality.

Obviously, a more accurate simulation method will be more complex and consequently the volume of calculations and the computational demand will be higher. This is the reason why when a simulation technique is chosen, a good balance between accuracy and computational cost should be found. The simulation techniques that usually give the best approach to reality are the full-wave methods, these techniques are based on numerical approaches to the resolution of Maxwell's equations, extracting from them the most accurate results in the case that all of the parameters of the simulated scenario are correctly introduced.

Finite-Difference Time-Domain (FDTD) is one of the most widely used deterministic methods not only with general purposes, but also in the dosimetry area [WANG 13b]. Method of Moments (MoM) is also a widely extended technique when dealing with electromagnetic problems [WANG 13b], particularly when scattering is dealt with.

One of the principal study areas where these kinds of simulation tools are used is the development and study of antennas, structures or conductors [HYUN 11], [STAK 03], [TOYO 08], [ZHAN 12]. However, the use of the method is extended to other areas, especially when it is hybridized with simpler methods, allowing a faster study of more extensive areas [WANG 00], [ZAHO 11].

At the other end, empirical models can offer results in a much shorter time but with less accuracy. These methods are obtained and calibrated from previous measurements and therefore they are strongly associated with the original scenario. This is the reason why when the topology or complexity of the scenario is different the results are a far cry from reality.

Most of them implement implicitly or explicitly the calculation of free space losses (2.1) and include other variables based on the measurements and the characteristics of different locations:

$$P_r(d) = \frac{P_i G_t G_r \lambda^2}{(4\pi)^2 d^2 L} \tag{2.1}$$

where Pr(d) is the received power, Pt is the transmitted power, Gt is the gain of the transmitter antenna, Gr is the gain of the receiver antenna, λ is the wavelength, d is the distance transmitter-receiver and L are the losses of the system not related with propagation.

Okumura is one of the most widely used empirical methods in urban scenarios. This model is the result of the measurements that Okumura did in Tokyo emitting from a base station to consider the attenuation produced when the signal was received in mobile devices [OKUM 68]. This model allows the use of distances from 1 to 100km utilizing frequencies in the range of 150 to 1500 MHz. The Hata model tries to complete Okumura model introducing a formula for the losses in free space and therefore working in the same frequency range, giving rise to the Okumura-Hata method [MEDE 00], [ALAM 12], [SCHN 96].

Other methods have been developed to model indoor environments. Whilst Cost 231 [CORR 09], ITU-RP 1238 [ITUR 12a] and Multi-Wall [SUJA 05] methods are able to take into account propagation losses produced by walls and floors, Linear Path attenuation model [DEVA 90] and Keenan-Motley method [KEEN 90] try to consider the calculated scenario by doing a preliminary measurement.

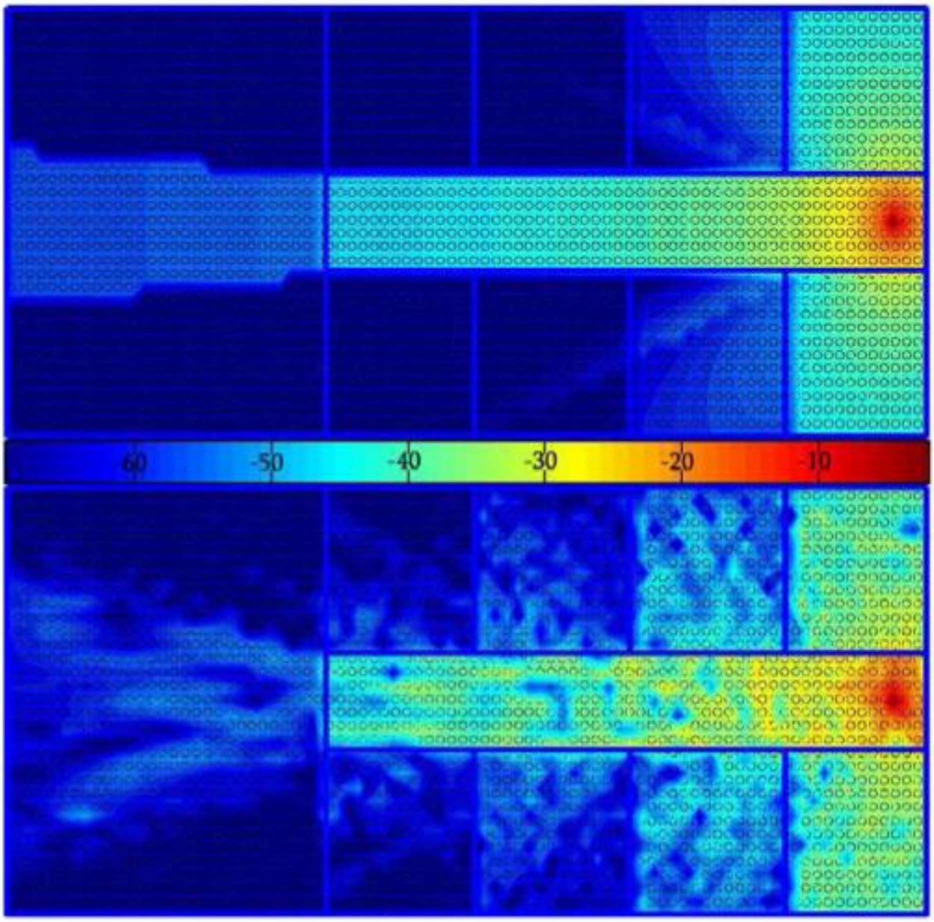

Figure 2.1 Comparison between the estimation of power distribution obtained from an empirical and a deterministic method [LOPE 12]

In [LOPE 12] a comparison between a deterministic and empirical method is presented. As it can be seen in Figure 2.1 the differences are large and the main reason is that the fundamental radiopropagation phenomena, which is multipath propagation, is obviated and the predominant considered phenomena is free space loss. The deterministic method utilized in [LOPE 12] is Ray tracing, one of the most used techniques due to the fact that it does not require as much computation time as the aforementioned deterministic methods.

Taking into account the good balance between processing time and accuracy, the three dimensional ray launching method has been chosen as the main tool in the development of this work. This algorithm has been entirely developed by students at the Public University of Navarre and has already proved its validity and good performance in several papers [AZPI 14], [AZPI 12], [MORE 12], [NAZA 12], [ITUR 12b].

It is based on Geometrical Optics (GO) and Geometrical Theory of Diffraction (GTD), providing GO approach the consideration of direct, reflected and refracted rays and introducing the consideration of diffracted rays through the use of GTD and its uniform extension, the Uniform Geometrical Theory of Diffraction (UTD). In Figure 2.2 the main phenomena considered are depicted.

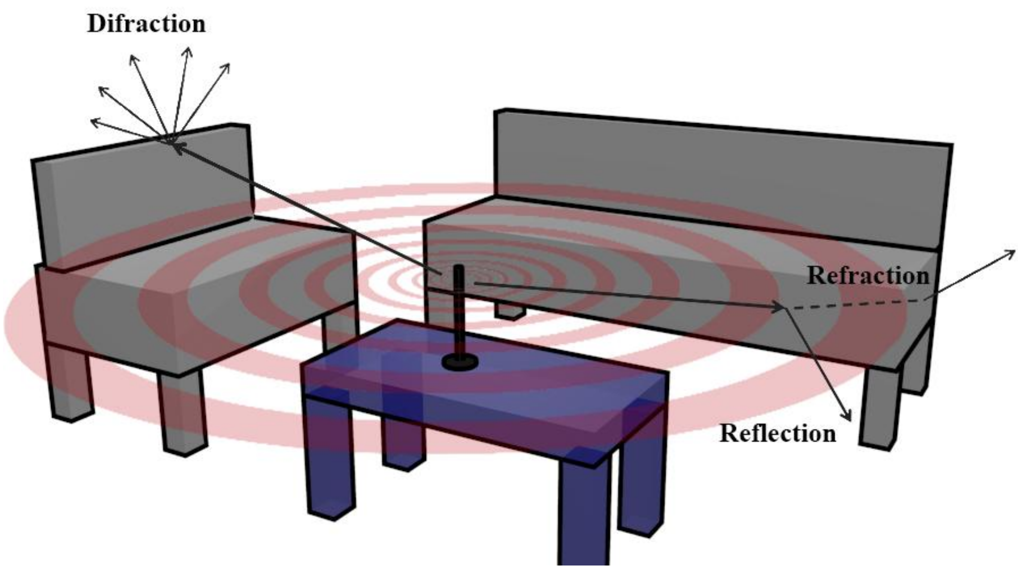

Figure 2.2 Phenomena that intervene in electromagnetic propagation and are considered in the 3D Ray Launching technique.

Since computers are not able to consider the continuity of reality, it must be discretized, giving rise to the concept of resolution. Two kinds of resolution are considered, spatial and angular resolution. Angular resolution is defined as the number of rays in which the electromagnetic wavefront produced by the antenna is divided. It must be taken into account that a higher angular resolution provides a greater resemblance to a real wavefront and consequently the results will be more accurate. However, the processing time will be higher when a greater number of rays are launched and therefore, in this case the appropriate balance between accuracy and computing time should be found again.

A spherical coordinate system in function of (θ,ϕ) angular variables is used to determine how the wavefront is discretized. In Figure 2.3 the division of the electromagnetic wave into rays is illustrated for the horizontal plane, Δϕ being the angle between two rays and therefore the angular resolution.

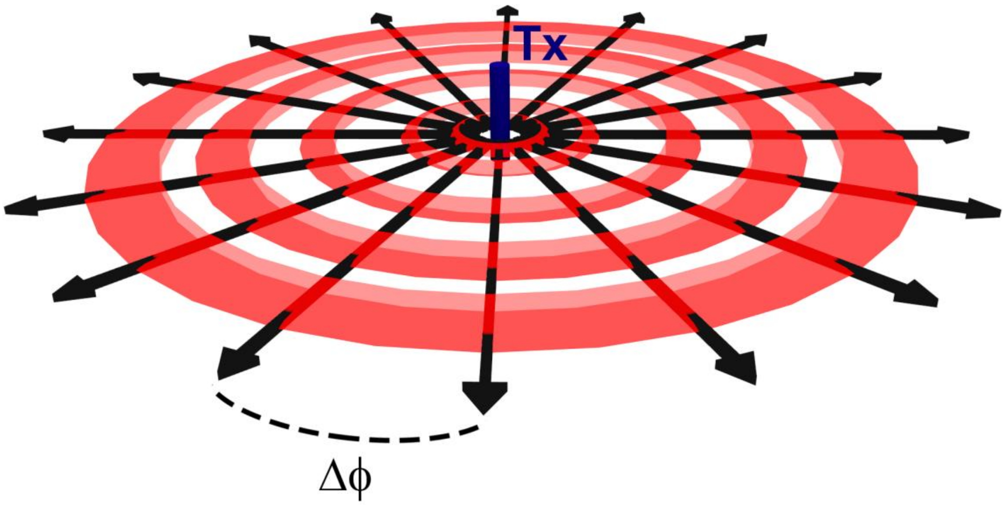

Figure 2.3 Illustration of the division of the wavefront in n finite components for one axis carried out by the 3D Ray Launching code.

On the other hand, the spatial resolution determines into how many parts the scenario will be divided. This three-dimensional entity will be called hereafter cuboid. Evidently this resolution follows the same rules as angular entity, when the space is divided into a higher number of cuboids, computational complexity is increased but reality is considered more precisely.

Related to resolution, it must be taken in account that its inadequate consideration may result in divergence problems. This means that if the scenario is overly big and the grid that divides it is too small, some rays never reach some cuboids that in the reality should pass through. This could also be a problem of angular resolution in the case that the number of launched rays is not enough.

In Figure 2.4 an example of this phenomenon is shown. An empty scenario is depicted and divided considering two different spatial resolutions. As it can be seen two rays are launched and in the case where the cuboids are larger, rays cross all of the divisions while in the other case more than one cuboid will not receive any rays. This example is an obvious simplification of the problem and its accuracy will be poor in both cases, nevertheless the principle is the same for more complex approaches.

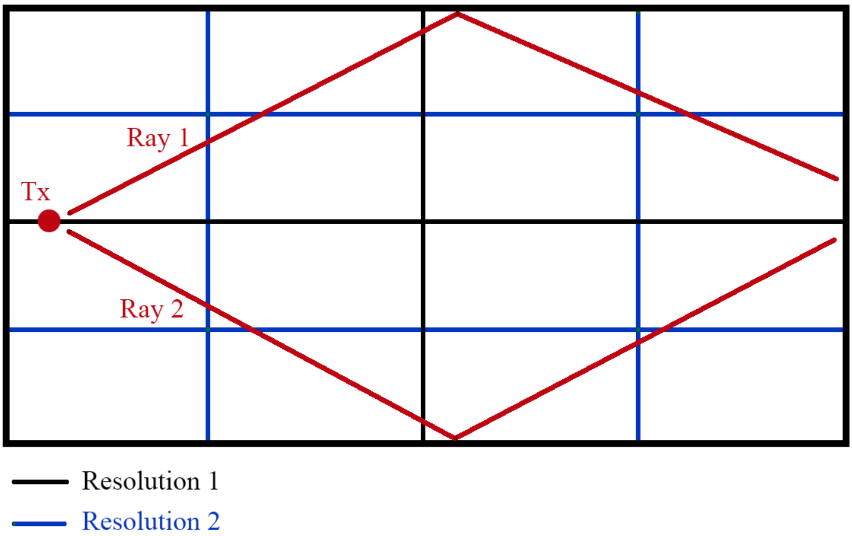

Figure 2.4 Explanation of divergence caused by the resolution differences.

Continuing with the previous example, it can be seen that if the number of ricochets were larger, rays would probably have reached more cuboids. Thus, the number of bounces or reflections must be taken in account; a large number of them also provide a better approach at the expense of doing more calculations.

Another characteristic of the simulation code is that it is programmed to work only with cubic objects and not with curved surfaces or angles, so the introduction of some kinds of objects is a challenge. This may not be a big problem considering that objects such as chairs, tables, closets and in general the furniture inside an indoor scenario are usually easily divided into rectangular parts. However, a human body is a very complex structure and it must be simplified. Fortunately this approach may not necessarily be critical considering that the wavelength is small if it is compared with the parts that compose the human body simplification.

2.2 [Paper A] ZigBee Radio Channel Analysis in a Complex Vehicular Environment

3D Ray Launching technique is tested in this paper, exhibiting good performance in an indoor environment. The selected scenario is a car due to the fact that nowadays some wireless technologies work together inside it and also, new technologies are developing for this environment. V2V (Vehicle to Vehicle) or V2I (Vehicle to Infrastructure) are the Vehicular ad-hoc Networks (VANET) that are being studied as an evolution of Mobile ad-hoc Networks (MANET).

This, combined with the fact that a car is a place where people are confined surrounded by metallic walls makes the car an ideal scenario for dosimetry analysis. However, this environment must be characterized and the correct operation of the simulation tool tested, because of the inherent complexity and the high number of reflections expected.

The selection of ZigBee as emitting technology is due to not only its suitability for this environment as a consequence of the flexibility and low energy consumption of ZigBee devices, but also for being one of the most extended Wireless Body Area Network (WBAN) technologies along with Bluetooth and RFID. Thus, a great number of applications can be developed exploiting Man-Vehicle communication through WPAN.

Once the goals have been introduced, the main features of this publication are the following:

- A transmitter is located over the dashboard taking into account the characteristics of a Xbee device and six receivers are considered, one for each seat and a last one over the back tray.
- The suitability of the code is supported through statistical estimations and comparing simulation results with real measurements.
- The behavior of radioelectric waves inside the car is studied calculating not only power distribution, but also power delay profiles and the delay spread, which are clear indicators of the impact of multipath propagation within the scenario.
- The feasibility of a ZigBee based system inside the scenario is proved thanks to current consumption calculation and obtaining the values of the Packet Error Ratio (PER).

PAPER A

IEEE Antennas and Propagation Magazine ***56(4)***
(2014)

ZigBee Radio Channel Analysis in a Complex Vehicular Environment

Peio López Iturri, Erik Aguirre, Leire Azpilicueta, Uxue Gárate and Francisco Falcone

upna
Universidad
Pública de Navarra
Nafarroako
Unibertsitate Publikoa

Artículo A eliminado en cumplimiento de la Ley de Propiedad Intelectual
(Real Decreto Legislativo 1/1996, de 12 de abril).

2.3 [Paper B] Characterization and Consideration of Topological Impact of Wireless Propagation in a Commercial Aircraft Environment

Since the topology of the scenario is essential for the radio-propagation and power distribution, the radio channel analysis is evaluated in different environments. Continuing with the philosophy of [Paper A], an entire aircraft is considered in [Paper B] due to the high concentration of people that usually can be found inside it and the high reflectivity of its walls.

Besides, nowadays new wireless technologies for passenger comfort in flight are developing, leading to a new situation where antennas are installed and operate inside airplanes. Therefore, the aim is to study not only radioelectric propagation but also the subsequent dosimetry analysis inside aircrafts.

In this paper, the schema is similar to the followed in [Paper A] but with the novelty of the introduction of an entire aircraft inside a 3D Ray Launching simulation tool considering all of its parts (e.g. seats, and porters). Therefore the main features of this publication are:

- All of the elements inside an Airbus A380 aircraft are considered in the simulation , being this one of the biggest commercial aircraft that is used nowadays with two floors and 550 seats distributed between them.
- Seven antennas are distributed all over the scenario placing them strategically with the aim of spreading electromagnetic power across the aircraft. Three different ISM (Industrial, Scientific and Medical) frequencies are considered (900 MHz, 2.4GHz and 5GHz) in order to compare the obtained results. This corresponds to the radioplanning analysis, which is the initial step for further coverage/capacity system level approaches.
- A statistical analysis of the scenario is done validating the use of the 3D RL simulation method.
- The obtained results are studied through horizontal power distribution planes, power distribution vs distance graphs, Power Delay Profiles (PDP) and delay spread distributions. As expected lower frequencies lead to higher power levels received all over the scenario and the number of ricochets are also higher since the rays propagate for longer distances (i.e., longer time distributions of reflected components in the PDP estimations). In any case more rebounds take place as a consequence of the existence of metallic walls.

PAPER B

IEEE Antennas and Propagation Magazine ***55(6)*** *(2013)*

Characterization and Consideration of Topological Impact of Wireless Propagation in a Commercial Aircraft Environment

Erik Aguirre, Peio López Iturri, Leire Azpilicueta, Javier Arpón and Francisco Falcone

Artículo B eliminado en cumplimiento de la Ley de Propiedad Intelectual (Real Decreto Legislativo 1/1996, de 12 de abril).

Chapter 3.

Dosimetric calculations through simulation techniques

This chapter describes the utilization of simulation tools in order to carry out dosimetric calculations and experimentations. The main human body models are also studied comparing their complexity as well as their possible uses with the aim of choosing the most suitable model for the used method. The chosen model is presented and deeply described, introducing not only its main characteristics, but also all the considerations behind its construction. Two original contributions are presented: (i) the human body model is introduced for the first time in a work performing a localized study considering the power distribution inside and outside the human body and comparing results with reality, (ii) a wide area study introducing the human body into an entire scenario when a real e-health system is working.

3.1 Simulation techniques and dosimetry

The use of simulation techniques when dosimetric issues are studied pose a great support since in some cases theoretical estimations are easier to carry out than the experimental ones. This is especially true when the absorption rate inside the human body is estimated, since a probe is not able to be placed, as an example, inside the brain of a person. This is the reason behind the wide utilization of FDTD simulation technique, it allows the study of the influence of electromagnetic waves in localized parts of the human body with high precision [NAGA 11a], [TAYL 95], [ALFA 05].

As an example, the SAR value obtained when someone is using the mobile phone is one of the most common measurements.

Nevertheless, when the area under analysis is larger as a consequence of the consideration of the environment where the human body is located, "lighter" techniques in terms of calculation loads must be used. In accordance with what has been shown in the previous chapter, the use of 3D RL technique is a good option as a consequence of its good simulation time/accuracy balance, although examples of empirical techniques can be found in the literature [DURN 79].

In any case, human body models should be considered when dosimetric estimations are done, especially when SAR is calculated since it measures the absorption produced in different tissues. The considered model is independent of the simulation technique chosen, however more accurate techniques usually consider more complex approximations, maintaining a higher global accuracy for all the process. More simple simulation techniques can implement more simple models since the technique will not be able to consider all the complexity of a more complete human body model.

These possible complexity levels force to carry out a deep study of the different possibilities considering not only the limitations of the simulation tool, but also the requirements of the study.

3.2 Human body models

The intrinsic complexity of the human body leads to the existence of different approaches when it comes to implementing it computationally. This variety goes from the simplest models where the morphology is not crucial to more complex models where the human body must be considered with total precision.

The most simplified human body models are constructed using only a basic geometric object, starting with the cylindrical modeling [POLJ 03], [RUAN 09], [GHAD 04], [PETR 14] where a cylinder is used to represent the entire human body. This cylinder is endowed with the dielectric properties of a biological tissue, usually the properties of skin [PETR 14].

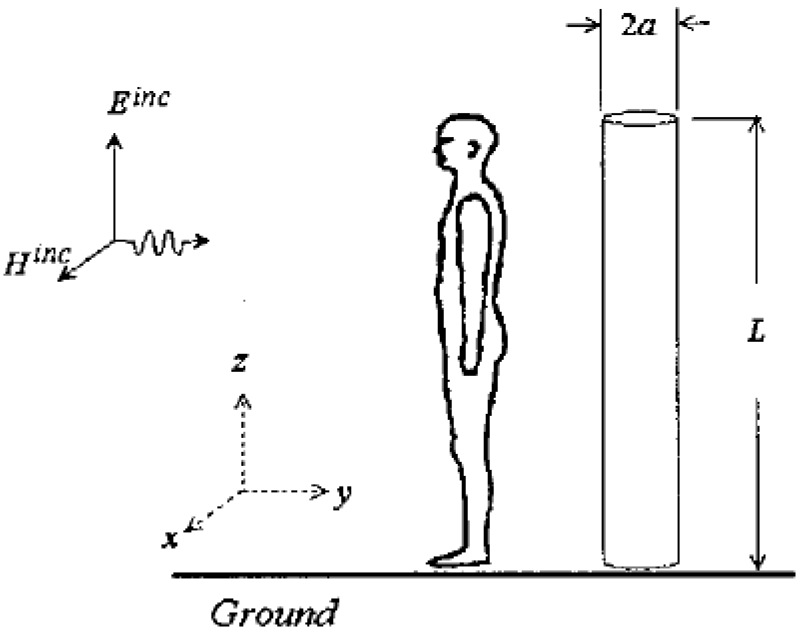

Figure 3.1 Cylindrical simplification of human body [POLJ 03]

Spheroidal [DURN 79], [UZUN 87], [REIV 99], [DURN 75] or ellipsoidal [CANS 03], [OZEN 01], [MASS 77] forms are also used to consider the complete human body and in this case the use is similar to what has been seen with cylinder. In some cases the simplified human body is divided in different layers [UZUN 87] to consider not only a unique tissue, but also more than one, introducing muscle, blood or any tissue present inside the human body.

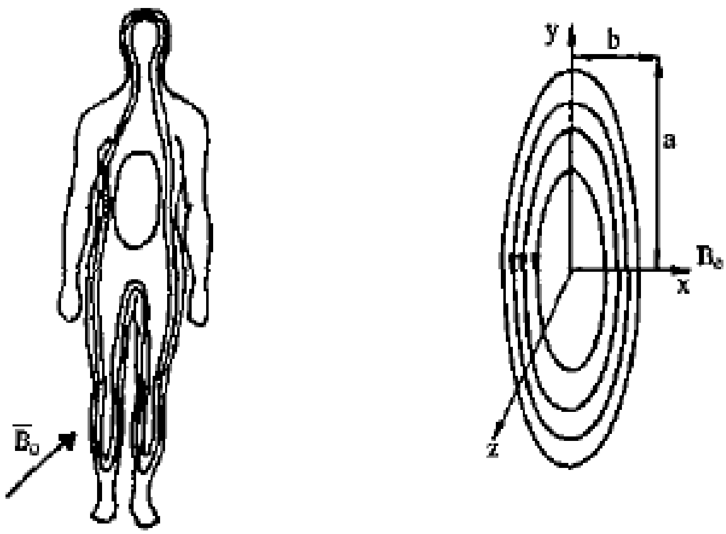

Figure 3.2 Human body divided in several layers and its corresponding spheroidal simplified model [UZUN 87]

In some cases these simplifications are used to simulate a particular part of the human body [SURD 08], [GOUZ 07], [BASH 10], evidently these models try to exhibit similar lengths to the original parts and this is the reason why complete body models are stretched while the head models can be a perfect sphere (Figure3.3).

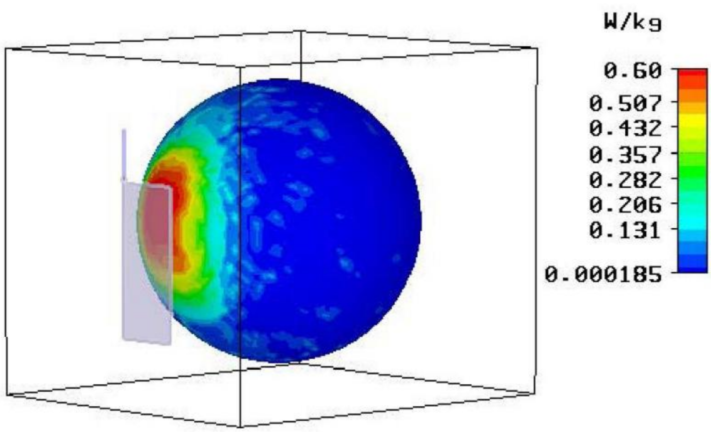

Figure 3.3 Spherical model for the study of the SAR distribution in the gray matter when it is exposed to electromagnetic waves [SUR 8]

In the next scale the simplified human body models with some morphological resemblance can be found [CHUA 97a], [CHUA 97b], [FUJI 06]. This kind of models show the basic human body structure considering head, arms and legs, nevertheless they are constructed with simple structures like rectangles.

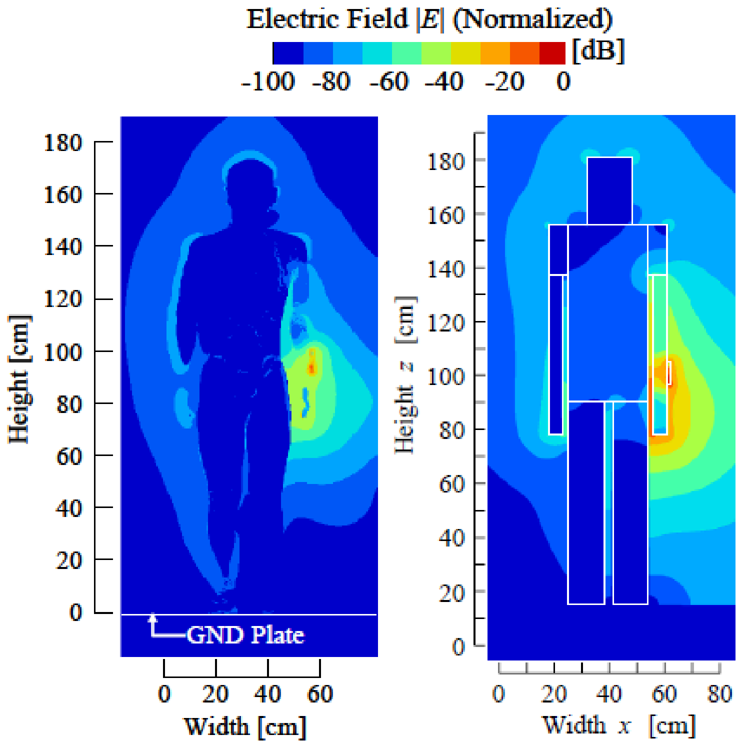

Figure 3.4 Electric field distribution considering a real model and its simplification [FUJ 2006].

Finally, high resolution models are defined [NAGA 08], [DAW 98], [NAGA 11b] termed this way because they represent the human body in a very precise way. The main difference with previous models is that the morphology of the human body is divided in smaller parts, leading to results which are more similar to reality.

One of the most important reference regarding human body modeling is called HUGO [SHIN 07], [VUCH 13], [RAAD 13], [MOTR 06] and it is implemented in CST (Computer Simulation Technology) [CST 13] based on Visible Human Project® [NLM 13]. Two human body cadavers was sectioned, one in 1993 belonging to a man and with a resolution of 1millimeter and another one two years later belonging to a woman with a resolution of 0.33 millimeters. From that dissection a complete and precise library of all the human body parts was obtained and it can be used for several purposes once a license has been obtained.

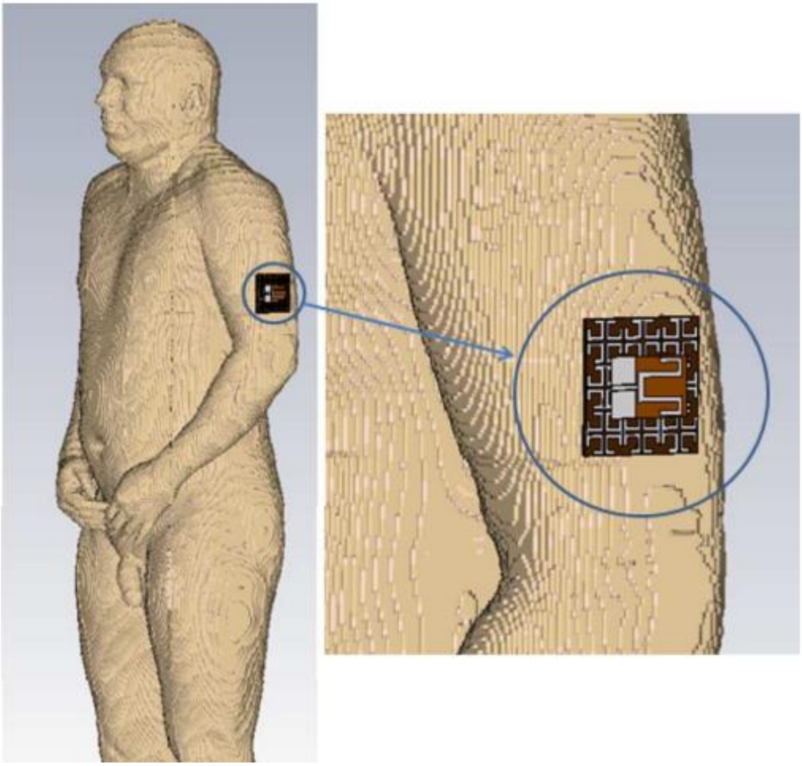

Figure 3.5 Example of the human body HUGO utilized for SAR calculation in [RAAD 13]

The parameterization of the two genders is important as long as not only the morphology is different but also some materials can have different properties. Those phenomena have also reproduced when persons of different ages are considered, especially when the subject under study is a child, the dielectric properties of the human body tissues change with age. Some computational human body models have been obtained utilizing Magnetic Resonance Imaging (MRI), in [NAGA 11b] [NAGA 09] National Institute of Information and Communications Technology (NICT) in Japan has computerized human body models of different ages, including pregnant woman models, to use them in electromagnetic dosimetry.

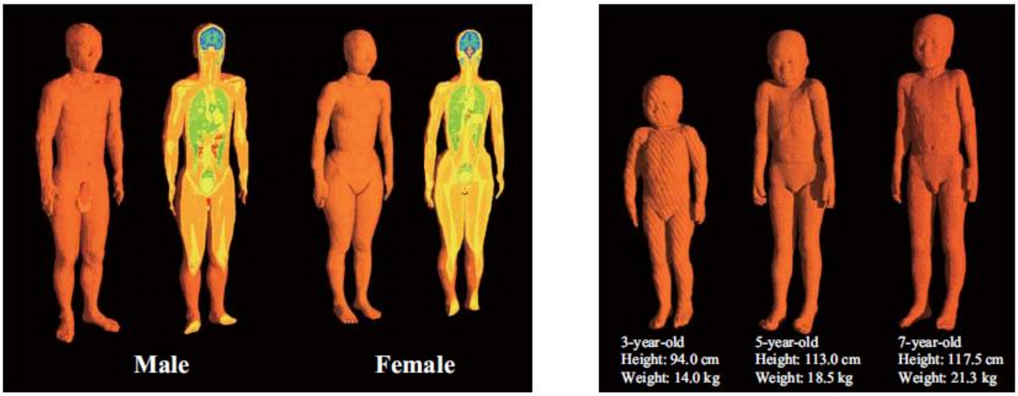

Figure 3.6 Human body models obtained by NICT [NAG 11] of two sexes and considering different ages.

In some cases and taking into account the high processing load produced by the consideration of the high resolution model, some researchers usually work using only a part of the human body [LAZZ 97] , [FASH 11], [DIMB 91]. In figure 3.7 an example where the electromagnetic source is placed next to the head is depicted, whereas the transmitter is a phone and they are usually used in this way, it is reasonable for the study be focused only on the area of the head.

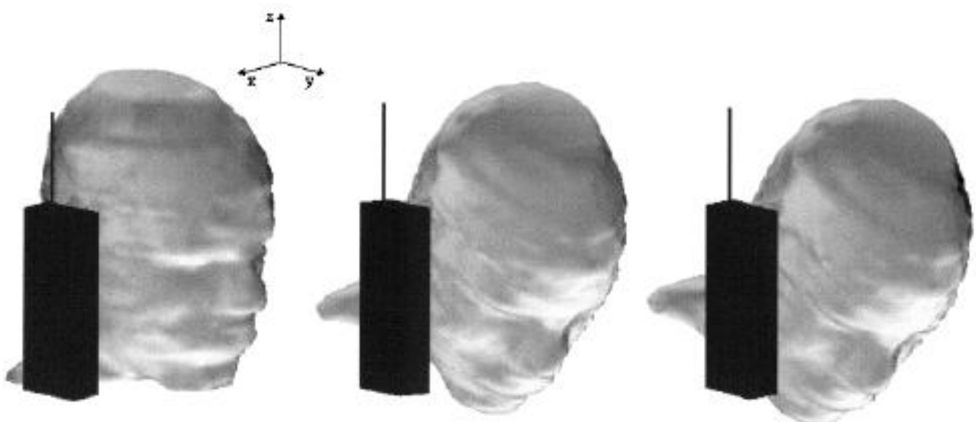

Figure 3.7 An example of a high resolution human head model utilized for the study of the influence of electromagnetic waves produced by a mobile phone when it is next to head. [LAZZ 97]

Finally, some researchers construct their own mannequins called phantoms, thus being able to compare computational results with more realistic data. Different scale of complexity can be also found in these models, depending on the resources or necessities of the designer. However, usually only a part of the body is reproduced and in most cases, a liquid or gel is utilized instead of a solid object [HAMB 03], [YAMA

13], [MACH 06], [WATA 10]. Those phantoms do not have to necessarily emulate a healthy tissue, in some cases they can take in account a cancerous tissue [ORTE 12].

At the other end, SAM (Specific Anthropomorphic Mannequin) is a widely extended morphologically realistic phantom that is usually utilized to measure SAR values inside head and also has a digital model that is used in numerical simulations [LEE 07], [LEE 11], [MONE 10]. This phantom has been created by SPEAG [SPEA 13a] that also has developed a entire human body phantom called POPEYE (POsable Phantom for Electromagnetic sYstems Evaluations) [SPEA 13b] that follows IEEE SCC34 [GROU 14], 3GPP TR 25.914 [3GPP 05] and CTIA [CTIA 13] standards.

As well as in digital versions of human body, phantoms must be correctly constructed, providing them the same properties as human body. When the aforementioned liquid or gel phantoms are created a mixture of different materials is implemented to give as similar characteristics as possible and in most cases they are similar to the materials shown in Table 3.1. It can be seen that each material provides a specific characteristic to the phantom and it is not strange that the main part of the mixture consists of water since the human body is principally composed of it.

Materials	Weight [g]	Effects
Purified water	3375	Main material
Polyethylene powder	337.5	Relative permittivity
NaCl	19.6	Conductivity
Agar	104.6	Forming
TX-151	82.93	Thickener
Sodium dehydroacetate monohydrate	2.0	Antiseptic

Table 3.1 Materials that are usually utilized in liquid or gel phantoms, their quantity and effect in the mixture [YAMA 13].

3.3 Developed human body model

Once the different human body models implemented have been studied, the most suitable and convenient model for the utilized ray launching code is selected. Taking into account the geometrical limitations imposed by the code but without forgetting that the morphology of an object could be essential when a correct propagation estimation is obtained, a simplified human body model with morphological resemblance is chosen.

This simplification poses a big challenge considering the complexity and irregularity of the human body, not only in its exterior but also in organs, bones and all the parts that compose the inner body. In any case, the morphology has been basically maintained by consulting several information sources for the exterior and interior of the human body.

The exterior dimensions have been extracted from [ERGO 14], [FIGU 14] and by performing several measurements in real individuals. It has been considered the widely known proportionality of the human body, programming a parameterized human body that respects those proportions depending on the introduced height.

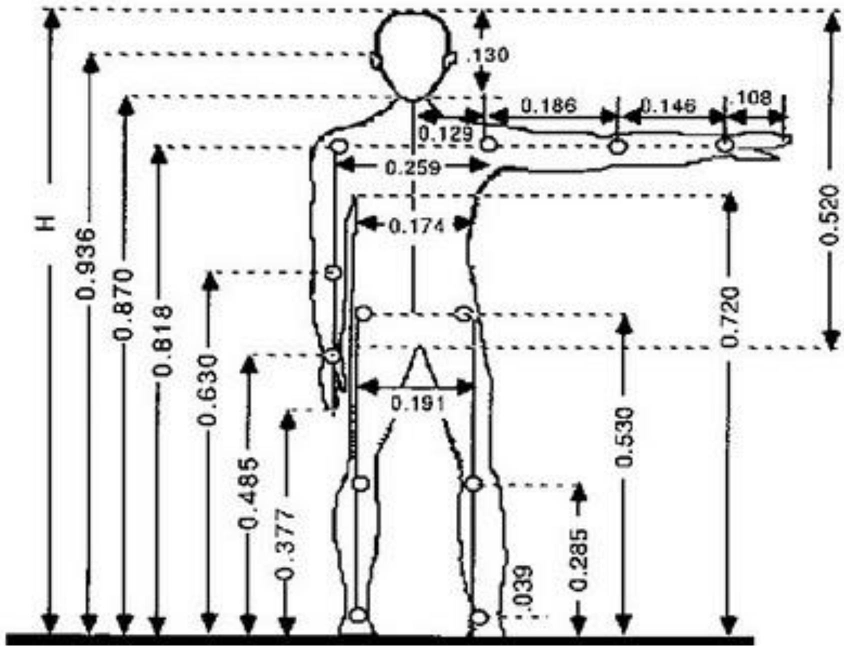

Figure 3.8 Standard proportions of the human body in accordance with [ERGO 14]

When dealing with the interior of human body apart from organs and bones, all the tissues that surround them should be considered. For this model three different layers have been defined over bones, skin layer, muscle layer and veins/arteries layers obtaining their thickness from [OCW 14]. Finally, dimensions of organs and bones consistent with anatomically realistic body models shown in Figure 3.9 and from [BIOD 14] where the dimensions and situation of the different organs are visible.

Figure 3.9 Anatomically realistic human body models and complete digitalized human anatomy(right) [BIOD 14]

The human body model has been implemented taking into account the possibility of considering different layers in simulation. Thus, four "resolution" levels are defined, giving the possibility of use spanning from a model with only skin properties until a model with all parts previously mentioned. With this possibility the processing time can be decreased considerably because fewer cubes will be used during simulation and therefore less calculations will be performed.

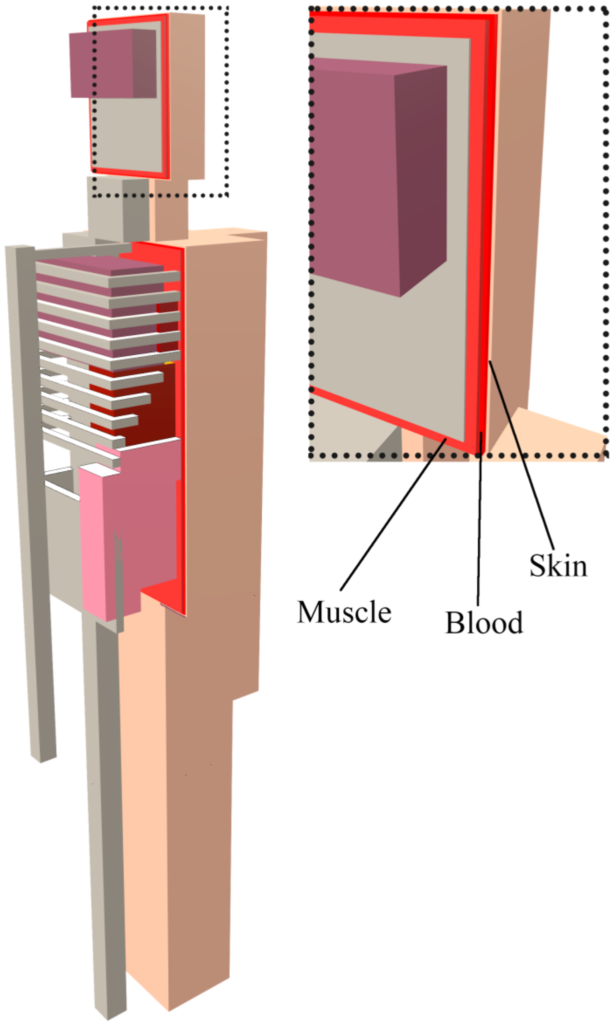

Figure 3.10 Developed human body model dissected with all the different layers visible.

The simplified body model has been endowed with more configurable possibilities starting from the option of changing its orientation so that it can lie down on the ground or be oriented to other sides. Its position can be also changed allowing the possibility of taking the sitting posture

The characteristic that complete the adequate functionality of the human body model is the correct implementation of the dielectric properties of the different tissues of which it is comprised. In this case and using the aforementioned formula extracted from [SANC 09], a human body model with frequency dependent tissue dielectric characteristics has been programmed.

As an example, in Figure 3.11 dielectric constant versus frequency is depicted for various biological tissues.

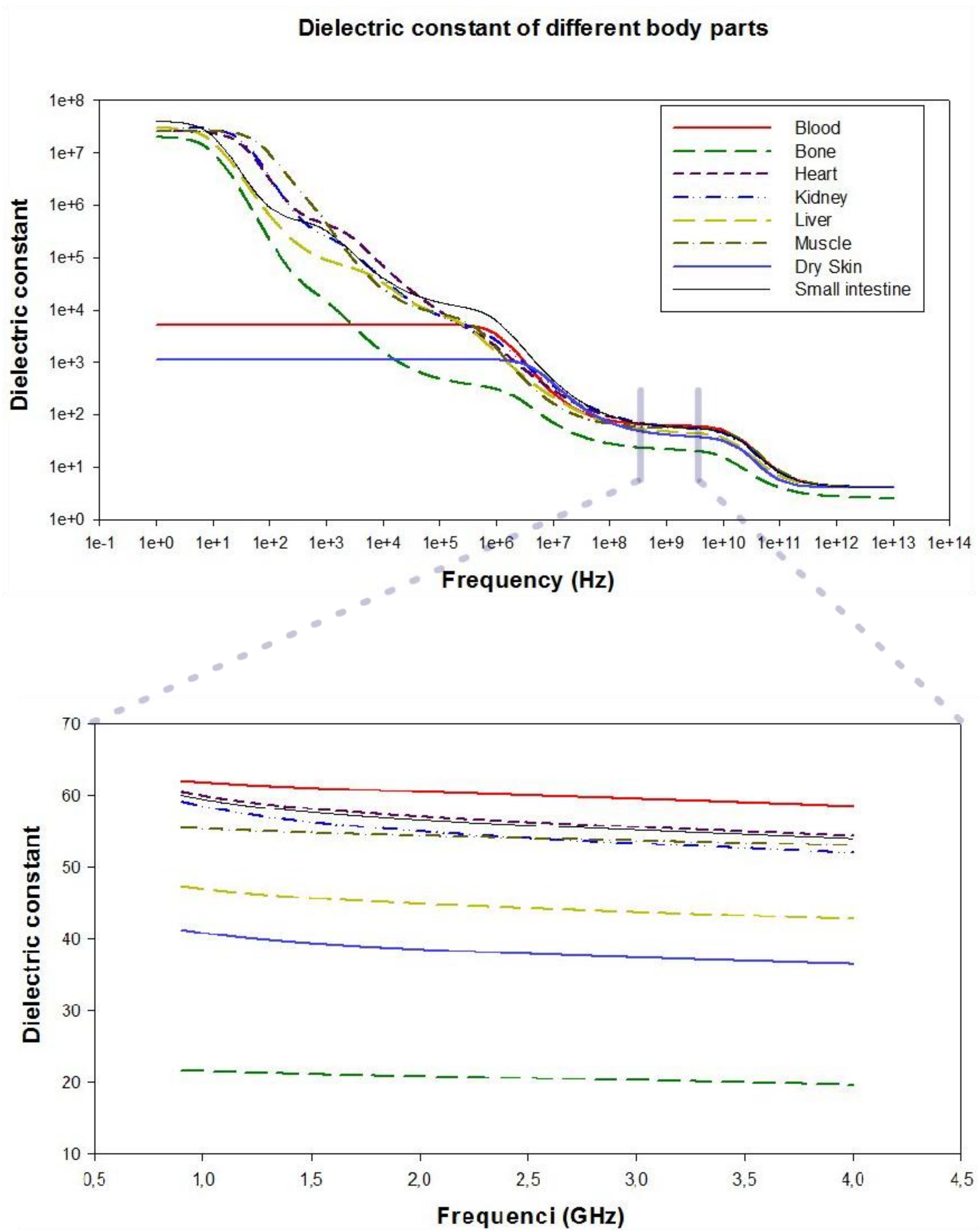

Figure 3.11 Dielectric constant vs Frequency for different biological tissues

3.4 [Paper C] Evaluation of electromagnetic dosimetry of wireless systems in complex indoor scenarios with human body interaction

Once the different human body models are studied and a simplified body is developed, it is tested utilizing the high resolution configuration where all parts of the human body are considered.

The developed human body model is introduced inside an entire floor of the Jerónimo de Ayanz building of the Public University of Navarre. Nevertheless, the human body is considered in a confined region by applying a technique of spatial resolution differentiation by zones. In this case, the human body is placed in a high resolution zone and the rest of the scenario has low resolution. This configuration allows the possibility of studying how the electromagnetic wave interacts with the materials that form human body when it is located inside a relatively large scenario, but decreasing considerably the processing time. The relevance of this communication can be summarized as follows.

- A deep study of different human body models and simulation techniques is presented to justify the use of the developed simplified human body model.
- The study of the power distribution inside a human body model is carried out when it is situated in a complex scenario and exposed to an antenna emitting in front of the model. Thus, not only the exposition of the human body is evaluated, but also the influence of the entire room to the rays that finally reach the person.
- The correct operation of the human body model is studied placing receivers over a real person and changing its position on the scenario for the comparison between simulated and measured results. Thus, good performance is achieved in all cases with low error rates.

PAPER C

*Progress in Electromagnetics Research B **43** (2012)*

Evaluation of electromagnetic dosimetry of wireless systems in complex indoor scenarios with human body interaction

Erik Aguirre, Javier Arpón, Leire Azpilicueta, Silvia de Miguel Bilbao, Victoria Ramos and Francisco Falcone

Progress In Electromagnetics Research B, Vol. 43, 189–209, 2012

EVALUATION OF ELECTROMAGNETIC DOSIMETRY OF WIRELESS SYSTEMS IN COMPLEX INDOOR SCENARIOS WITH HUMAN BODY INTERACTION

E. Aguirre[1], J. Arpón[1], L. Azpilicueta[1], S. de Miguel[2], V. Ramos[2], and F. Falcone[1, *]

[1]Electrical and Electronic Engineering Department, UPNA, Pamplona, Navarra, Spain

[2]Telemedicine and E-Health Research Unit, Health Institute Carlos III, Madrid, Spain

Abstract—In this work, the influence of human body within the estimation of dosimetric values is analyzed. A simplified human body model, including the dispersive nature of material parameters of internal organs, skin, muscle, bones and other elements has been implemented. Such a model has been included within an indoor scenario in which an in-house 3D ray launching code has been applied to estimate received power levels within the complete scenario. The results enhance previous dosimetric estimations, while giving insight on influence of human body model in power level distribution and enabling to analyze the impact in the complete volume of the scenario.

1. INTRODUCTION

The use of wireless systems has experienced great growth in the last decade, mainly due to the adoption of communication systems that are of use in a broad range of applications. One of the areas experiencing more growth is the adoption of wireless systems in indoor scenarios, with the advent of Wireless Sensor Networks for health monitoring and home automation system of the evolution of mobile wireless systems, with Long Term Evolution being the main driver in femtocell deployment. In the case of a conventional household, several wireless systems can be operating simultaneously, such as WLAN in different versions, personal area network such as Bluetooth or ZigBee, or distribution in wireless fashion of DVB-T

Received 9 July 2012, Accepted 21 August 2012, Scheduled 23 August 2012

* Corresponding author: Francisco Falcone (francisco.falcone@unavarra.es).

signals, among others. Also, Ambient Assisted Living scenarios make intensive use of wireless sensors in order to perform monitoring and control tasks, adding new elements of use within the wireless spectrum (mainly based on 802.15 standard as well as GSM/UMTS backup). Because of this growth of wireless technology it is highly important to have the knowledge of the effects that exposure to electromagnetic fields has in the human body. Related to this, there are several organizations that are devoted to legislate issues and recommendations in this area, establishing maximum limits to which a person may be exposed [1, 2]. In this scenario, dosimetric assessments acquire great importance due to the fact that they determine whether new legislation should be implemented and anticipating potential changes in actual regulations, with an extensive set of dosimetric assessments reported in literature [3–6], with different techniques and different approaches of the human body more or less accurate or simplified.

A priori, the most precise way to estimate electromagnetic exposure and perform dosimetric evaluation is obtained by in situ measurements. However, to obtain insight on the potential impact of different wireless devices and their integration as complete systems requires the use of theoretical estimations. On the other hand, these theoretical estimations exhibit some problems, related to the accuracy of the radio propagation parameters and to the human body characteristics. This leads to a commitment between the computational complexity in terms of calculation time and the final accuracy of the results.There is a great assortment of ways to estimate radio propagation and a large ways of representing the human body. The most accurate method to perform dosimetric estimation is directly solving Maxwell's equations,in which SAR calculations are achieved using full wave techniques such as Finite Difference Time Domain [7–9], or equivalent methods. However, the large requirements in terms of memory use and the high computational cost make them inappropriate for large area calculations at high frequency bands. The search for optimized evaluation of SAR values has lead to enhanced estimation procedures, including modification of the measurement setup to maintain level of exposure and field uniformity, such as described in [10].

Geometrical optics techniques offer a good approximation with a lower computational cost. This group includes a great number of methods, being one of the most widespread the Shooting and Bouncing Rays (SBR) [11–13]. Another approach is the use of empirical methods, traditionally applied for initial coverage estimation of broadcast wireless systems. They give rapid results but require calibration based on measurements to give an adequate fit of the results based on initial regression methods (elimination of mean error component and reduction of standard deviation). These methods are not optimal for dosimetry studies due to the complexity of the human body in morphological as well as topological terms, although they have been used to perform initial estimations [14].

The human body model designed for simulations can be more or less complex depending on the required analysis and the frequencies of operation of the wireless systems under consideration.Several studies simplify the human body by representing it cylindrically [15–17], spherically [14, 18–20] or with ellipsoidal shape [21–23]. Generally, the aim of these studies is the analysis of the influence of the total human body in the environment, although there are also studies related to specific body parts [24].

Within the variety of morphologically similar human body models, there are high resolution models [25–27], which show a dense volume meshing; or simpler ones [28–30] that respect the basic structure of the arms, legs, head, etc.. It should be noted that depending of the aim of the analysis or the substantial processing time, many studies that implement a high resolution model focus in a localized area of the body and not in the overall human body [31, 32]. Many of these models are also studied experimentally, with the so-called phantom models, which are designed similarly with a variety of shapes [33, 34].

The goal of this work is to obtain dosimetric assessments in large spaces considering the interaction of the environment and the objects that are located within this scenario and not an isolated human body or a fraction of it. This is achieved by an adequate balance between computational time and accuracy of data, with the best combination of radio propagation estimation technique with simplified model of the human body. Considering all methods described, geometrical optics technique is optimal because although it is not as accurate as full wave techniques, it offers good results, with standard deviations of 5–8 dB [35], with a fairly low computational cost. As far as the simplified model of the human body is concerned, the use of cylindrical model could be interesting, providing good results in high intermediate frequencies (400 MHz to 7 GHz) [36]. Nevertheless, is recommendable a high resolution model, considering the computational time and the complexity of implementation, for more precise analysis.

In the literature, electromagnetic and thermal analysis has been performed in the human head due to RF exposure [37, 38], relating interaction of electromagnetic fields in the calculation of Specific Absorption Rate. Non-thermal effects have also been analyzed, basically on the influence of time and frequency hopping mechanisms in REM sleep stages as well as in alpha waves [39, 40]. In both cases, the estimation of the received electromagnetic field value is a key parameter in the rf exposure analysis. The aim of this article is to assess in the computation of received electromagnetic field values, which can later on be employed as an estimation of compliance with international, national and local standards. This methodology is actually employed by Spanish Ministry of Health in the verification of regulation compliance, by means of RMS measurement of 1 second samples in a 6 minute time span per measurement location of E-field values. The goal is an analysis of an indoor scenario with the presence of a human body model to verify his influence in the environment. It is shown that the topology and morphology of the scenario strongly influence the behavior of the wireless channel. A deterministic method based on three-dimensional (3D) ray launching has been implemented within our research team based on Matlab$^{\text{TM}}$ programming environment. A simplified human body model has been developed for this code. This model implements the basic organs considering their frequency dispersive material characteristics, in order to analyze their influence on the environment. The combination of a simplified human body model with an efficient simulation technique enables to assess the impact of wireless systems within the complete scenario under analysis, not limited to specific body sections.

2. DEFINITION OF SIMULATION SCENARIOS AND RESULTS

Deterministic methods [41–47] are based on numerical approaches to the resolution of Maxwell's equations, such as ray launching and ray tracing, or full-wave simulation techniques (method of moment (MoM), finite difference time domain (FDTD) [48], FITD, etc.). These methods are precise but are time-consuming to inherent computational complexity. As a midpoint, methods based on geometrical optics, offer a reasonable trade-off between precision and required calculation time [49]. As stated in the introduction, a 3D ray launching algorithm has been implemented in-house based on Geometrical Optics (GO) and Geometrical Theory of Diffraction (GTD). The rays considered in GO are direct, reflected and refracted rays interacting within the elements of the scenario under analysis. To complement the GO theory, the diffracted rays are introduced with the GTD and its uniform extension, the Uniform GTD (UTD) [50–52]. The purpose of these rays is to remove the field discontinuities and to introduce proper field corrections, especially in the zero-field regions predicted by GO. The basic procedure of the ray launching algorithm [50–52] is, first, to launch a ray from the transmitting antenna (noted as Tx). Then, the ray is traced to see if it hits any object or is received by the receiving antenna. When the ray impacts with an obstacle, reflection, transmission and diffraction will occur, depending on the geometry and the electric properties of the object. Once all possible paths have been identified, high-frequency electromagnetic techniques, such as UTD [50] are applied to the rays to compute the amplitude, phase, delay, and polarization of each ray. The implemented algorithm takes into account Fresnel equations, discretized within the cuboids present in the simulation volume, in which the reflection coefficient $R^{\perp}$ and transmission coefficient $T^{\perp}$ are calculated by

$$T^{\perp} = \frac{E_t^{\perp}}{E_i^{\perp}} = \frac{2\eta_2 \cos(\Psi_i)}{\eta_2 \cos(\Psi_i) + \eta_1 \cos(\Psi_t)} \tag{1}$$

$$R^{\perp} = \frac{E_r^{\perp}}{E_i^{\perp}} = \frac{\eta_2 \cos(\Psi_i) - \eta_1 \cos(\Psi_t)}{\eta_2 \cos(\Psi_i) + \eta_1 \cos(\Psi_t)} \tag{2}$$

where $\eta_1 = 120\pi/\sqrt{\varepsilon_{r1}}$, $\eta_2 = 120\pi/\sqrt{\varepsilon_{r2}}$ and Ψ_i, Ψ_r and Ψ_t are the incident, reflected and transmitted angles respectively. Several transmitters can be placed within the scenario, in which power is modeled as a finite number of rays launched within a solid angle. Parameters such as frequency of operation, radiation patterns of the antennas, number of multipath reflections, separation angle between rays, and cuboids dimension are introduced. The material properties for all the elements within the scenario are considered, given the dielectric constant and the loss tangent at the frequency range of operation of the system under analysis.

Figure 1 shows the principle of ray launching method. The transmitter antenna launches rays in different directions following

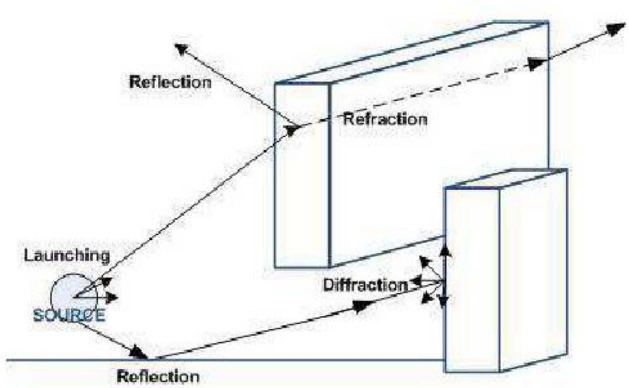

Figure 1. Principle of ray launching method.

the radiation pattern of the antenna. The reflection and refraction coefficients are calculated using the well-known Fresnel's equations and the diffraction coefficients by the Uniform Theory of Diffraction (UTD) [50]. The commitment between accuracy and computational time is acquired with the number of launching rays and the cuboids size of the considered scenario. The considered scenario is an indoor room of dimensions 6.5 m × 5.5 m × 2.5 m with different objects and with a human body model in the center. Objects are defined as different hexahedrons in the algorithm. By this basic geometric shape it is highly easy to form another objects much more complex, such as tables, chairs and shelves, and placing them into the room. In a generic room, walls can be formed by windows, doors, frames, etc. So, to characterize the walls of a room, each discontinuity on the wall must be characterized. This will define each part of the wall like an object by its central position (x_0, y_0, z_0), the width in each dimension (Δx, Δy, Δz) and the material that is made. A schematic view of the simulated scenario is depicted in Figure 2, with some typical objects of an office

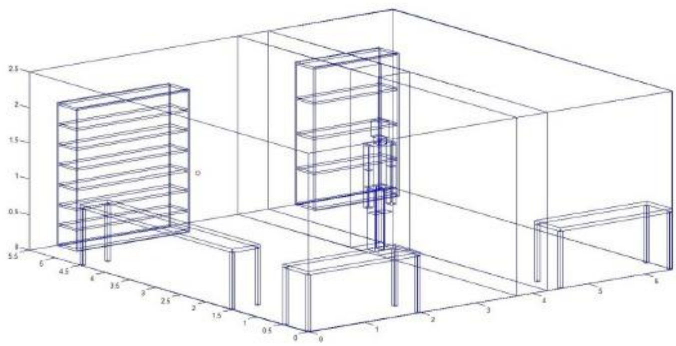

Figure 2. Schematic view of the considered scenario.

Table 1. Simulation parameters employed by the RL code developed at UPNA.

PARAMETERS IN THE RAY LAUNCHING SIMULATION	
Frequency	2 GHz 2.4 GHz
Vertical plane angle resolution $\Delta\theta$	1°
Horizontal plane angle resolution $\Delta\varphi$	1°
Reflections	7
Transmitter Power	4.5 dBm

room, specifically three tables and two shelves.The transmitter antenna has been placed at the point (0.75 m, 3 m, 1.5 m). Simulations have been done for two different working frequencies, 2 GHz and 2.4 GHz. Table 1 shows the parameters used in simulation.

In the analyzed scenario, two different areas have been considered to perform a more precise analysis of the influence of electromagnetic waves in the human body, to optimize computational cost without compromising accuracy. Therefore, a high resolution and low resolution areas have been defined. The high resolution area (Figure 3) is located at the center of the scenario (Figure 2), with a reduced size $0.55\,\mathrm{m} \times 0.55\,\mathrm{m} \times 2.5\,\mathrm{m}$, in which the model of the human body is located.

Resolution is defined in the 3D Ray launching algorithm by the size of the cuboids in which the room is divided to estimate the power level in each of them. In this way, the resolution of the small zone in which the human body has been introduced employs cuboids of size $0.03\,\mathrm{m} \times 0.03\,\mathrm{m} \times 0.2\,\mathrm{m}$. As far as the human body model is concerned, it has been performed with the greatest detail as possible, taking into

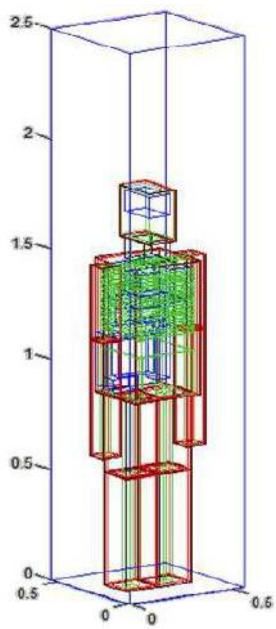

Figure 3. Detail of the high resolution zone, which the different organs that are embedded in the human body model.

account parts such as bones, internal organs, muscles, blood and skin, all with their respective values of dielectric constant and conductivity parameterized to the given frequency range, as given by [53, 54]. Table 2 shows the materials taken into account for simulation. The human body model has been parameterized in such a way that body proportions (i.e., relative dimensions between head, limbs and torso) are maintained for any given height of the person that is needed to be modeled.

To reduce computational cost, it is possible to consider less resolution in the design of the human body model. In this way only skin and bones could be considered, adding organs gradually up to four different types of human body models. In this work, the highest resolution for the human body has been considered. The behavior of such materials is strongly dispersive, as seen in Figures 4 and 5, by parametric calculation of the materials parameters which is automatically performed by the in house code that has been developed for this purpose. Therefore, a dynamic variation of the material properties to take into account the estimation of interaction of electromagnetic waves with different organs is considered in the overall simulation result.

The results of the received power correspond to the high resolution area, which is depicted with the human body in Figure 2. Figures 6 and 7 show horizontal planes of received power in two different heights ($Z = 1\,\mathrm{m}$ and $Z = 1.6\,\mathrm{m}$) for operating frequencies of a wireless source of 2 GHz and 2.4 GHz, respectively. Figures 8 and 9 depict the vertical sections of the zone of high resolution keeping constant the value of X in 0.3 m.

Table 2. Dielectric constant and conductivity for different parts of the body at different frequencies.

	ε_r		**Conductivity [S/m]**	
Frequency	**2 GHz**	**2.4 GHz**	**2 GHz**	**2.4 GHz**
Blood	60.50	60.12	18.01	17.01
Bone	20.86	20.63	4.75	4.83
Heart	57.08	56.43	15.75	15.07
Kidney	55.03	54.27	17.45	16.47
Liver	44.91	44.42	11.46	11.16
Muscle	54.44	54.16	11.69	11,29
Dry skin	38,53	38,03	11,41	10.82
Small intestine	56.66	56.03	24.04	21.94

It can be seen that the wave impinges with more power on the left side of the human body model, due to the fact that the source is located in this direction and direct wave has more power than the reflected waves. The morphology of the human body also influences the way in which power is distributed through space. There is an important difference between one meter height, where is the waist of the body and the height of 1.6 m where the wave hits the head, given by the consideration of different material parameters embedded in the model. It can also be seen that the election of the frequency plays a key role in the characterization of the radio propagation channel, with a higher estimation of received power for lower frequencies.

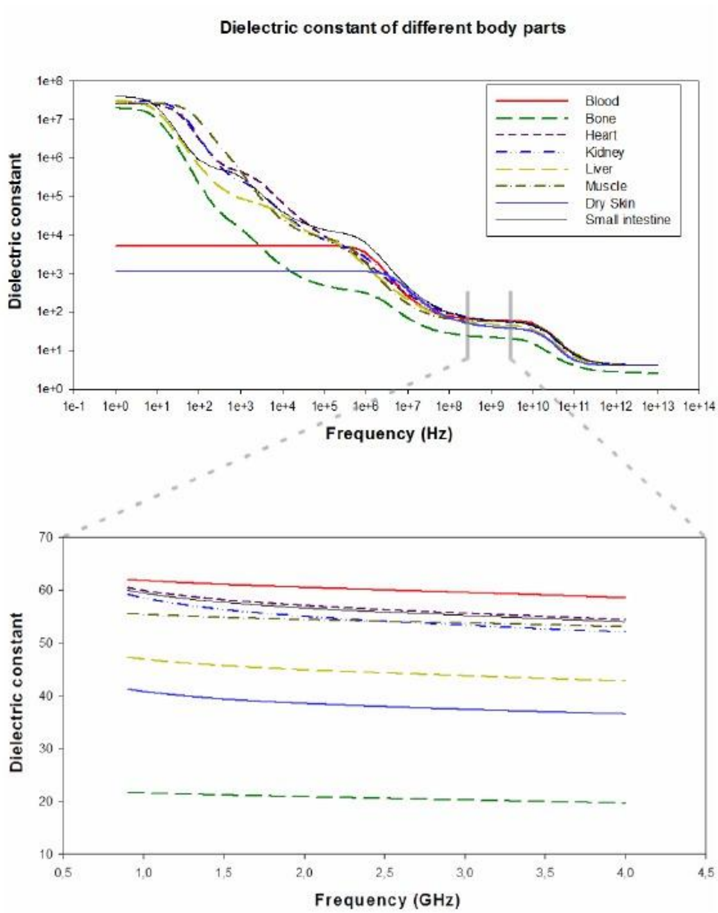

Figure 4. Estimation obtained of the dielectric constant shift versus frequency for different parts of the human body model developed.

In order to analyze more thoroughly the data, Figure 10 represents the estimation of received power for the high resolution zone with the Y axis value of 0.275 m and Z dimension ranging for different heights, between 0.4 m to 2 m.

As expected, the estimated received power decreases with higher frequencies. Such behavior is dictated by the radio propagation characteristic and the frequency response of dispersive materials presenting in the human body model. It is also observed strong degree of variability in the received power. This is due to the fact that the fundamental propagation phenomena in an indoor environment is multipath propagation, which is characterized by the temporal

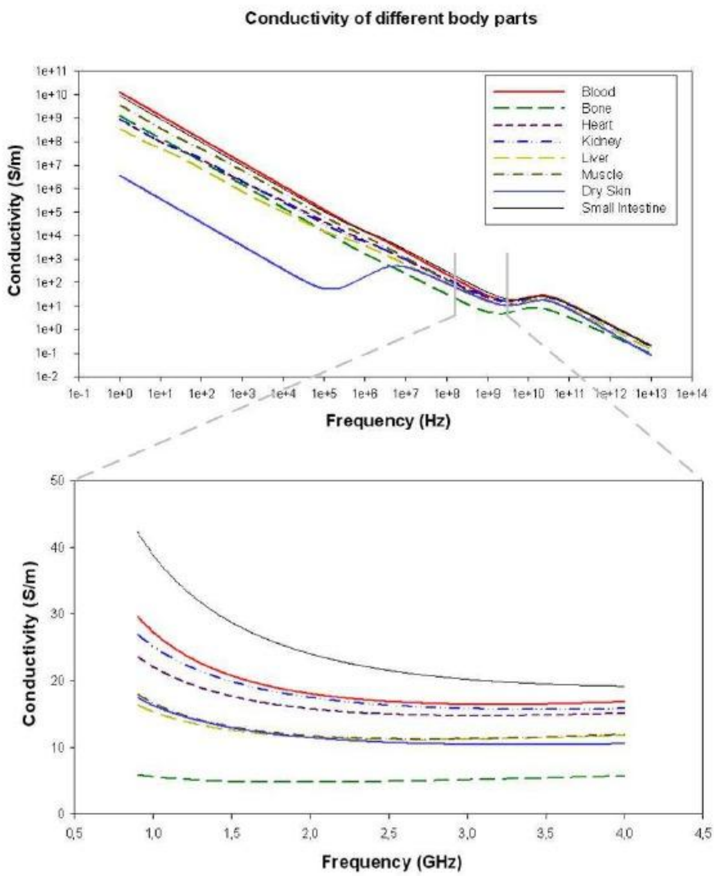

Figure 5. Estimation obtained of the Conductivity shift versus frequency for different parts of the human body model developed.

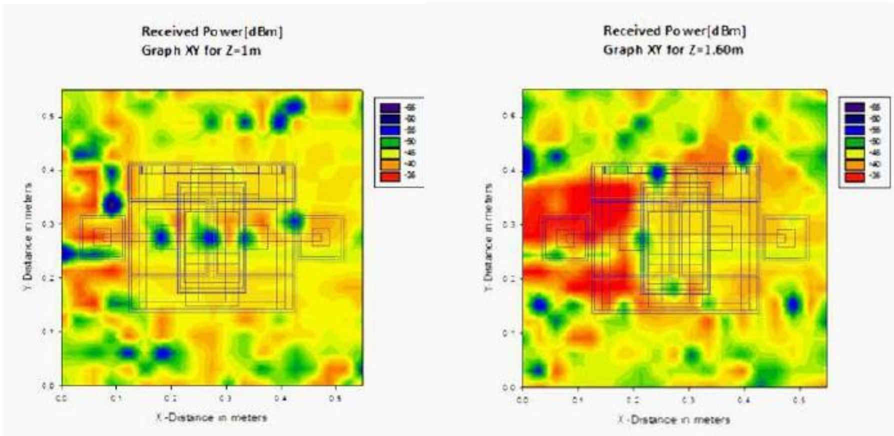

Figure 6. Estimation of Received power for two different heights in the XY plane with the human body model overhead (2 GHz).

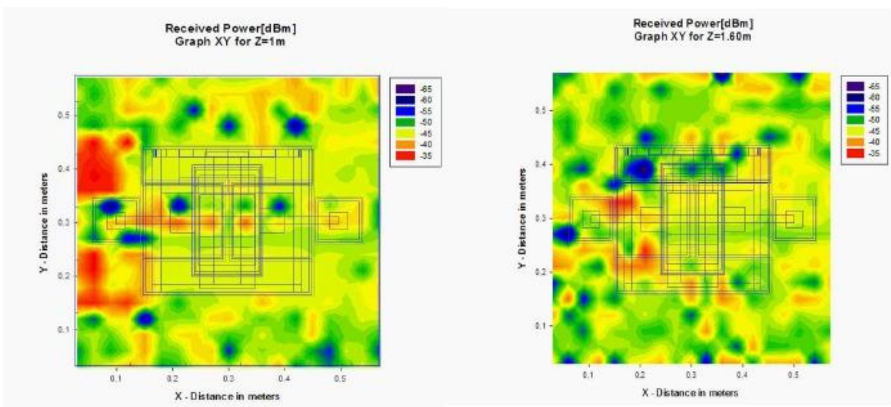

Figure 7. Estimation of Received power for two different heights in the XY plane with the human body model overhead (2.4 GHz).

dispersion of the signal and the frequency dispersion due to temporal variations of the received amplitude.

3. MEASUREMENT RESULTS

To validate previous predictions, measurements in a real scenario with a real person have been performed. For this purpose, the ground floor of the research center Jerónimo de Ayanz of the Public University of Navarre has served as the set up for the experiments, whose geometry is shown in Figure 11. All materials within the scenario have been taking into account for the simulation, like concrete for the walls and columns, glass for the windows, metal for the elevator and wood for the doors, considering their dielectric constant and conductivity for the given frequency of operation. The scenario dimensions are 19.6 m × 13.6 m × 3.8 m.

The wideband measurements were performed with 100 MHz bandwidth at 2.4 GHz frequency. The transceivers are from Texas Instruments, specifically the CC2530 that is a true system-on-chip (SoC) solution for IEEE 802.15.4 ZigBee. The radiation pattern of the transceivers is omnidirectional with linear polarization and 0.82 dBi gain. Measurements have been made with the transmitter fixed at the point XY (8.51 m, 11.29 m) with a 0.60 m height. The transmitter power is 4.5 dBm.

In order to perform the measurements, three different positions of

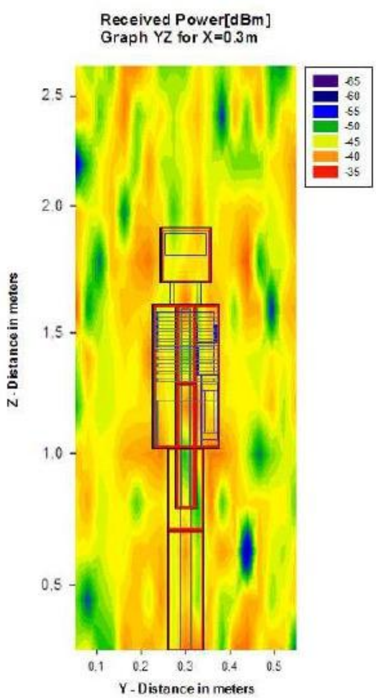

Figure 8. Estimation of received power for the plane YZ (2 GHz).

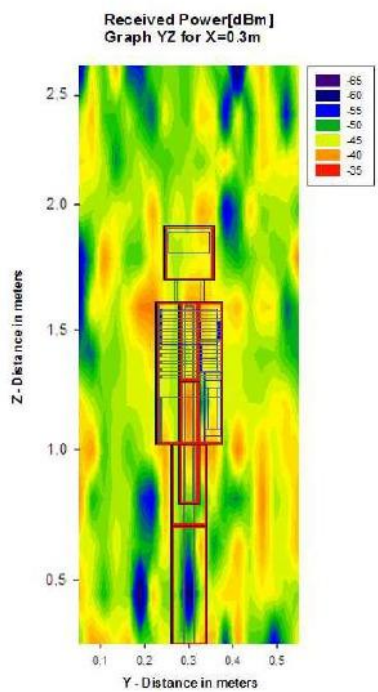

Figure 9. Estimation of received power for the plane YZ (2.4 GHz).

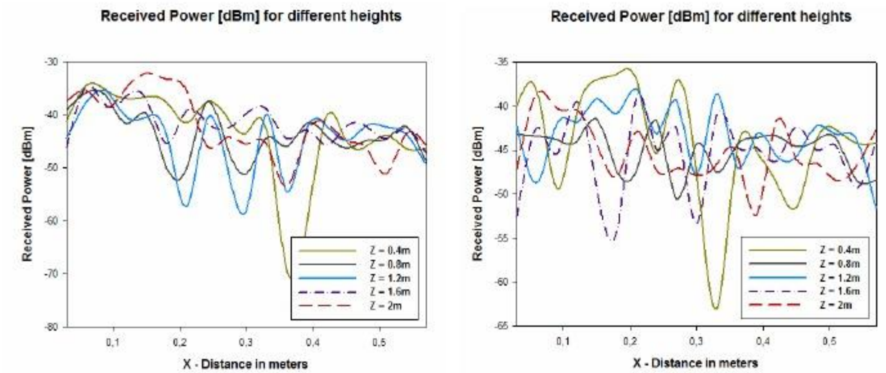

(a) (b)

Figure 10. Estimation of received power for different heights within the simulation scenario. (a) $f = 2\,\text{GHz}$, (b) $f = 2.4\,\text{GHz}$.

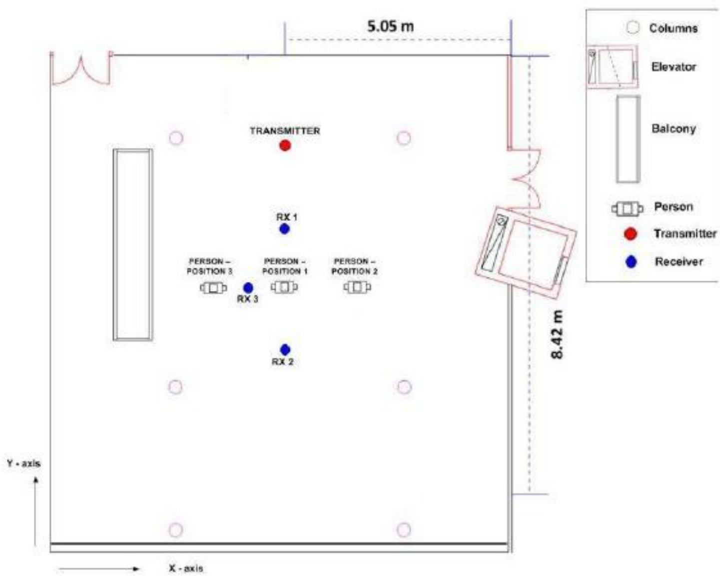

Figure 11. Scenario considered for the measurements.

the person have been considered, which are depicted in Figure 11 and correspond to the points XY (6.07 m, 7.69 m), (8.61 m, 7.69 m) and (11.23 m, 7.69 m). For each position of the person in the considered scenario, nine measurements have been performed. The first three measurements correspond to the three points of reception shown in Figure 11. The election of these points is designed to assess the

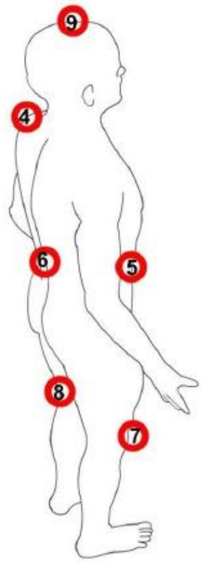

Figure 12. Measurement points in the real person.

influence of the human body in different points of the environment, taking into account free space between transmitter and receiver for RX 1 and the presence of a person between them for RX 2. The remaining six measurement points agree with the points represented in Figure 12 for different parts of the human body. In the process of measures, the person was always looking ahead to the transmitter. To evaluate the influence of the different organs which make up the human body in the environment, different points of the front of the human body have been chosen, specifically, the abdomen and the right knee and the shoulder and back knee for the rear of the body.

A portable spectrum analyzer from Agilent (N9912 Field Fox) has been used for the experiments. The measurement time at each point was 60 seconds, and the power value represented by each point was the higher peak of power shown by the spectrum analyzer for the considered bandwidth (*MaxHold* function in the spectrum analyzer of Agilent).

Figure 13 shows the comparison between simulation and measurements, exhibiting good agreement with a mean error around 2 dB for all cases. The differences are mainly due to approximations made in simulation. It is also important to consider the fast fading, which is a relevant effect in indoor environments that occur due to the multipath components which are very significant. It is observed that

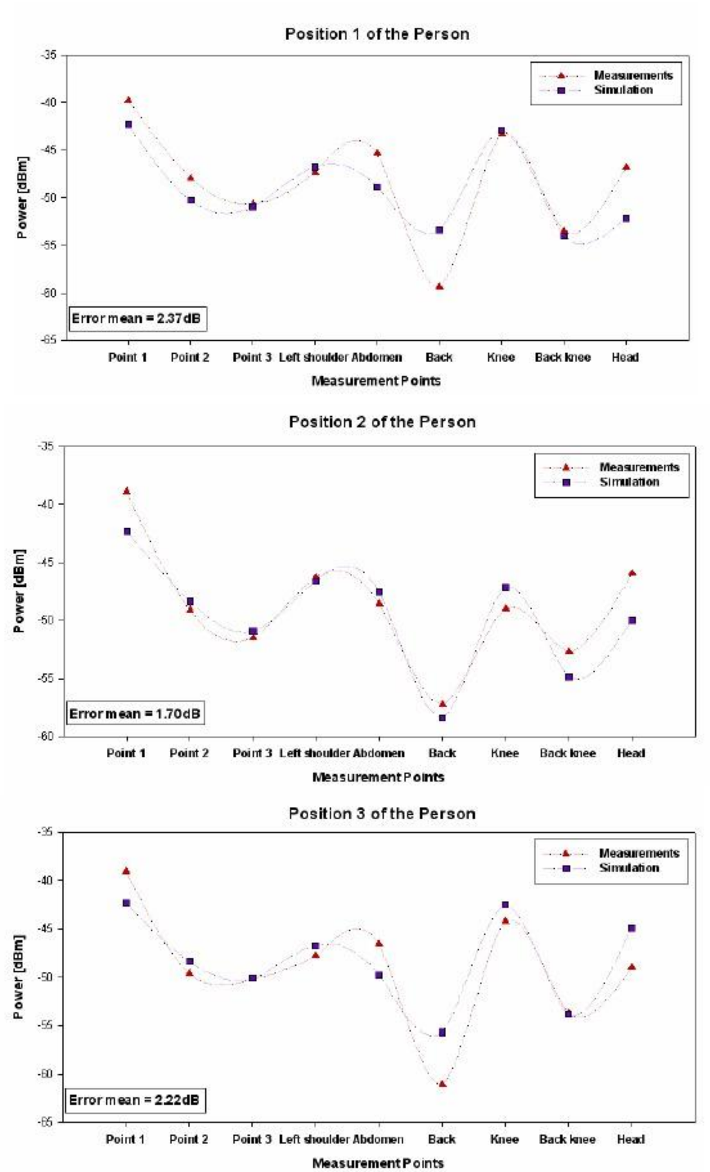

Figure 13. Comparison simulation versus measurements for different positions of the person.

there are no significant differences between the three positions of the person in terms of power levels received at each position. Nevertheless, for the three cases, received power level is lower for the position 2 of the receiver (RX 2 of Figure 11) due to the presence of the human body between the transmitter and the receiver. It is also shown that the influence of the person for point 3 (RX 3 of Figure 11) is also considerable, comparing with the position 1 (RX 1 of Figure 11) which is facing the transmitter. It is also perceived that the received power levels for the measurement points of the front part of the body, specifically the abdomen and the knee (Point 5 and 7 of Figure 12), are higher values than the rear part, back and back knee (Point 6 and 8 of Figure 12). This is due to the human body penetration losses which are present in the radio electric path. It is observed that these losses are bigger in the abdomen part of the body than in the knee, due to the higher volume of mass as well as to the higher volume of liquid content in the first case.

4. CONCLUSIONS

In this work, the influence of a human body in dosimetry evaluations has been analyzed. A simplified human body model, including the dispersive nature of material parameters of internal organs has been implemented. The use of deterministic 3D ray launching algorithm implemented in-house combined with the human body model allows the performance of dosimetric estimations for indoor scenarios considering the electromagnetic sources and the presence of several persons in the same scenario. Simulations as well as measurement results have been presented, showing good agreement between them. This simulation approximation can be used in order to assess the influence of electromagnetic exposure due to the combined operation of several wireless systems in indoor heterogeneous scenarios, with results given for the full extent of such simulation scenario.

ACKNOWLEDGMENT

The authors wish to acknowledge the financial support of project FASTER, funded by the Consejería de Industria, Gobierno de Navarra.

REFERENCES

1. World Health Organizations, "Framework for developing health-based EMF standards," EMF Project, http://www.who.int/peh-emf/standards/framework/en/index.html.
2. http://www.icnirp.org/documents/emfgdl.pdf.

3. *Biologic Effects and Health Hazards of Microwave Radiation*, Polish Medical Publication, Warsaw, 1974.
4. Wang, J. and O. Fujiwara, "Uncertainty evaluation of dosimetry due to plastic holder for restraining small animal in Vivo near field exposure setup," *IEEE Trans. on EM Comp.*, Vol. 46, No. 2, May 2004.
5. Wang, J. and O. Fujiwara, "Dosimetricanalysis of a small animal locally exposed to near fields by electrically short antennas," *International Symposium Electromagnetic Compatibility*, 1999.
6. Zhadobov, M., R. Sauleau, Y. L. Dréam, S. I. Alekseev, and M. C. Ziskin, "Numerical and experimental millimeter-wave dosimetry for in vitro experiments," *IEEE Trans. on Microwave Theory and Techniques*, Vol. 56, No. 12, Dec. 2008.
7. Tinniswood, A. D. and C. M. Furse, "Computations of SAR distributionsfor two anatomically-basedmodels of the human head using CAD files of commercial telephonesand the parallelized FDTD code," *1997 Digest IEEE Antennas and Propagation Society International Symposium*, 1997.
8. Nagaoka, T. and S. Watanabe, "GPU-based 3D-FDTD computation for electromagnetic field dosimetry," *IEEE Africon 2011 — The Falls Resort and Conference Centre*, 13–15, Livingstone, Zambia, Sep. 2011.
9. Tailor, H. C., J. W. Hand, and R. W. Lau, "FDTD modelling for microwave dosimetry and thermcigraphy," *IEEE Colloquium on Application of Microwaves in Medicine*, Feb. 28, 2005.
10. Angulo, L. D., S. G. Garcia, M. F. Pantoja, C. C. Sanchez, and R. G. Martín, "Improving the SAR distribution in petri-dish cell cultures," *Journal of Electromagnetic Waves and Applications*, Vol. 24, Nos. 5–6, 815–826, 2010.
11. Sato, R., H. Sato, and H. Shirai, "A SBR algorithm for simple indoor propagation estimation," Faculty of Education and Human Sciences, Niigata University, Faculty of Science and Engineering, Chuo University, Tokyo, Japan, 2005.
12. Shirai, H., R. Sato, and K. Otoi, "Electromagnetic wave propagation estimation by 3-D SBR method," *International Conference on Electromagnetics in Advanced Applications, ICEAA*, Sep. 2007.
13. Ling, F., Q. Sheng, and J. M. Jin, "Hybrid MoM/SBR and FEM/SBR methods for scattering by large bodies with inhomogeneous protrusions," *1997 Digest IEEE Antennas and Propagation Society International Symposium*, Jul. 13–18, 1997.
14. Durney, C. H., M. F. Iskander, H. Massoudi, and C. C. Johnson,

"An empirical formula for broad-band SAR calculations of prolate spheroidal models of humans and animal," *IEEE Trans. on Microwave Theory and Techniques*, Vol. 27, No. 8, Aug. 1979.

15. Poljak, K. and N. Kovac, "The electromagnetic-thermal analysis of human exposure to radio base station antennas," *17 International Conference on Applied Electromagnetics and Communications*, Dubrovnik, Croatia, Oct. 1–3, 2003.
16. Ruan, F., T. Duglosz, D. Shi, and Y. Gao, "Cylinder model of human body impedance based on proximity effect," *3rd IEEE International Symposium on Microwave, Antenna, Propagation and EMC Technologies for Wireless Communications*, Oct. 27–29, 2009.
17. Ghaddar, M., L. Talbi, and T. A. Denidni, "Human body modelling for prediction of effect of people on indoor propagation channel," *Electronics Letters*, Vol. 40, No. 25, Dec. 9, 2004.
18. Uzunoglu, N. K. and E. A. Angelikas, "Field distributions in a three-layer prolate spheroidal human body model for a loop antenna irradiation," *IEEE Trans. on Antennas and Propagation*, Vol. 35, No. 10, Oct. 1987.
19. Reivomen, S., T. Keikko, J. Isokorpi, and L. Korpinen, "Internal currents in a human body with spheroidal model in 400 kv switching substation," *IEEE Symposium on High Voltage Engineering*, No. 461, Aug. 21–22, 1999.
20. Durney, C. H., C. C. Johnson, and H. Massoudi, "Long-wavelength analysis of plane wave irradiation of a prolate spheroid model of man," *IEEE Trans. on Microwave Theory and Techniques*, Feb. 1975.
21. Canseven, A. G. and N. Seyhan, "Ellipsoid models for human and guinea pigs exposed to magnetic fields," *IEEE International Symposium on Electromagnetic Compatibility*, May 11–16, 2003.
22. Özen, S., S. Çömlekçi, and O. Çerezci', "An evaluation for coupling of human to magnetic fields in human ellipsoidal models with frequency up to 100 kHz," *Proceedings of the 23rd Annual IEEE EMBS International Conference*, 25–28, Oct. 2001.
23. Massoudi, H., C. H. Durney, and C. C. Johson, "Long-wavelength electromagnetic absorption in ellipsoidal model man and animals," *IEEE Trans. on Microwave Theory and Techniques*, Vol. 25, No. 1, Jan. 1977.
24. Surda, J., E. Cocherova, and O. Ondracek, "Tissue parameters influence on the microwave energy absorption in biological objects," *14th Conference on Microwave Techniques*, 1–4, 2008.

25. Nagaoka, T. and S. Watanabe, "Development of anatomically realistic whole-body models of children and their use in electromagnetic dosimetry," *Cairo International Biomedical Engineering Conference*, 2008.
26. Dawson, T. W. and M. A. Stuchly, "High-resolution organ dosimetry for human exposure to low-frequency magnetic fields," *IEEE Transactions on Magnetics*, Vol. 34, No. 3, May 1998.
27. Nagaoka, T. and S. Watanabe, "Japanese voxel-based computational models and their applications for electromagnetic dosimetry," *XXXth URSI General Assembly and Scientific Symposium*, 2011.
28. Chuang, H. R. and W. T. Chen, "Computer simulation of the human-body effects on a circular-loop-wire antenna for radio-pager communications at 152, 280, and 400 MHz," *IEEE Trans. Veh. Tech.*, Vol. 46, No. 3, Aug. 1997.
29. Fujii, K., M. Takahashi, K. Ito, and N. Inagaki, "Study on the electric field distributions around whole body model with a wearable device using the human body as a transmission channel," *First European Conference on Antennas and Propagation*, 2006.
30. Chuang, H. R., "Numerical computation of fat layer effects on microwave near-field radiation to the abdomen of a full-scale human body model," *IEEE Trans. on Microwave Theory and Techniques*, Vol. 45, No. 1, Jan. 1997.
31. Lazzi, G. and O. P. Gandhi, "Realistically tilted and truncated anatomically based models of the human head for dosimetry of mobile telephones," *IEEE Transactions on Electromagnetic Compatibility*, Vol. 39, No. 1, Feb. 1997.
32. Fahs, H., A. Hadjem, S. Lanteri, J. Wiart, and M. F. Wong, "Calculation of the SAR induced in head tissues using a high-order DGTD method and triangulated geometrical models," *IEEE Trans. on Antennas and Propagation*, Vol. 59, No. 12, Dec. 2011.
33. Iskander, M. F., H. Massoudi, C. H. Durney, and S. J. Allen, "Measurements of the RF power absorption in spheroidal human and animal phantoms exposed to the near field of a dipole source," *IEEE Transactions on Biomedical Engineering*, Vol. 28, No. 3, Mar. 1981.
34. Commens, M. and L. Williams, "Strategies for effective use of EM simulation for SAR," *International Symposium on Electromagnetic Compatibility*, 2004.
35. Seidel, S. Y. and T. S. Rappaport, "Site-specific propagation prediction for wireless in building personal communication system design," *IEEE Trans. Veh. Tech.*, Vol. 43, 879–891, Nov. 1994.

36. Durney, C. H., "Electromagnetic dosimetry for models of humans and animals: A review of theoretical and numerical techniques," *Proceedings of the IEEE*, Vol. 68, No. 1, Jan. 1980.
37. Bernardi, P., M. Cavagnoro, S. Pisa, and E. Piuzzi, "Specific absorption rate and temperatura increases in the head of celular-phone user," *IEEE Trans. on Microwave Theory and Techniques*, Vol. 48, No. 7, 1118–1126, Jul. 2000.
38. Gritsenko, N. V., A. Y. Bijamov, A. Razmadze, L. S. Shoshiashvili, and R. S. Zaridze, "Simulation of the thermal effects in the human head due to the RF exposure," *Proceedings of the 9th International Seminar/Workshop on Direct and Inverse Problems of Electromagnetic and Acoustic Wave Theory, 2004, DIPED 2004*, 87–89, Oct. 2004.
39. Salford, L. G., A. Brun, J. Eberhardt, L. Malmgren, and B. Persson, "Electromagnetic field-induced permeability of the blood-brain barrier shown by immunohistochemical methods," *Interaction Mechanism of Low-Level Electromagnetic Fields in Living Systems*, B. Nordén and C. Ramel, eds., 251–258, Oxford University Press, Oxford, 1992.
40. Salford, L. G., A. Brun, K. Sturesson, J. L. Eberhardt, and B. R. R. Persson, "Permeability of the blood-brain-barrier induced by 915 MHz electromagnetic-radiation, continuous wave and modulated at 8, 16, 50 and 200 Hz," *Microscopy Research and Technique*, Vol. 27, No. 6, 535–542, 1994.
41. Lee, S.-H., "A photon modeling method for the characterization of indoor optical wireless communication," *Progress In Electromagnetics Research*, Vol. 92, 121–136, 2009.
42. Lee, D. J. Y. and W. C. Y. Lee, "Propagation prediction in and through buildings," *IEEE Trans. Veh. Tech.*, Vol. 49, No. 5, 1529–1533, 2000.
43. Tan, S. Y. and H. S. Tan, "A microcellular communications propagation model based on the uniform theory of diffraction and multiple image theory," *IEEE Trans. on Antennas and Propagation*, Vol. 44, No. 10, 1317–1326, 1996.
44. Kanatas, A. G., I. D. Kountouris, G. B. Kostaras, and P. Constantinou, "A UTD propagation model in urban microcellular environments," *IEEE Trans. Veh. Tech.*, Vol. 46, No. 1, 185–193, 1997.
45. Dimitriou, A. G. and G. D. Sergiadis, "Architectural features and urban propagation," *IEEE Trans. on Antennas and Propagation*, Vol. 54, No. 3, 774–784, 2006.
46. Franceschetti, M., J. Bruck, and L. J. Schulman, "A random

walk model of wave propagation," *IEEE Trans. on Antennas and Propagation*, Vol. 52, No. 5, 1304–1317, 2004.

47. Blas Prieto, J., R. M. Lorenzo Toledo, P. Fernández Reguero, E. J. Abril, A. Bahillo Martínez, S. Mazuelas Franco, and D. Bullido, "A new metric to analyze propagation models," *Progress In Electromagnetics Research*, Vol. 91, 101–121, 2009.
48. Schuster, J. W. and R. J. Luebbers, "Comparison of GTD and FDTD predictions for UHF radio wave propagation in a simple outdoor urban environment," *IEEE Antennas and Propagation Society International Symposium*, Vol. 3, 2022–2025, 1997.
49. Iskander, M. F. and Z. Yun, "Propagation prediction models for wireless communications systems," *IEEE Trans. on Microwave Theory and Techniques*, Vol. 50, 662–673, 2002.
50. Kouyoumjian, R. G. and P. H. Pathak, "A uniform theory of diffraction for an edge in a perfectly conducting surface," *Proceedings of the IEEE*, Vol. 62, No. 4, 1448–1462, 1974.
51. Seidel, S. Y. and T. S. Rappaport, "Site-specific propagation prediction for wireless in-building personal communication system design," *IEEE Trans. Veh. Tech.*, Vol. 43, No. 4, 879–891, 1994.
52. Luebbers, R. J., "A heuristic UTD slope diffraction coefficient for rough lossy wedges," *IEEE Trans. on Antennas and Propagation*, Vol. 36, No. 2, Feb. 1989.
53. Gabriel, C., "Compilation of the dielectric properties of body tissues at RF and microwave frequencies," Tech. Rep. AL/OE-TR-1996–0037, Brooks Air Force, Brooks AFB, TX, 1996.
54. Sánchez-Hernández, D. A., *High Frequency Electromagnetic Dosimetry*, Artech House, Inc., 2009.

3.5 [Paper D] Analysis and Description of HOLTIN Service Provision for AECG monitoring in Complex Indoor Environments

Since the human body is composed by water in a high percentage its absorption rate is high and it should be considered in all simulations where a person is involved. The study of WBAN systems is a paradigmatic case where its consideration is compulsory, taking into account that by definition human body will be a part of the system.

HOLTIN is a novel e-Health service for monitoring and electrocardiogram (ECG) analysis developed by LQTAI (Life Quality Technology Accessibility and Innovation) [LQTA 14]. Combining this tool with other monitoring system a complete patient tracking system could be developed based on WBAN and Bluetooth [MARTI 09].

In [Paper E] the HOLTIN device is studied considering the influence of a person through the use of the human body model in an indoor complex scenario. Therefore, the main features of this publication are:

- The influence of the human body in the performance of real WBAN system based on Bluetooth is studied and furthermore, it is shown how the power distribution changes when a person is introduced as a consequence of its high absorption rate.
- Given the RSSI values obtained from HOLTIN system, simulation results are compared and a good accuracy is obtained demonstrating again the suitability of the selected simulation method.
- The low resolution configuration is used, demonstrating that when the inner portion of the human body is not going to be studied, the consideration of skin dielectric properties are sufficient and a good approach to reality is obtained.

PAPER D

Sensors ***13(4)*** *(2013)*

Analysis and Description of HOLTIN Service Provision for AECG monitoring in Complex Indoor Environments

Santiago Led, Leire Azpilicueta, Erik Aguirre, Miguel Martinez de Espronceda, Luis Serrano and Francisco Falcone

Sensors **2013**, *13*, 4947-4960; doi:10.3390/s130404947

OPEN ACCESS

sensors

ISSN 1424-8220
www.mdpi.com/journal/sensors

Article

Analysis and Description of HOLTIN Service Provision for AECG monitoring in Complex Indoor Environments

Santiago Led, Leire Azpilicueta, Erik Aguirre, Miguel Martínez de Espronceda, Luis Serrano and Francisco Falcone *

Electrical and Electronic Engineering Department, Edificio Los Tejos, 1 Planta, UPNA, Pamplona, 31006 Navarra, Spain; E-Mails: santiago.led@unavarra.es (S.L.); leyre.azpilicueta@unavarra.es (L.A.); aguirrerik@gmail.com (E.A.); miguel.martinezdeespronceda@unavarra.es (M.M.E.); lserrano@unavarra.es (L.S.)

* Author to whom correspondence should be addressed; E-Mail: francisco.falcone@unavarra.es; Tel.: +34-616-929-743; Fax: +34-948-167-20.

Received: 11 March 2013; in revised form: 9 April 2013 / Accepted: 10 April 2013 / Published: 12 April 2013

Abstract: In this work, a novel ambulatory ECG monitoring device developed in-house called HOLTIN is analyzed when operating in complex indoor scenarios. The HOLTIN system is described, from the technological platform level to its functional model. In addition, by using in-house 3D ray launching simulation code, the wireless channel behavior, which enables ubiquitous operation, is performed. The effect of human body presence is taken into account by a novel simplified model embedded within the 3D Ray Launching code. Simulation as well as measurement results are presented, showing good agreement. These results may aid in the adequate deployment of this novel device to automate conventional medical processes, increasing the coverage radius and optimizing energy consumption.

Keywords: ambulatory electrocardiogram; U-Health; HOLTIN; 3D ray launching

1. Introduction

Ambulatory Electrocardiogram (AECG) monitoring services are among the most relevant Ubiquitous Health (U-Health) applications due to the high prevalence of cardiovascular disease [1,2]. There are a large number of cardiac pathologies, but healthcare specialists show great interest in diagnosing some of them. Of particular interest are pathologies whose symptoms are palpitations, dizziness and sporadic syncopes, *i.e.*, cardiac conditions that require long-term monitoring systems in order to be diagnosed. The detection of arrhythmic cardiac events (ventricular tachycardia, atrial fibrillation, bradycardia, *etc.*) allows the cardiologist to provide the patient with the most appropiate treatment, usually based on drug administration or pacemaker/ICD implantation. Furthermore, cardiac event detection may be really useful in order to diagnose relevant chronic diseases, such as heart failure. Thus, AECG services that allow continuous and long-term patient monitoring are required to improve diagnosis and treatment of cardivascular diseases. In this sense, cardiologists are very interested in new U-Health services aimed at monitoring of patients that suffer from paroxysmal arrhythmias and sporadic syncopes. Besides from the clinical utility, these new healthcare services should be capable of improving the patient's quality of life [3].

Nowadays, AECG monitoring services used by cardiologists are based on conventional Holter devices and implantable loop recorder systems [4–6]. These systems fulfill the patient's cardiac activity monitoring and allow detecting several types of arrhythmias. However, these systems also present several limitations such as the duration of the monitoring session due to a limited storage capacity and reduced ergonomics. These features may be improved using U-Health approaches. Thus, the new so-called HOLTIN (for INtelligent HOLTer) service has been designed in-house at the Public University of Navarre [7,8]. This service is focused on monitoring of patients that are at low risk, and whose sympthoms are sporadic arrhythmias (ventricular tachycardia, bradycardia), asystolic pauses, and syncopes. Moreover, essential aspects related to development and delivery of U-Health services have been considered in HOLTIN system such as: service goals definition, healthcare professional requirements, technology selection, clinical evaluation, satisfaction of patients, *etc*. A comparative analysis between the HOLTIN service and conventional AECG monitoring systems is shown in Table 1.

Table 1. Comparison of Features and Functionalities found in AECG systems.

	HOLTIN	**Holter Monitor**	**Insertable Loop Recorder (Reveal® Plus)**
Implantable	No	No	Yes
Ergonomics	+++	+	+++++
Automatic detection of cardiac events	Yes	No	Yes
Patient notification of syncopes	Yes	No	Yes
Service autonomy	Medical prescription Rechargeable battery 5 days (60 seconds cardiac events detected every 10 minutes)	24/48 hours	14 months
Storage type Storage capacity	Event recorder +++	Continuous ECG+	Event recorder +
Configurability	Yes	No	Yes
Availability of diagnostic data	Fast	Slow	Medium
Cost	++	+	+++++
Clinical utility	++++	++	+++++

The remainder of this paper is organized as follows: Section 2 describes the implementation of the HOLTIN service, with special emphasis on the wearable ECG device used by the patient and its functional model. Section 3 presents the behaviour of the device modeled in a complex radioelectric environment by means of in-house 3D ray launching code coupled to a simplified human body model. Section 4 presents the measurement results obtained in order to validate the performance of the ECG device, as well as to perform a radioplanning analysis of the optimal location within the operational environment of the HOLTIN system. Finally, Section 5 lists the conclusions of the work.

2. Description of the HOLTIN Service's Architecture

The HOLTIN platform consists of a wearable ECG device, a smartphone (data Gateway), a server (data management center) and a set of connecting monitoring clients. The platform shows highly innovative features such as multisystem wireless connectivity, wearable technology and health data management. Besides this technological platform, the service includes a functional model with a detailed description of system operation according to healthcare professional requirements. The elements of the HOLTIN platform are the following (see Figure 1):

- *Wearable ECG recorder*. This device is placed on patient's chest through several disposable wet electrodes avoiding the uncomfortable connection leads used in convetional AECG systems (Figure 2). It performs the ECG waveform (lead II) acquisition, detection of outstanding arrhythmias and its transmission to a Smartphone device via Bluetooth® v2.1 + EDR wireless technology. The ECG recorder has been designed in a small form factor, very low power consumption and high ergonomics in order to improve the patient comfort level.
- *Smartphone*. This gateway device is implemented in a commercial Smartphone with customized service software based on Android 4.0 OS. It receives the acquired ECG data and transmits it to the data management center. This transmission is perfomed via 3G mobile telecomunications technology and a propietary application-level protocol based on commands. The Smartphone also performs tasks related to functional operation of HOLTIN service: mainly ECG recorder association, malfunction warnings, and operation messages.
- *Management center*. This system receives the patients' ECG data and stores it in a database together with demographic information. In this way, healthcare professionals diagnose the patients using online personalized tools.

It is worthwhile to pay attention to several features of the system. On one hand, the use of a wearable acquisition device provides the patient with high comfort and mobility levels. On other hand, the use of a short-range wireless technology for communication between ECG recorder and Smartphone device increases the overall functionality in terms of mobility and battery lifetime. In this sense, Bluetooth® technology provides the whole technical features (frequency hopping spread spectrum, low power consumption, authentication and data encryption, flow control, *etc*.) for being used in this type of system. Although Bluetooth® technology provides a recent release (Bluetooth® v4.0) for very low power applications, the HOLTIN platform uses the Bluetooth® v2.1 + EDR version. It provides a sufficient data rate (up to 3 Mbps) for sending cardiac information with reduced average power consumption and short transmission times; this feature is really important in event recorder devices.

Figure 1. Overview of the HOLTIN platform.

Figure 2. Image of the HOLTIN wearable ECG recorder (**a**) placed on a patient chest (**b**) detail of the device.

(**a**) (**b**)

From a functional point of view, the HOLTIN service consists of an extremely elaborated functional model that includes the whole requirements of healthcare staff and takes into account the technological solutions that make possible to fulfill them. ECG recorder performs several operational tasks:

- During the start-up process, the device performs a real time ECG monitoring of the patient in order to allow the healthcare specialist configuring and verify its correct operation. Once the ECG recorder has been initialized, the continuous cardiac event detection process is started.
- The ECG recorder is able to detect and store the patient's outstanding cardiac information in two different operation modes: automatic detection and patient notification. In automatic operation, the device performs a continuous ECG signal processing and detects automatically specific types of cardiac arrhythmic events based on the patient's heart rhythm and several diagnostic settings established by the cardiologist. The device is able to acquire the outstanding data associated to following cardiac events: ventricular tachycardia, bradycardia, and asystolic pauses. In patient notification mode, the patient can trigger a manual event recording process using the Smartphone when he/she feels some arrhythmia symptom (syncope, dizziness). These notifications cause the establishment of Bluetooth® communication between the ECG recorder and the Smartphone for exchanging specific application data.
- The device stores temporarily all detected/notified cardiac events. When storage capacity reaches a specific configurable level, the ECG recorder establishes wireless communication

with the Smartphone device in order to transmit all the ECG information. In this way, a permanent Bluetooth® communication with high power requirements is avoided and no relevant patient information is lost.

Although the ECG recorder provides high storage capacity, a reliable wireless communication link is required due to the fact some patients suffer frequent cardiac event episodes. Moreover, this reliability should guarantee the correct operation of the HOLTIN service, independently of the environment where the device is used by the patient. Indoor monitoring is surely one the most regular environments. Thus, it compulsory to model the wireless behavior of the ECG recorder in indoor complex scenarios, where unexpected degradation of the wireless links, especially in the HOLTIN-Smartphone short range communication can occur mainly due to energy absorption and strong multipath components.

3. Channel Modeling

Once the HOLTIN ECG recorder has been described, it will be tested to foresee potential limitations derived from the wireless link. For an efficient setup of an indoor wireless sensors network the knowledge of path loss and field coverage in the wireless channel is essential. The behavior of the radio channel in indoor scenarios [9,10] is not a trivial issue and heavily depends of the complexity of the environment. The occurrence of shading effects fundamentally due multipath components but also of phenomenon like reflection, refraction, diffraction and diffuse scattering among others, makes the study of the associated radio channel a complex task. The most straightforward way is to estimate the path loss by means of empirical models based on analytical expressions derived from non-linear regression of the scenario under analysis (*i.e.*, COST 231, Walfish-Bertoni, *etc*.). These models give rapid results, but don´t take into account site-specific features related with topology and morphology, require on site calibration and therefore are prone to higher mean error levels as well as higher standard deviation. As an alternative, numerical techniques have been proposed that can fully or partially capture the site-specific features. These methods include ray launching and ray tracing algorithms (based on geometrical approximations) or full wave simulation techniques, such as finite-difference-time-domain (FDTD) [11,12] and pure-full-wave time and frequency domain approaches [13]. These methods are precise, but are time consuming due to inherent computational complexity. As a mid-point, methods based on geometrical optics, for radio planning calculations with strong diffractive elements, offer a reasonable trade-off between precision and required calculation time [14–16].

In this work, the estimation of wireless coverage of an indoor scenario has been obtained by means of a 3D ray-launching method for simulating radio wave propagation and penetration. The aim of this analysis is the assessment of the wireless channel between the HOLTIN ECG device and the gateway in terms of capacity and coverage. The algorithm has been implemented in-house at UPNA, based on the Matlab™ programming environment. It is based on Geometrical Optics (GO) and Geometrical Theory of Diffraction (GTD). To complement the GO theory, the diffracted rays are introduced with the GTD and its uniform extension, the Uniform GTD (UTD). The purpose of these rays is to remove field discontinuities and to introduce proper field corrections, especially in the zero-field regions predicted by GO. The principle of the ray launching method is to consider a bundle of transmitted rays that may or may not reach the receiver. The number of rays considered and the distance from the transmitter to the receiver location determines the available spatial resolution and, hence, the accuracy of the model. A finite sample of the possible directions of the propagation from the transmitter is chosen and a ray is launched for each such direction. If a ray hits and object, then a reflecting ray and a refracting ray are generated. If a ray hits a wedge, then a family of diffracting rays is generated, as represented in Figure 3. Rays are launched from the transmitter at an elevation angle θ and with an azimuth angle Φ, as defined in the usual coordinate system. Antenna patterns are incorporated to include the effects of antenna beamwidth in both azimuth and elevation. The material properties for all the elements within the scenario are also taking into account, given the dielectric constant and permittivity at the frequency range of operation of the system under analysis.

Figure 3. Principle of operation of the 3D ray launching method implemented in-house to perform indoor coverage analysis.

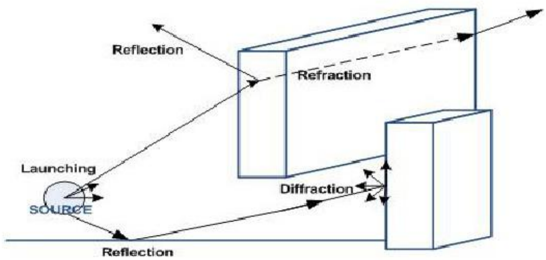

A plane electromagnetic wave falling to the planar interface between two regular semi-infinite media 1 and 2 gives rise to two plane waves: reflected and transmitted (or refracted). According to the Snell's law [17], the reflection coefficient $R^{\perp}$ and transmission coefficient $T^{\perp}$ are calculated by:

$$T^{\perp} = \frac{E_t^{\perp}}{E_i^{\perp}} = \frac{2\eta_2 \cos(\Psi_i)}{\eta_2 \cos(\Psi_i) + \eta_1 \cos(\Psi_t)} \tag{1}$$

$$R^{\perp} = \frac{E_r^{\perp}}{E_i^{\perp}} = \frac{\eta_2 \cos(\Psi_i) - \eta_1 \cos(\Psi_t)}{\eta_2 \cos(\Psi_i) + \eta_1 \cos(\Psi_t)} \tag{2}$$

where $\eta_1 = 120\pi/\sqrt{\varepsilon_{r1}}, \eta_2 = 120\pi/\sqrt{\varepsilon_{r2}}$ and Ψ_i, Ψ_r and Ψ_t are the incident, reflected and transmitted angles respectively.

Once the parameters of transmission T and reflection R are calculated, and the angle of incidence Ψ_i and Ψ_t, the new angles (θ_r, ϕ_r) of the reflected wave and (θ_t, ϕ_t) of the transmitted wave can be calculated. The finite conductivity two-dimensional diffraction coefficients are given by [18,19] as:

$$D^{\|\perp} = \frac{-e^{(-j\pi/4)}}{2n\sqrt{2\pi k}} \left\{ \begin{array}{l} \cot g(\frac{\pi + (\Phi_2 - \Phi_1)}{2n}) F(kLa^{+}(\Phi_2 - \Phi_1)) \\ + \cot g(\frac{\pi - (\Phi_2 - \Phi_1)}{2n}) F(kLa^{-}(\Phi_2 - \Phi_1)) \\ + R_0^{\|\perp} \cot g(\frac{\pi - (\Phi_2 + \Phi_1)}{2n}) F(kLa^{-}(\Phi_2 + \Phi_1)) \\ + R_n^{\|\perp} \cot g(\frac{\pi + (\Phi_2 + \Phi_1)}{2n}) F(kLa^{+}(\Phi_2 + \Phi_1)) \end{array} \right\} \tag{3}$$

where $n\pi$ is the wedge angle, F, L and $a\pm$ are defined in [18], $R_{0,n}$ are the reflection coefficients for the appropriate polarization for the 0 face or n face, respectively. The Φ_2 and Φ_1 angles in Equation (3) are depicted in Figure 4.

Figure 4. Geometry for wedge diffraction coefficients.

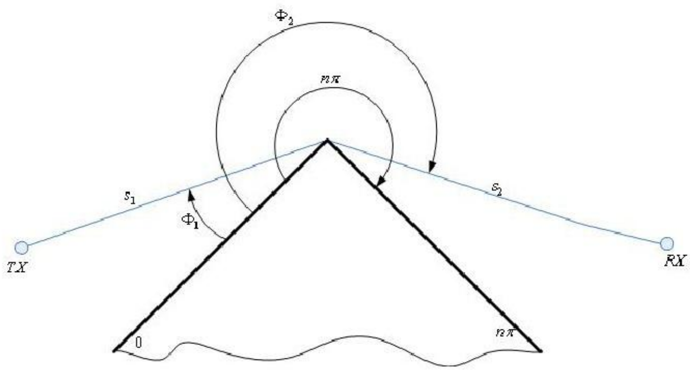

4. Results and Discussion

4.1. 3D Ray Launching Simulation Results

Simulations and measurements have been performed in a room of the Jerónimo de Ayanz Communications Research Center of the Public University of Navarre.

The considered scenario, depicted in Figure 5, could be considered as a typical indoor room of a patient's house. It is a complex environment composed of different types of walls (concrete, plywood, *etc*.) and a variety of different furniture (metallic cupboards, tables, chairs, computers, *etc*.) heavily affected by signal degradation due to multipath components. Simulations and measurements have been performed for the HOLTIN transmitter device with a person carrying the transmitter in his chest and afterwards, the device by itself without human body effect.

Figure 5. Image of R&D Communications Center laboratory N° 2, in which simulation and measurement results of operation of the HOLTIN system have been performed

Within the considered indoor scenario, several radiofrequency sources can be placed, in which wireless power is converted into a finite number of rays launched within a solid angle. Parameters such as frequency of operation, radiation diagram of the antennas, number of reflections, separation angle between rays and cuboid dimensions can be fixed. A schematic view of the indoor scenario is shown in Figure 6(a).

Figure 6. (**a**) R&D Communication's Center laboratory N°2, proposed for deterministic radio channel simulation; (**b**) Detail of the simplified human body model, with the different organs that are embedded within it.

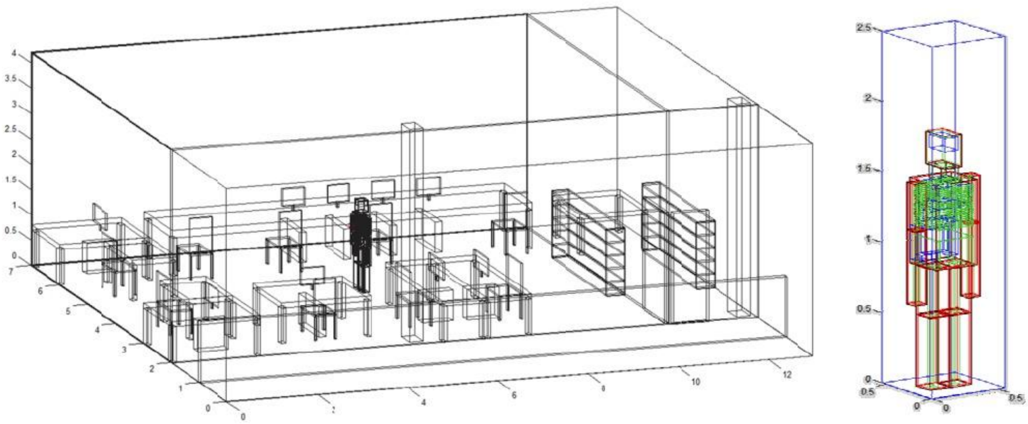

(**a**) (**b**)

In order to fully account for the effect of the presence of patients in the device operation, a simplified human body model has been specifically developed for this 3D ray launching code [20]. This model implements the basic organs considering their frequency dispersive material characteristics, following a Cole-Cole model, in order to analyze their influence on the environment. Figure 6(b) shows a detail of the simplified human body model, which has been performed with the greatest detail as possible, taking into account part such as bones, internal organs, muscles, blood and skin, all with their respective values of dielectric constant and conductivity parameterized to the given frequency range. The human body model has been parameterized in such a way that body proportions (*i.e.*, relative dimensions between head, limbs and torso) are maintained for any given height of the person that is needed to be modeled. The combination of a simplified human body model with an efficient simulation technique enables to assess the impact of wireless systems within the complete scenario under analysis.

Two simulations have been performed for the considered scenario to assess the influence of the presence of a person in the environment, as well as to verify the performance of the HOLTIN transmitter device. The transmitter antenna of the HOLTIN device has an omnidirectional radiation pattern with 1.89 dBi gain. The first simulation was with a simplified human body model located at the center of the room, with the HOLTIN transmitter device placed on the chest of the person. After that, the same simulation has been performed without the human body model. The parameters used for both simulations are the shown in Table 2.

Table 2. Parameters considered for the deterministic technique of ray launching.

Frequency	2.44 GHz
Transmitter power	0 dBm
Transmitter Antenna gain	1.89 dBi
Receiver Antenna gain	0.82 dBi
Horizontal plane angle resolution ($\Delta\Phi$)	1°
Vertical plane angle resolution ($\Delta\theta$)	1°
Reflections	5
Cuboids resolution	3 cm × 3 cm × 3 cm

Figure 7 shows the bidimensional distribution of received power for both cases, with and without the human body model in the indoor scenario with the transmitter location fixed at the point with coordinates (5.67 m, 4.67 m, 1.30 m), which correspond with the chest of the person.

Figure 7. Spatial distribution of Received Power [dBm] for 1.30 meters height in the indoor scenario with (**a**) the presence of a human body model in the center (**b**) without the human body model.

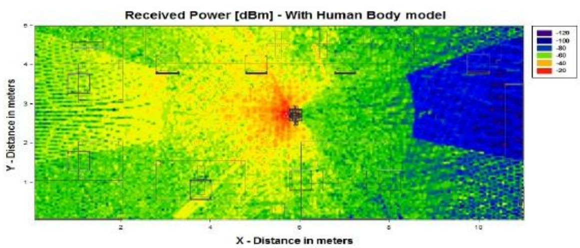

(**a**)

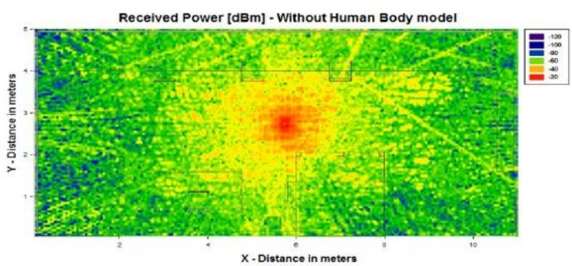

(**b**)

The results obtained clearly show the strong influence in the signal degradation by the presence of the human body in it, as well as the topological and morphological dependence of the received power in relation to the indoor scenario itself. In order to further illustrate the dependence with the human body model and the spatial distribution, Figure 8(a) represents the received power distribution along the X-axis for Y = 4.67 meters, which correspond to the Y-position of the transmitter. It can be seen that with the presence of a person, the received power decreases in the rear location of the person. The strong dips in received power level are due to destructive addition of multipath components, described by statistically by fast fading.

Figure 8. (**a**) Distribution of Power for Y = 4.67 meters along the X-axis for both cases, with and without the presence of a person (**b**) Power-Delay Profile at Point (3.41, 4.67, 1.35) meters in the indoor scenario.

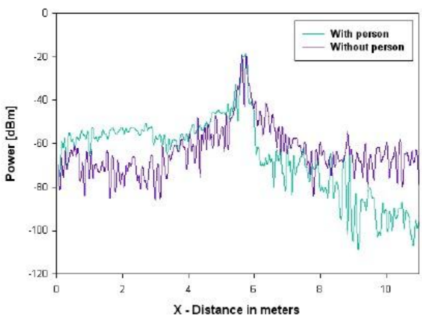

(**a**)

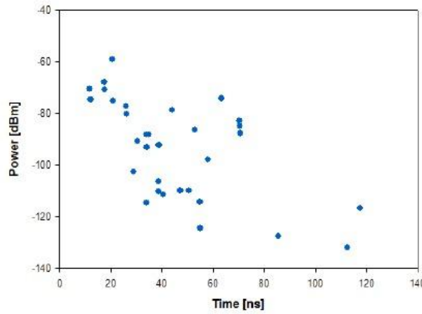

(**b**)

To illustrate the relevance of multipath propagation, which is very significant in this type of scenarios, the power delay profile for a given point of the scenario has been computed and is shown in Figure 8(b). As it can be seen, there are a large number of echoes in the scenario, within a time span of approximately 15 ns to 120 ns, corresponding to trajectories for the rays from 4.5 meters to 36 meters including all the reflections. The large amount of echoes within such distance for the rays is coherent with the complexity of the scenario as well as the material properties at the frequency of operation of the Bluetooth link under analysis.

4.2. Measurement Results

To validate previous predictions, measurements in a real scenario with a real person have been performed. For this purpose, the experimental setup has been deployed in room N°2 of the Jerónimo de Ayanz Research Center of the Public University of Navarre, described in the previous section. The layout of the considered scenario is shown in Figure 9. All materials within the scenario have been taken into account for the simulation, like concrete for the walls and columns, glass for the windows, wood for the doors, considering their dielectric constant and conductivity for the given frequency of operation. Radiochannel measurements have been performed for three different positions, shown in Figure 9, with and without the presence of the human body model, with the transmitter fixed at the coordinate point (5.67 m, 4.67 m, 1.30 m).

Figure 9. Layout of the measurement scenario.

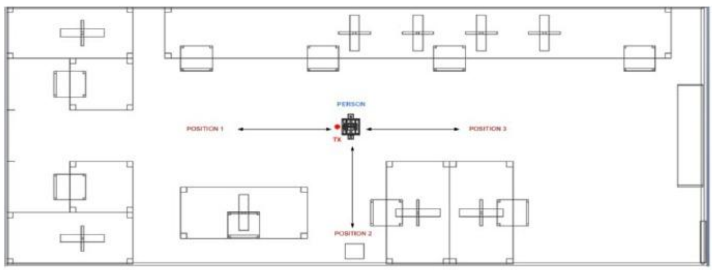

The receiver antenna is from Antenova (Cambridge, United Kingdom), specifically a Picea 2.4 GHz Swivel Antenna, which is a vertical monopole with 0.82 dBi gain. The HOLTIN ECG recorder performs frequency hopping in each Bluetooth® channel randomly to transmit the data. The storage capacity of the device is 32 Mbits, which is equivalent to two hours 75 minutes of continuous ECG signal, considering the sampling frequency of the HOLTIN which is 200 samples/s and 2 Bytes/sample. To visualize the frequency variation with time (and hence, the possible influence of external interference), a spectrogram has been measured in the scenario. Figure 10 shows the measured spectrogram in *Max Hold* mode, for Position 1 in the considered scenario, with the aid of portable spectrum analyzer (Agilent N9912 Field Fox, Agilent Technologies, Santa Clara, CA, USA).

Figure 10. Measured spectrogram in 2.4 GHz ISM band, in the operating region of the Bluetooth wireless link of the HOLTIN-Smartphone connection.

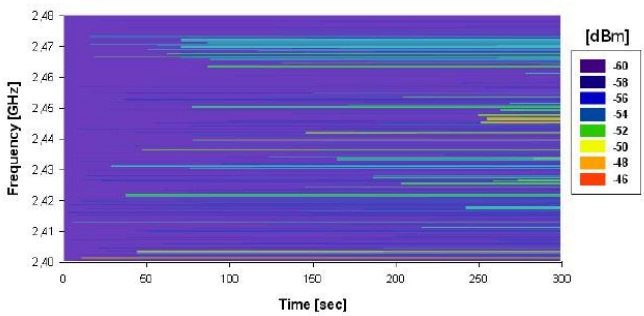

In order to analyze pre-existent interference in the scenario, the spectrum without transmitting any data with the HOLTIN ECG recorder has been measured and is shown in Figure 11(a), where certain levels of interference in some channels of the 2.4 GHz ISM band are observed, which corresponds with a Wifi transmission in the room. Figure 11(b) shows the measured RF power in the same bandwidth with the HOLTIN ECG recorder transmitting data. Measurements have been performed during a continuous period of five minutes. From the measurement results, it can be seen that almost all channels transmit some data along the observed time span and therefore, some channels could be interfered with the pre-existent interfering signals previously shown.

Figure 11. Measured spectrum without transmitting any data with the HOLTIN device (**b**) measured spectrum with the HOLTIN device is transmitting data.

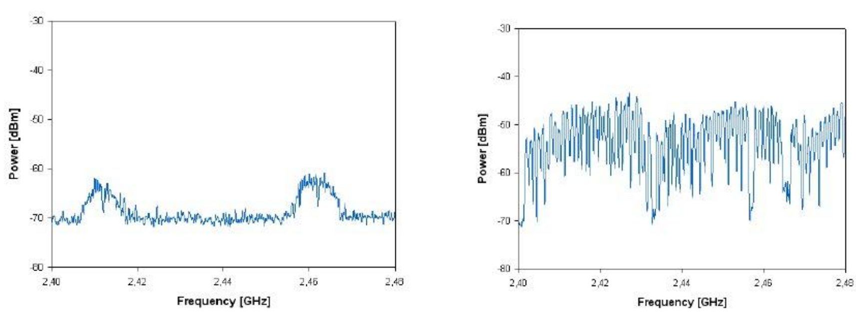

(**a**) (**b**)

Due to the presence of the pre-existent interference levels, the selected frequency of operation for comparison with simulations has been chosen to 2.44 GHz. As stated previously, two simulation calculations have been performed with the 3D ray launching algorithm for this frequency of operation. Figure 12 shows the comparison between simulation and measurements, for the three positions depicted in Figure 9. As it can be seen, they exhibit good agreement with a mean error around 2 dB for both cases. The differences are mainly due to geometrical approximations made in simulation, related with the inherent matrix calculation approach. It is also important to consider fast fading, which is a relevant effect in indoor environments due to multipath components which are very significant. It is observed that with the presence of the person, there are more variations in received power level between Position 1 and Position 3 of Figure 9. This is due to human body penetration losses which are present in the radio electric path and are dependent on human body position, which due to the material consideration embedded in the human body model implemented, is intrinsically considered.

Figure 12. Comparison simulation versus measurements for different positions of the receiver in the considered scenario (**a**) With person (**b**) Without person.

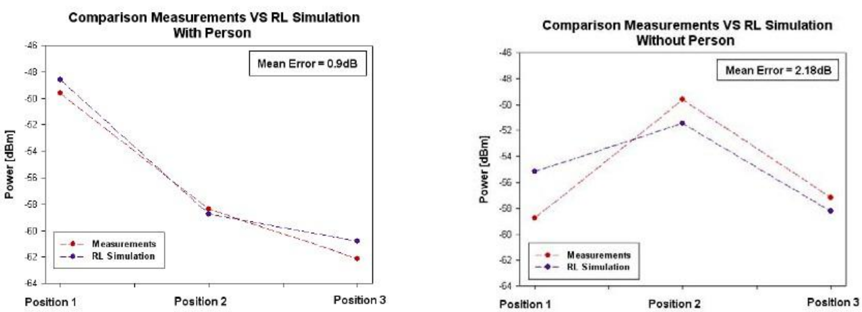

(**a**) (**b**)

Figure 13. Real ECG waveform transmitted by the HOLTIN in the indoor scenario. Visualization in a proprietary software application for the HOLTIN platform has been developed specifically.

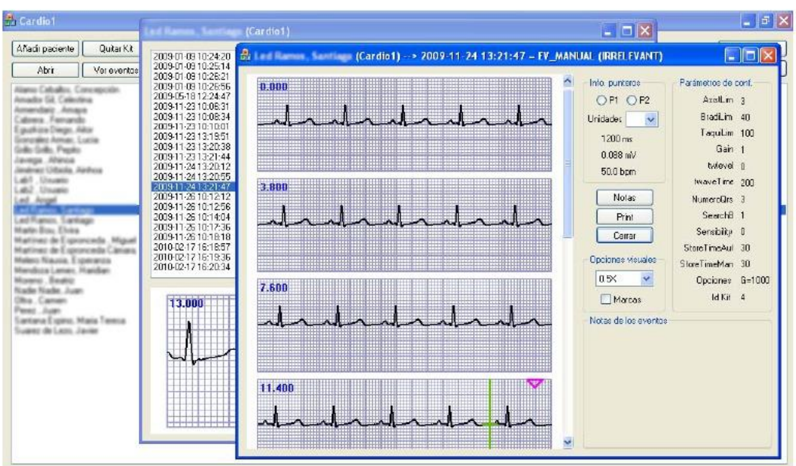

Once the assessment of the wireless channel between the HOLTIN ECG recorder and the gateway has been done in a typical indoor environment, it is shown that link quality is above nominal receiver sensitivity (−90 dBm). Accordingly, the relevant biomedical data is transported along the short range Bluetooth link (from HOLTIN device to the Smartphone acting as a gateway element) and later on via GPRS/UMTS Smartphone connection to the Application Server of the HOLTIN system. The image in Figure 13 is the actual representation that the medical specialist would remotely see, for example, in the hospital while the patient is located in his home.

5. Conclusions

In this paper, a novel platform for AECG monitoring implemented in-house, called HOLTIN, has been described and analyzed in terms of radiochannel quality. Indoor scenarios are one of the most common scenarios in which potential patients may use HOLTIN device for remote medical monitoring. Therefore, the analysis of the overall device's performance is needed. An in-house 3D Ray Launching code has been employed, in combination with an *ad-hoc* simplified human body model in order to estimate radiopropagation losses and hence sensitivity requirements of the short range Bluetooth link between the HOLTIN wearable ECG and a smartphone that acts as a gateway to the final monitoring application. Simulation results show the dependence with topology and morphology of the indoor scenario, in which material absorption as well as strong multipath components are mainly responsible for radio signal losses. Measurement results from the pre-existent signals in the indoor scenario, as well as from the operation of the short range communication link of the HOLTIN device have been performed, showing good agreement with the on-body measurements. Both the position on the human body and the relative transmitter-receiver location are relevant parameters in the overall performance of the device. The application of deterministic radioplanning techniques definitively aid in designing an optimal system layout, minimizing interference as well as reducing energy consumption. As an overall result, the HOLTIN system may represent a new step in U-Health services, reducing health assistance costs and increasing quality of life of patients.

Acknowledgments

The authors wish to thank the support given under project ENEIDA TEC2010-21563-C02-01, funded by the Ministry of Economy and Competitiveness of Spain.

References

1. World Heart Federation. Available online: http://www.world-heart-federation.org/ (accessed on 7 March 2013).
2. Kario, K.; Yasui, N.; Yokoi, H. Ambulatory blood pressure monitoring for cardiovascular medicine. *IEEE Eng. Med. Biol. Mag.* **2003**, *22*, 81–88.
3. Jayaraman, S. Enhancing the quality of life through wearable technology. *IEEE Eng. Med. Biol. Mag.* **2003**, *22*, 41–48.
4. Philips Healthcare. Available online: http://www.healthcare.philips.com/ (accessed on 7 March 2013).
5. Welch Allyn. Available online: http://www.welchallyn.com/ (accessed on 7 March 2013).

6. Medtronic. Available online: http://www.medtronic.com/ (accessed on 7 March 2013).
7. Led, S.; Fernández, J.; Serrano, L. Design of a wearable device for ECG continuous monitoring using wireless technology. *Conf Proc IEEE Eng Med Biol Soc.* **2004**, *2*, 3318–3321,
8. Led, S.; Serrano, L.; Galarraga, M. Intelligent Holter: A New Wearable Device for ECG Monitoring Using Bluetooth Technology. In Proceedings of European Medical and Biological Engineering Conference EMBEC, Prague, Czech Republic, 20–25 November 2005.
9. Hashemi, H. The indoor radio propagation channel. *Proc. IEEE* **1993**, *81*, 943–968.
10. Fink, J.; Michael, N.; Kushleyev, A.; Kumar, V. Experimental Characterization of Radio Signal Propagation in Indoor Environments with Application to Estimation and Control. In Proceedings of Intelligent Robots and Systems (IROS), St. Louis, MO, USA, 10–15 October 2009.
11. Yun Z.; Iskander M.F.; Zhang Z. A hybrid technique based on combining ray tracing and FDTD methods for site-specific modeling of indoor radio wave propagation. *IEEE Trans. Antennas Propag.* **2000**, *48*, 743–754.
12. Wang, Y.; Chaudhuri, S.K.; Safavi-Naeini, S. An FDTD/Ray tracing analysis method for wave penetration through inhomogeneous walls. *IEEE Trans. Antennas Propag.* **2002**, *50*, 1598–1605.
13. Alighanbari, A.; Sarris, C.D. Rigorous and efficient time-domain modelling of electromagnetic wave propagation and fading statistics in indoor wireless channels. *IEEE Trans. Antennas Propag.* **2007**, *55*, 2373–2381.
14. Tümer, A.E.; Gündüz, M. Energy-efficient and fast data gathering protocols for indoor wireless sensor networks. *Sensors* **2010**, *10*, 8054–8069.
15. Iskander, M.F.; Yun, Z. Propagation prediction models for wireless communications systems. *IEEE Trans. Microw. Theory Tech.* **2002**, *50*, 662–673.
16. Reza, A.W.; Sarker, M.S.; Dimyati, K. A novel integrated mathematical approach of ray-tracing and genetic algorithm for optimizing indoor wireless coverage. *Progress Electromagn. Res.* **2010**, *110*, 147–162.
17. Hristov, H.D. *Fresnel Zones in Wireless Links, Zone Plate Lenses and Antennas*; Artech House: Norwood, MA, USA, 2000.
18. Luebbers, R.J. A heuristic UTD slope diffraction coefficient for rough lossy wedges. *IEEE Trans. Antennas Propag.* **1989**, *37*, 206–211.
19. Luebbers, Raymond J. Comparison of lossy wedge diffraction coefficients with application to mixed path propagation loss prediction. *IEEE Trans. Antennas Propag.* **1988**, *36*, 1031–1034.
20. Aguirre, E.; Arpón, J.; Azpilicueta, L.; de Miguel, S.; Ramos, V.; Falcone, F. Evaluation of electromagnetic dosimetry of wireless systems in complex indoor scenarios with human body interaction. *Progress Electromagn. Res. B* **2012**, *43*, 189–209.

Chapter 4.

Dosimetric estimation of complex scenarios

In this chapter dosimetry is studied simulating different complex scenarios and the existing guidelines which determine maximum exposure levels. Three original contributions are introduced in this chapter: (i) the consideration of a commercial aircraft is obtaining E-field strength values as well as "guideline compliance" maps, (ii) E-field values when a ZigBee system is emitting inside a car comparing then with real values obtained from a dosimeter, (iii) dosimetry estimations using the developed human body model through E-field strength and SAR.

4.1 [Paper E] Estimation of Electromagnetic Dosimetric Values from Non-Ionizing Radiofrequency Fields in an Indoor Commercial Airplane Environment

In spite of the fact that ICNIRP guidelines are only recommendations and as aforementioned each government decides their own legislative regulation for electromagnetic exposure, those recommendations are a good indicative when dosimetric estimations are performed since most of the laws are based on it. In fact, ICNIRP recommendations are widely used in several papers [BORN 09], [QABA 07], [GRAS 12].

As mentioned previously, in [Paper B], an aircraft is a suitable location for dosimetric estimation analysis. In [Paper F] a smaller commercial airplane has been chosen, specifically an Airbus A320. Nevertheless, it can be also considered as a big and complex indoor scenario since it has dimensions of 32.5 x 3.67 x.2.3 m.

In this case the 3D Ray Launching tool is used to calculate Electric field values, converting it from received power with the following formula.

$$\frac{e^2}{120\pi}m^2 \tag{4.1}$$

where P is the received power values in watts, m^2 is the area of the cuboids defined in the simulation and e is the electric field value. This equation an approximation to the received spherical wave:

$$\frac{e^2}{120\pi}\frac{\lambda^2}{4\pi} \tag{4.2}$$

where λ is the wavelength of the transmitted signal. The main features of this contribution can summarized as follows:

- ICNIRP guidelines and their adequacy to the different countries in Europe are studied as well as the different simulation techniques.
- An antenna is situated in the center of the aircraft emitting in two frequencies, 2.4GHz and 5GHz obtaining the E-field distribution through the scenario.
- Not only the ICNIRP thresholds are considered to determine in what parts of the aircraft the limit is surpassed but also IEEE C95.1 thresholds are also taken into account. It is shown that ICNIRP guidelines are more restrictive in both frequencies
- Received limitations are only higher than the limit in the center of the aircraft, when the considered point is in the vicinity to the emitting antenna.

PAPER E

Electromagnetic Biology and Medicine (2013)

Estimation of Electromagnetic Dosimetric Values from Non-Ionizing Radiofrequency Fields in an Indoor Commercial Airplane Environment

Erik Aguirre, Javier Arpón, Leire Azpilicueta, Peio López Iturri, Silvia de Miguel, Victoria Ramos and Francisco Falcone

Artículo E eliminado en cumplimiento de la Ley de Propiedad Intelectual (Real Decreto Legislativo 1/1996, de 12 de abril).

4.2 [Paper F] Analysis of Estimation of Electromagnetic Dosimetric Values from Non-Ionizing Radiofrequency Fields in Conventional Road Vehicle Environments

In [Paper G] the scenario used in [Paper A] is considered for the dosimetric calculation. In this paper a ZigBee system and different mobile technologies (GSM, UMTS) are simulated and measured using not only the FieldFox analyzer but also EME Spy 121 personal dosimeter.

Depending on different factors mobile technologies emit different power and this is considered when the simulations are performed, introducing as a result of this upper as well as lower power thresholds.

With the aim of calculating the received electric field values, formula (4.1) and formula (4.2) have been used for the calculation of E-field extracted from the simulation and spectrum analyzer respectively. The contribution of this paper is summarized as follows:

- Technologies that usually can be operating together inside a car are studied and the obtained E-field maximum values are in all cases far away from the ICNIRP guideline thresholds.
- With the comparison between simulation and measurement results, especially with the values obtained from dosimeter, the suitability of the simulation method as dosimetric estimation tool is proved.

PAPER F

Electromagnetic Biology and Medicine (2014)

Analysis of Estimation of Electromagnetic Dosimetric Values from Non-Ionizing Radiofrequency Fields in Conventional Road Vehicle Environments

Erik Aguirre, Peio López Iturri, Leire Azpilicueta, Silvia de Miguel, Victoria Ramos and Francisco Falcone

Artículo F eliminado en cumplimiento de la Ley de Propiedad Intelectual (Real Decreto Legislativo 1/1996, de 12 de abril).

4.3 [Paper G] Evaluation of Electromagnetic Interference and Exposure Assessment from s-Health Solution based on Wi-Fi Devices

Although the electric field strength is widely used when dosimetry is studied, SAR is the standard indicator to determine the exposure of a person to radioelectric waves and therefore it is considered in most research works. Employing formula (4.1) the absorbed energy by a specific tissue can be calculated starting from the received E-field value.

In this work both, E-field strength and SAR values are considered when a Wi-Fi transceiver is emitting. A Wireless Local Area Network (WLAN) has been chosen since WBANs usually require a higher area network to transmit the received information collected from sensors.

An indoor room has been chosen as the scenario under study, taking into consideration that a wireless device as presented in this work could be operating inside a hospital room or a patient´s home. The main features of this publication are:

- Near field values are measured accurately thanks to the aid of automated system and an E-field probe within an anechoic chamber. Those results exceed the established threshold in the International Electrotechnical Commission Standard of Electromedical Devices.
- However, the values received in far field are far from the threshold established by ICNIRP for the utilized frequency. The electric field estimation has done with measurements and using the 3D RL simulation tool demonstrating once again the accuracy of the tool.
- Two different situations have been considered theoretically, populating the room with people or leaving it empty. The difference is notorious since the E-field values are higher when the human body is introduced. This experiment supports the assumption of the high influence that the human body has in the overall power distribution.
- The influence of the human body is also visible when received power, PDP and Delay spread are compared in the case of empty and populated situations.
- SAR values are calculated in one of the considered human body models, obtaining as a result that the absorbed energy is low according to ICNIRP guidelines.

PAPER G

Biomed Research International (2014)

Evaluation of Electromagnetic Interference and Exposure Assessment from s-Health Solution based on Wi-Fi Devices

Silvia de Miguel-Bilbao, Erik Aguirre, Peio López Iturri, Leire Azpilicueta, José Roldan, Victoria Ramos and Francisco Falcone

Evaluation of Electromagnetic Interference and Exposure Assessment from s-Health Solutions based on Wi-Fi Devices

Silvia de Miguel-Bilbao, Erik Aguirre, Peio Lopez Iturri, Leire Azpilicueta, José Roldán, Victoria Ramos and Francisco Falcone,

[1]Telemedicine and eHealth Research Unit, Health Institute Carlos III, Madrid, Spain
[2]Electrical and Electronic Engineering Dept, Universidad Pública de Navarra, Pamplona, Navarra, Spain
E-mail: sdemiguel@isciii.es, aguirrerik@gmail.com, peio.lopez@unavarra.es, leyre.azpilicueta@unavarra.es, vramos@isciii.es, francisco.falcone@unavarra.es

Abstract: In the last decade the number of wireless devices operating at the frequency band of 2.4 GHz has increased in several settings, such as healthcare, occupational and household. In this work, the emissions from WiFi transceivers applicable to context aware scenarios are analyzed in terms of potential interference and assessment on exposure guideline compliance. Near field measurement results as well as deterministic simulation results on realistic indoor environments are presented, providing insight on the interaction between the WiFi transceiver and implantable/body area network devices as well as other transceivers operating within an indoor environment, exhibiting topological and morphological complexity. By following approaches (near field estimation/deterministic estimation), co-located body situations as well as large indoor emissions can be determined. The results show in general compliance with exposure levels and the impact of overall network deployment, which can be optimized in order to reduce overall interference levels while maximizing system performance.

Index Terms: Wi-Fi devices, electric field, exposure threshold, near field exposure, 3D ray launching code.

I. Introduction

Mobile communication devices have become omnipresent in almost all fields of daily life, including home, health, and labor environments and even the displacements. Since the point of view of the healthcare all these fields of application are not disjoint and are involved in the concept of Smart Health (s-Health). The widespread use of wireless technologies and the great interest in ubiquitous communications, seeking connection anywhere and anytime, has meant the emergence of the concept of s-Health as the results of the natural synergy between mobile health (m-health) and smart cities, from the information and communications technology (ICT) perspective and also from that of individuals and society [1].

In healthcare environment, the introduction of wireless communication systems has promoted the improvement in the efficiency of patient care and health management. One of the scenarios of applicability of wireless communication systems in healthcare environments are the ubiquitous healthcare networks [2] that allow the patient care and the assistance regardless their location.

Body Area Networks (BAN) are used in several healthcare scenarios: ambulances, emergency rooms, operating rooms, postoperative recovery, clinics and even homes. BANs are characterized by the following components: the network nodes are sensors (or telemetry devices) that measure biological parameters and the router that collects information detected by sensors and then transmit it to the control center. Regarding the type of interfaces that form the BAN, are considered the following types: short range interface that connects the telemetry devices (or sensors) with the router or gateway, and wide area networks (WAN) that allow connectivity between the router and the control center. Ideally, seeking greater ubiquity in patient care the network interfaces are wireless.

Typically BAN devices are incorporating Wi-Fi interfaces to communicate with the router, and contain low-powered radiofrequency (RF) transceivers that support wireless local area networks (WLANs). The component of the BAN that acts as a router is provided with a Wi-Fi interface and a WAN interface to route the patient information to the control center. In this context the Wi-Fi devices generally work in proximity to persons, which can lead to an excessive perception of risks related to electromagnetic field (EMF) exposure. Moreover, interference to other devices within this framework which can lead to potential malfunction requires assessment.

This paper deals with the evaluation of the electric field strength levels from Wi-Fi systems, both in situations in which the transceivers are co-located with the body and within a larger indoor environment. A near field measurement procedure is followed in the initial case, whereas a deterministic simulation approach, employing 3D ray launching is employed in the latter case, owing to computational complexity constraints. The emission levels have been obtained in far field and near field conditions in order to test the compliance with the recommended standard to assure the safety of people. The European standards are essentially based on the guidelines formulated by the International Commission on Non-Ionizing Radiation Protection (ICNIRP) a nongovernmental organization, formally recognized by the World Health Organization (WHO), which establish exposure limits by taking into account ascertained health effects.

ICNIRP defines limits that have been established in the great majority of countries in the world. Two classes of guidance are presented [3]: basic restrictions of ICNIRP are derived from the considerations related to established adverse health effects and are given in terms of dosimetric quantities, i.e., induced current density for low frequency and specific absorption rate (SAR) for radio frequency and microwaves. As these quantities cannot be measured outside the body, reference levels are provided for practical exposure assessment to determine whether the basic restrictions are likely to be exceeded. Reference levels are given in terms of radiometric quantities, such as electric and magnetic field strengths. Compliance with the reference levels will ensure compliance with the relevant basic restriction [4]. If the measured or calculated value exceeds the reference level, it does not necessarily imply that the basic restriction will be exceeded. However, whenever a reference level is exceeded it is compulsory to test compliance with the relevant basic restriction and hence, to determine whether additional protective measures are necessary.

Compliance with the present guidelines may not implicitly avoid interferences with, or effects on, medical devices such as metallic prostheses, cardiac pacemakers and defibrillators, and cochlear implants [5]. It is worth noting that interference with pacemakers may occur at levels below the recommended reference levels.

In this context, it is worth noting the new Directive 2013/35/EU of the European Parliament and of the Council of 26 June 2013 on the minimum health and safety requirements regarding the exposure of workers to the risks arising from physical agents. The limit values for exposure to electromagnetic fields, and the levels at which the employer must take action, must now be based on the new, more stringent recommendations of ICNIRP [6].

Within the framework of s-Health, ambient assisted living and other context aware scenarios, the impact of the potentially massive use of wireless transceivers, mainly in Industrial, Scientific and Medical bands must be correctly assessed, in terms of electromagnetic exposure as well as interference emission compliance. The elaboration of new directives such as 2013/35/EU require in depth analysis on the use of such devices.

The paper is structured as follows: Section II will describe the near field measurement setup and results; Section III is devoted to indoor characterization, simulation and measurement; Section IV provides discussion on the results obtained, finally leading to the conclusions.

II. NEAR FIELD CHARACTERIZATION

The first step in the characterization of potential radiated interference from WLAN transceiver elements within a context aware scenario is to analyze near field behavior. Thus, potential impact to implantable devices as well as impact on other elements which form part of a Body Area Network can be determined. Initial measurements were performed with the aid of a DASY5PRO automated system with a coupled E-field probe, within an anechoic chamber, as shown in Fig. 1 [7].

The specific Wi-Fi module was a WiFly GSX 802.11 b/g Wireless LAN Module that operates with the protocol 802.11g, whose maximum allowed power is 10 dBm. A specific architecture to generate traffic from the Wi-Fi module was implemented in order to operate the employed Wi-Fi module, depicted in Fig. 2. Transmission routines of the Wi-Fi module have been programmed with Arduino, and a specific connection is established with an auxiliary Access Point (AP).

The AP is connected to a laptop where specific software controls the traffic received from, and transmitted to, the Wi-Fi module. The AP and the laptop are connected through an Ethernet connection. The control functions of the communication between the module and the AP have been implemented through a Xampp Server, installed in a laptop. The Xampp Server is an independent server platform, which consists on a MySQL database, an Apache web server and interpreters for scripting languages such as PHP. The server allows setting the operating parameters of the AP, receives the data sent by the module, and establishes the connection with the database to store the received data.

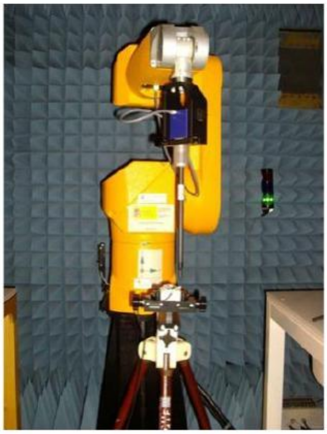

Fig 1. Near Field Measurement setup based on a DASY5PRO near field porbe and a tripod holding the device under test.

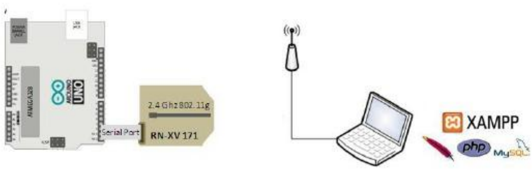

Fig 2. Components of the system to generate the communication from the Wi-Fi module. It consists in a WiFi module connected to an Arduino microcontroller and an Access Point connected to a Xampp application server.

The E-field measurements were taken in the interpolated points belonging to a predefined grid whose dimensions are 8.1cm×8.1cm×4.1cm, with differential distances of dx=1 mm, dy=1 mm, and dz=1 mm. The E-field levels were measured in points of the predefined grid that belong to the three planes: (x, y), (x, z), (y, z).

At 2.4 GHz, the wavelength is about 12.5 cm, which means the reactive near field extends to around 2 cm from the source. Taking into account that the length of the antenna of the Wi-Fi module is 3 cm, the radiating near field extends no further than around 1.44 cm at 2.4 GHz. The minimum distance between the probe and the antenna is 2 mm, so the great majority of the measurements during this work were made in the far field region with respect to the source.

The obtained E-field values were compared with the thresholds of the recommended exposure levels (ICNIRP-98) [3], and the thresholds for the safety and basic performance of the electromedical equipment (IEC 60601-1-2) [8]. Fig. 3 shows the E-field values in the three axes: (x,z), (y,z), and (x,y).

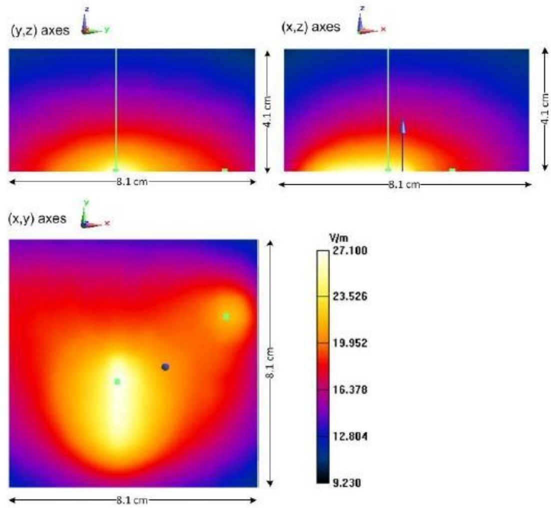

Fig 3. E-field around the tested device in the (x,z), (y,z) and (x,y) planes.

As it can be seen from the results obtained from the near field measurement setup, the highest measured level of the E-field is 27.1 V/m, which exceeded the most restrictive value of 3 V/m that is established in the International Electrotechnical Commission Standard of Electromedical Devices [8]. Therefore, use of the proposed transceiver must be carefully evaluated in terms of maximum allowed transmit power, in order to comply with previously stated guidelines. These near field results will complemented with emission and interference estimation in a conventional indoor scenario in the following section.

III. Deterministic Indoor characterization of WiFi Transceiver Emission

The quantification of the E-field in the proximity of the device is enough for the assessment of EMI or exposure level analysis for many study cases, as the radiated E-field level is required for a complete scenario. These scenarios are usually complex indoor scenarios, where the radio wave propagation is affected by electromagnetic phenomena such as reflection, refraction, diffraction and different effects due to multipath propagation. In order to pursue this issue, an in-house developed 3D ray launching algorithm, based on Geometrical Optics (GO) and Geometrical Theory of Diffraction (GTD), has been used. This method is a midpoint between the analytical methods, which require low computational cost and provide limited accuracy [9-10], and full wave techniques such as FDTD (Finite-Difference Time-Domain) or MoM (Method of Moments), which exhibit precise results but require high computational cost [11], which in many instances renders the approach unfeasable. Therefore, the presented deterministic 3D ray launching method, implemented in-house at the Public University of Navarre, offers an adequate compromise between calculation time and accuracy, and it has been previously validated in several complex indoor scenarios, for different applications such as the analysis of wireless propagation in indoor scenarios [12-13], EMI analysis [14] or electromagnetic dosimetry evaluation [15].

In order to validate the presented in-house ray-launching software within the indoor scenario where the WiFly module will be tested, simulations have been made and radio propagation measurements have been taken. The chosen scenario is a typical office-laboratory environment that can be found at the research building of the Public University of Navarre.

Figure 4 shows the real scenario and its schematic representation considered for simulations. The scenario has the inherent complexity of this kind of indoor environments, with different types of walls (concrete and plywood), chairs, computers, tables, etc. The real dimensions of the objects within the scenario as well as their material properties (dielectric constant and loss tangent) at the frequency range of operation are considered by the 3D ray launching algorithm. Other parameters that have been set for the simulations are summarized in Table I.

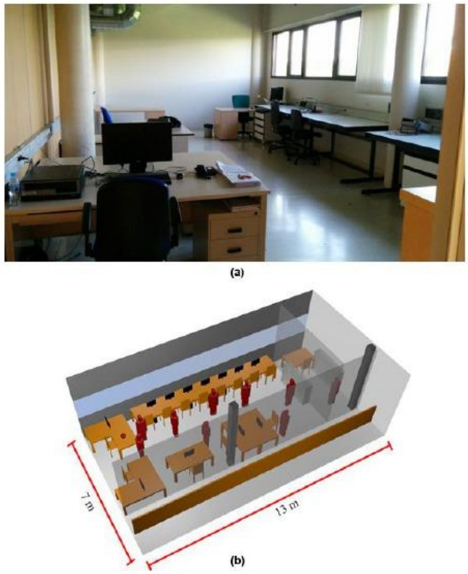

Fig 4. Laboratory of the University Public of Navarre (a) and its 3d representation (b) where the situation of Wifly is depicted (red point) and people have been randomly introduced

TABLE I
RAY LAUNCHING SIMULATION PARAMETERS

Parameter	Value
Frequency of operation	ISM 2.4 GHz
Radiation pattern	Monopole
Transmitted power	10 dBm
Resolution (cuboids size)	10 cm x 10 cm x 10 cm
Maximum reflections permitted	5
Vertical and Horizontal launched rays resolution	1°

Note that the schematic image of the scenario in Fig. 4b is populated with people. However, the simplified human body model is only used in the simulations where the real device is considered and therefore, the following results belong to the empty room.

As the WiFly devices operate at ISM 2.4 GHz band, two different simulations have been launched for two different frequencies within this range: 2.4 GHz and 2.45 GHz. The transmitter has been placed randomly on a table (at coordinates X = 9.94m, Y = 4.5m, at 0.60m high) and the transmitted power has been set to 10 dBm, the maximum value allowed by the motes. In Fig. 5 and Fig. 6 the comparison between the simulation results and measurements for randomly chosen linear paths within the scenario are shown, for 2.4 GHz and 2.45 GHz respectively. Good agreement between measurements and estimated values can be seen, with a mean error of 0.0027 V/m at 2.4 GHz, and 0.0092 V/m at 2.45 GHz.

The measurements taken for the comparison shown in Figure 5 and Figure 6 have been carried out with a RF signal generator with a monopole antenna, emulating a transmitting device, and a N9912 Field Fox portable spectrum analyzer of Agilent, which provided the peak value for each measurement point.

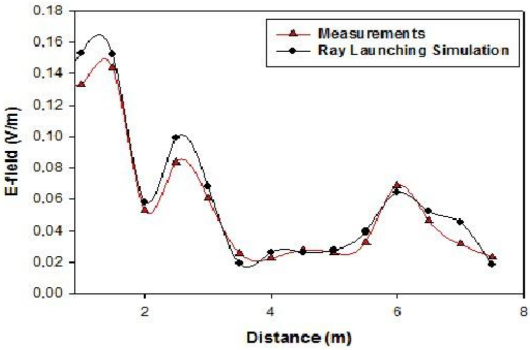

Fig 5. Received electric field values versus distance of measurements and Ray Launching simulation for the first control experiment.

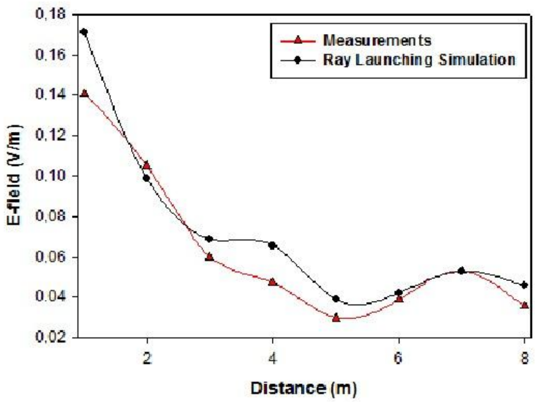

Fig 6. Received electric field values versus distance of measurements and Ray Launching simulation for the second control experiment.

Once the correlation between estimated values and measurements has validated the simulation method within the presented scenario, the study with the WiFly device has been carried out. The red point in Figure 4(b) indicates the location where the device has been placed, emitting with a power of 10dBm. The received power has been measured placing the Fieldfox RF Analyzer every one meter in front of the device.

The device usually needs to communicate with a data base as it can be shown in Figure 3, however, the power contributed by the Access Point is larger than the signal emitted by the wearable device. With the aim of accounting only for the WiFly transceiver, the AP has been switched off and the power received when the device is signaling. Nevertheless, the power emitted by other Wireless networks must be considered. With this aim the spectrogram of the power received in the whole Wi-Fi band has been measured and it is depicted in Figure 7.

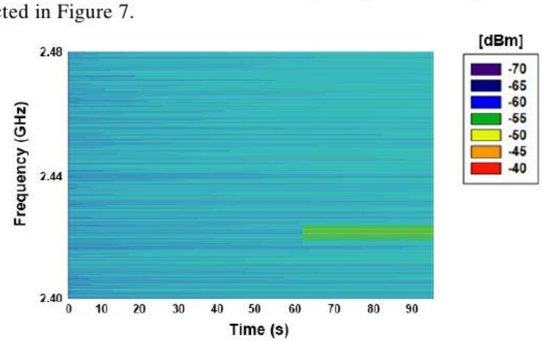

Fig 7. Measured spectrogram when the Wifly transceiver is disconnected (background power spectrum of the scenario).

It is visible that in one of the first channels where Wi-Fi works a device is transmitting. Considering that the Wi-Fi module is programmed for working in the channel 11 (2.462 GHz), this problem is avoided and consequently the measurements can be carried out without interferences.

Since the exposure level and SAR values are directly related with the human body, not only the empty scenario has been considered in simulation, but also people have been randomly introduced along the scenario The employed simplified human body model, implemented in house in order for it to be coupled to the 3D ray launching code has been previously tested, exhibiting adequate performance [15,16].

In Figure 8 the comparison between measurements and simulation results is depicted. Note that the introduction of the human body inside the room changes absolutely the received power in the considered points and in fact, the simulation results obtained in this case are far away from the real received power. As expected, the empty scenario results are similar to measures, having only a mean error of 0.002V/m. In any case, both, the measurements and simulation results, comply with the recommendations proposed by ICNIRP, being the maximum allowed level of 61 V/m and 0.05V/m the received electric field level in the worst case.

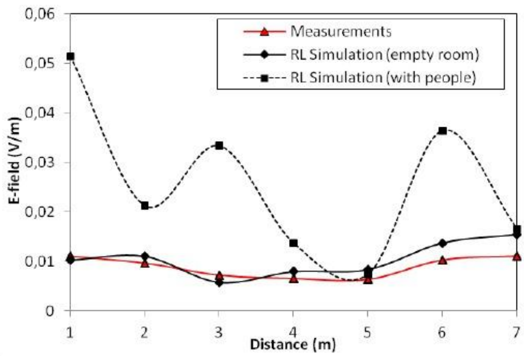

Fig 8. Received electric field values versus distance of measurements and Ray Launching simulation in empty scenario and with people considering Wifly as emitter.

The influence of the human body introduction is more visible in Figure 9 where the receiver power distribution obtained in simulation is depicted for both, the empty scenario and the scenario with people inside it.

In spite of the fact that in figure 8 the simulated points receive more power in the case where people is considered, it is visible that the received power in the global of the scenario is lower when the human body is inside it. This behavior is caused by the high absorption rate of the human body, although the ricochets produced by it could cause higher levels in some areas.

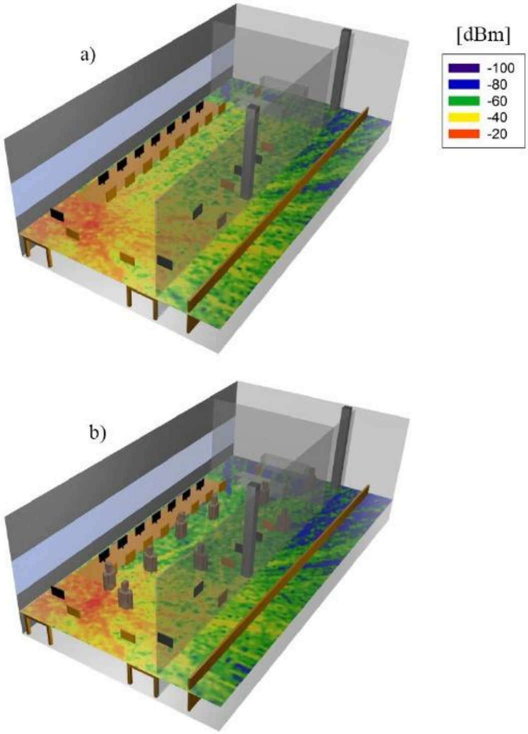

Fig 9. Simulated power distribution when the Wifly device is emitting without people(a) and with people(b).

In order to stress the influence of the presence of human body models, the power difference between the two scenarios is depicted in Figure 10. As it can be seen, significant differences can be observed, due to the inclusion of the human body models, introducing high levels of absorption losses as well as other elements of interaction, such as reflection components which interact with the rest of propagating contributions within the scenario.

In Figure 11 power delay profile estimation is depicted comparing both scenarios. The obtained results shows the number of ricochets which cross one point of the space and as expected not only the number of bounces is lower when there are human bodies inside the scenario, but also they arrive with more power when it is empty. Those results support the aforementioned hypothesis, considering that the human body has absorbed a part of the emitting power which in the other case has reached that point.

In order to provide more insight in the effect of the complex indoor environment the Delay Spread estimation for all points of the scenario in 0.9m height can be shown. In both figures, 11 and 12, it is visible that the considered scenario is a very reflective room. Like it can be seen also in Figure 9, the morphological dependence of the distributed power is also demonstrable. For example, once the electromagnetic wave reach the wall situated around the principal room, the received power decreases and consequently the delay spread times either.

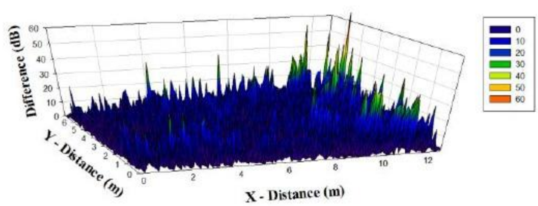

Fig 10. Difference between the received power distribution when the scenario is empty and when people presence is considered

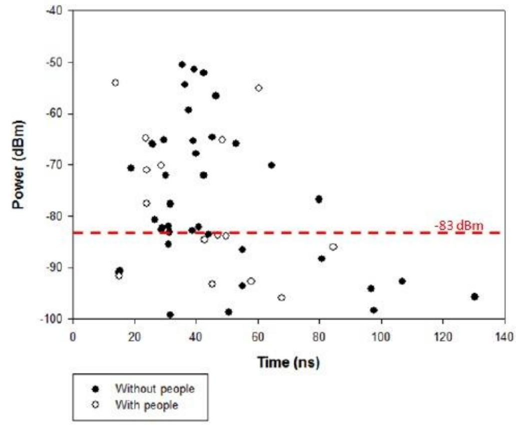

Fig 11. Power delay profile considering empty and full scenario with the sensitivity of the device overexposed.

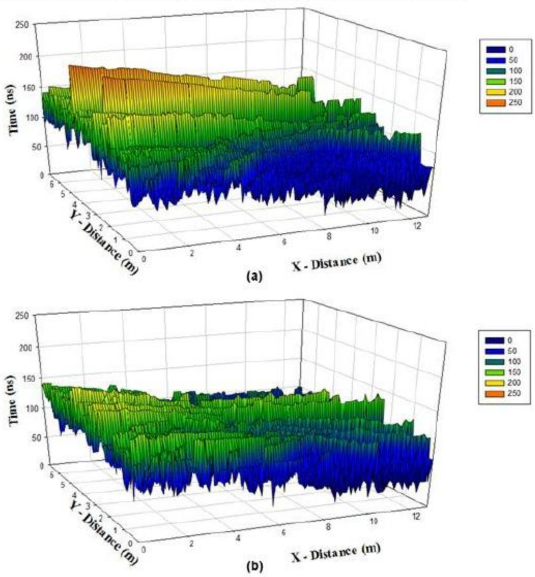

Fig 12. Delay Spread for the scenario without (a) and with people (b).

Finally, is important to stress again upon the influence of the people considered inside the room and the fact that most of the launched rays are absorbed by them decreasing considerably the number of rays and the delay spread time.

Once the measurements and the simulations have been compared and validated, SAR will be calculated utilizing the introduced human body models in the scenario. These values are obtained with the aid of Eq. (1), an approach that has been employed in similar studies previously [17-19]. The skin properties have been considered with a value for conductivity (σ) of 10.18 m/s[15] and a density(ρ) of 1043 Kg/m^3[20].

$$SAR = \frac{\sigma}{\rho}\left|\vec{E}\right|^2 \qquad (1)$$

In Figure 13, SAR values for the person who is nearest to the antenna is depicted. In this case the human body is situated in profile to the antenna and therefore, the highest SAR values are received in the right side of the body. Nevertheless and considering the low electric field and power received in aforementioned experiments, SAR values are far away from the recommendations collected in ICNIRP guidelines [3], reaching 0.00037 W/Kg mean in whole body and being 0.08 W/Kg the limit value which ICNIRP recommends.

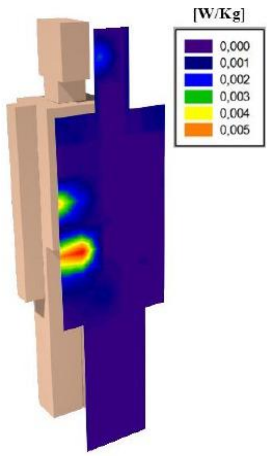

Fig 13.Estimation of received SAR by a human body inside the scenario

IV. Discussion

The objective of this study is to quantify the exposure in the proximity of the device due to the increasing use of Wi-Fi wireless devices that operate in the band of 2.4 GHz, and to analyze the compatibility between equipment and networks in different environments.

For the near field setup, the lower sensitivity limit of the E-field probe (2 V/m) has not been reached. The value of the E-field is 27.1 V/m, this involves that the more restrictive threshold of 3 V/m, established in the International Electrotechnical Commission Standard of Electromedical Devices [8], is exceeded. It is important to consider that the device under test was transmitting information continuously while the measurement campaign have been carried out, which means a duty factor of 100 %. The duty factor is referred as the relation between the time interval of effective transmission and the total duration of the transmission. Usually, Wi-Fi devices do not transmit information continuously; depending on traffic demands, Adaptive Modulation and Coding Schemes and additional Quality of Service constraints. It has been documented that exposure levels of the EM field depend on the data rate at which the information is being transmitted [21]. Regarding the influence of wireless local area networks (WLAN), no electromagnetic interference caused by the WLAN technology was documented by using in vitro testing of pacemakers and implantable cardioverter defibrillators (ICD) [22] In order to avoid medical device malfunction, it is recommend maintaining a distance from the transmitting device greater than 1 m.

It is worth noting that all the field strengths recorded in this study are well below the corresponding ICNIRP reference level of 61 V/m defined for the general public at the working frequency (2.4 GHz) [3].

The near field data is complemented with the analysis provided of interaction of devices and users in an indoor scenario in which complex topo-morphological considerations can be taken into account. Due to the interaction with the elements within the environment, strong multipath components appear which modify the emission levels from the WiFly device. In the case of analyzing emissions not co-located in the human body, estimated field levels are in compliance with exposure guidelines, given by strong attenuation of the propagated signal due mainly to multipath components. Moreover, the location of potential transceivers as well as the distribution of the indoor environment plays a key role in the observable power distributions, as well as the inclusion of adequate human body models.

V. Conclusion

Wireless transceivers will play a fundamental role in the adoption of context aware environment, with application in multiple scenarios such as building automation, ambient assisted living, e-health and s-health environments, among others. In this sense, the characterization of a WiFi transceiver has been performed both in near field as well as in a full indoor complex scenario, emulating the real behavior of this device. The results find application both in electromagnetic exposure as well as in interference assessment.

Measurements have been realized in an anechoic chamber with the measurement system DAISY5PRO that is provided with the possibility of measure the E-field in predefined and programmed positions. Under usual operating conditions the levels of E-field caused by the tested social alarm device do not exceed the limits of personal exposure according to ICNIRP 1998 [3]. In the cases of very small distances from the tested device, the highest level of E-field strength exceeds the more restrictive threshold of 3 V/m that is established in the International Electrotechnical Commission Standard of Electromedical Devices [8]. The measurement conditions are characterized by a duty factor of the transmission of 100 %, while in real conditions the duty factor is considerable lower. In practice the duty factor does not usually exceed 65%, hence providing estimations for the worst case.

The analysis has also been extended to a larger indoor scenario, with the aid of an in-house implemented deterministic 3D ray launching code, in which scenario elements as well as human body models have been included. By following this approach, estimations can be obtained in large complex scenarios maintaining an adequate compromise between accuracy and computational complexity. The results show that emission levels are in principle in compliance with emission level guidelines, although capable of introducing non-desired components which could act as interferers to other systems. Therefore, taking into account the role of wireless transceivers in the advent of context aware scenario, where massive deployments are expected, electromagnetic emission analysis by means of deterministic modelling can aid in providing overall interference and exposure assessment. The proposed technique, tested on a WiFi device can be readily extended to include multiple systems, such as IEEE 802.15 devices or 3G/4G mobile devices.

ACKNOWLEDGMENT

This work has been realized thanks to the valuable cooperation and help offered by the staff of the Radio Frequency Laboratory El Casar of the General Direction of Telecommunications and Information (Spanish Ministry of Industry, Energy, and Tourism).

REFERENCES

[1] A. Solanas, C. Patsakis, M. Conti, I. Vlachos, V. Ramos, F. Falcone, O. Postolache, P. Pérez-Martínez, R. Di Pietro, D. Perrea, A. Martínez-Ballesté. Smart Health: A Context-Aware Health Paradigm within Smart Cities. Technical Report, Universitat Rovira i Virgili, 2013

[2] A. Soomro, D. Cavalcanti, "Opportunities & Challenges using WPAN and WLAN Technologies in Medical Environments," *IEEE Communications Magazine*, vol. 45, no. 2, p. 114-122. Feb 2007.

[3] International Commission on Non-Ionizing Radiation (ICNIRP), "Guidelines for limiting exposure to protection time-varying electric, magnetic and electromagnetic fields (up to 300 GHz)," Health Phys., vol. 74, no. 4, p: 494–522, 1998.

[4] M. Barbiroli, C. Carciofi, D. Guiducci, "Assessment of Population and Occupational Exposure to Wi-Fi Systems: Measurements and Simulations," *IEEE Transactions on Electromagnetic Compatibility*, vol. 53, no. 1, p: 219-228. Feb 2011.

[5] S. de Miguel-Bilbao, M.A. Martín, A. del Pozo, V. Febles, J.A. Hernández, J.C. Fernández de Aldecoa, V. Ramos,, " Analysis of exposure to electromagnetic fields in a healthcare environment: simulation and experimental study, " Health Phys., vol. 105, no. 5, p. S209-S222, 2013.

[6] Directive 2013/35/EU of the European Parliament and Council of 26 June 2013 on the minimum health and safety requirements regarding the exposure of workers to the risks arising from physical agents (electromagnetic fields).

[7] S. de Miguel-Bilbao, J. Roldán, J. García, V. Ramos, J. Fernández, O. J. Suárez, "Assessment of Exposure from Wi-Fi Devices", 9th IEEE International Symposium on Medical Measurement and Applications, Lisbon, Portugal, June 2014

[8] International Electrothecnical Commission (IEC) Standard IEC 60601-1-2 Electromedical devices. 2007.

[9] M. Hata, "Empirical formula for propagation loss in land mobile radio services," *IEEE Transactions on Vehicular Technology*, vol. 29, no. 3, pp. 317-325, 1980.

[10] F. Ikegami, S. Yoshida, T. Takeuchi, M. Umehira, "Propagation factors controlling mean field strength on urban streets," *IEEE Transactions on Antennas and Propagation*, vol. 32, no. 8, pp. 822-829, 1984.

[11] A. Dimitriou, G. Sergiadis, "Architectural features and urban propagation," *IEEE Transactions on Antennas and Propagation*, vol. 54, no. 3, pp. 774-784, 2006.

[12] L. Azpilicueta, F. Falcone, J. J. Astráin, J. Villadangos, I. J. García Zuazola, H. Landaluce, I. Angulo, A. Perallos, "Measurement and modeling of a UHF-RFID system in a metallic closed vehicle," Microwave and Optical Technology Letters, vol. 54, no. 9, pp. 2126-2130, 2012.

[13] J. A. Nazábal, P. Iturri López, L. Azpilicueta, F. Falcone and C. Fernández-Valdivielso, "Performance Analysis of IEEE 802.15.4 Compliant Wireless Devices for Heterogeneous Indoor Home Automation Environments," *International Journal of Antennas and Propagation*, Hindawi Publishing Corporation, 2012.

[14] P. L. Iturri, J. A. Nazábal, L. Azpilicueta, P. Rodriguez, M. Beruete, C. Fernández-Valdivielso, F. Falcone, "Impact of High Power Interference Sources in Planning and Deployment of Wireless Sensor Networks and Devices in the 2.4GHz frequency band in Heterogeneous Environments," *Sensors*, vol. 12, no. 11, pp. 15689-15708, 2012.

[15] E. Aguirre, J. Arpón, L. Azpilicueta, S. de Miguel, V. Ramos and F. Falcone, "Evaluation of electromagnetic dosimetry of wireless systems in complex indoor scenarios within body human interaction," *Progress In Electromagnetics Research B*, vol. 43, pp. 189-209, 2012.

[16] S. Led, L. Azpilicueta, E. Aguirre, M. Martínez de Espronceda, L. Serrano, F. Falcone, "Analysis and Description of HOLTIN Service Provision for AECG monitoring in Complex Indoor Environments," Sensors, 2013, vol. 13, Issue 4, pp. 4947-4960.

[17] D. A. Sánchez-Hernández, High Frequency Electromagnetic Dosimetry, Artech House, Inc., 2009.

[18] B. Loader, A. Gregory, D. Bownds, F. Seifert, " Evaluation of an optical electric field sensor for measurement of specific absorption rate (SAR) during magnetic resonance imaging," *International Symposium on Electromagnetic Compatibility*, p. 1-4. Sept. 2012

[19] K. Kininami, T. Iyama, T. Onishi, S. Uebayashi, "Evaluation of an optical electric field sensor for measurement of specific absorption rate (SAR) during magnetic resonance imaging, " *IEEE Transaction on Electromagnetic Compatibilit*, vol. 50, no. 4, p. 828-836. Nov. 2008.

[20] H. J. Krzywicli, K. S. K. Chinn "Human Body Density and Fat of an Adult Male Population as Measured by Water Displacement," *The American Journal of Clinical Nutrition*, vol. 20, no. 4, p. 305-310. Apr. 1967.

[21] A. Peyman, M. Khalid, C. Calderon, D. Addison, T. Mee, M. Maslanyj, S. Mann, "Assessment of exposure to electromagnetic fields from wireless computer networks (Wi-Fi) in schools; results of laboratory measurements," *Health Phys.,* vol. 100, no. 6, p. 594-612, 2011.

[22] J. L. Tri, J. M. Trusty, D. L. Hayes, "Potential for Personal Digital Assistant interference with implantable cardiac devices," *Mayo Clin Proc* vol. 79, no. 12, p. 1527-1530, 2004

Chapter 5.

Application of the human body model to alternative simulation techniques

The exportation of the human body model to other simulation techniques is studied including one original contribution related with precursors: (i) basic morphology of the human body and its dielectric characteristics are used in another context.

5.1 [Paper H] Evaluation of the Brillouin precursor performance for ultra wide band intra-body technologies

When an ultrawideband (UWB) signal interacts with a dispersive and absorptive material each frequency have a different absorption rate and also travels a different phase velocity[MOHA 12]. As a result of these effects, precursors are defined as the characteristic wave patterns caused by the dispersive nature of the material when the main wave is propagating inside it.

They are usually considered as negative a contribution, nevertheless the advantages of this phenomenon have been considered in several applications, since they become predominant at greater depths instead of the carrier frequency of the signal. Due to this characteristic the main applications are related with imaging and remote sensing [ONG 03], [DAWO 12a], [JIAN 11], [SAFI 09], [DAWO 12b], [LUKO 09].

Forerunners were explained by the first time in 1914 by Sommerfeld and Brillouin [OLSO 11] and in fact high frequency precursor (above resonance) is called Sommerfeld precursor and low frequency precursor (bellow resonance) is known as Brillouin [OUGH 05].

When a precursor is considered in a dispersive medium with a cole-cole behavior, such as a human body, the achieved electromagnetic wave penetration can be useful for imaging purposes. However, when the dosimetry is studied this penetration leads to a heat of internal tissues as it can be concluded from [NAJA 10] where the carrier frequency heats the surface of the water and decays rapidly with tissue depth, but when the precursor is considered, heat distribution is more constant and decays slower. In Figure 5.1 the concept of precursor formation through the human body is depicted.

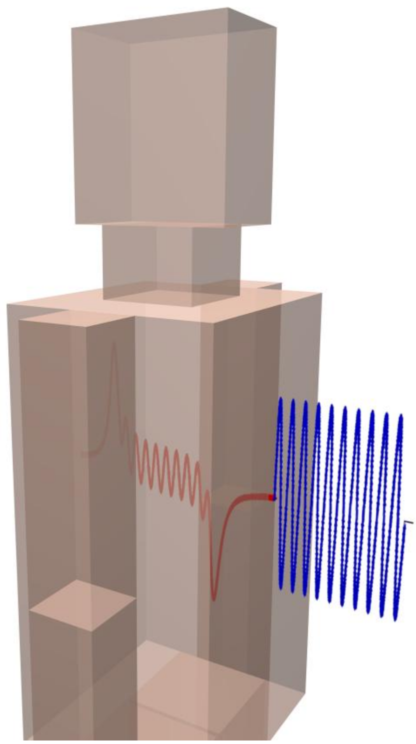

Figure 5.1 Brillouin precursor formation (red) through the human body when a properly configured input signal (blue) is considered.

When EM propagation inside the human body and interaction between different organs or parts inside the human body with radioelectric waves is calculated, full wave techniques are more suitable as a consequence of their precision and for being localized simulations in a specific human body part.

In this work a Frequency-domain simulation technique combined with the simplified human body model is used to study precursors. Thus, the possibility of combining this model with other simulation techniques is carried out. The main features of this publication are:

- All the different parts of the human body model are considered with their dielectric characteristics with the aim of studying Brillouin precursor through the human body.
- Those characteristics are extracted from the human body model presented in this thesis and therefore the possibility of export this model to other simulation techniques is corroborated.
- The characteristics of the Brillouin pulse are demonstrated since a higher amplitude level is received when it is used in a dispersive media like the human body.

PAPER H

Journal of Electromagnetic Waves and Applications
27(17) *(2014)*

Evaluation of the Brillouin precursor performance for ultra wide band intra-body technologies

Ana Vazquez Alejos, Francisco Falcone, Muhammad Dawood, Erik Aguirre and Leire Azpilicueta

Artículo H eliminado en cumplimiento de la Ley de Propiedad Intelectual (Real Decreto Legislativo 1/1996, de 12 de abril).

General discussion of results, current work and future lines

From the work presented in this thesis some aspects of the dosimetric calculation through simulation methods are covered, specifically aspects centered in the deterministic 3D Ray Launching simulation technique. While the human body model as well as its implementation in some full wave simulation techniques is usual in the bibliography for dosimetric calculation in localized zones of the human body, the study of the influence of the human body as well as the dosimetric evaluation in different environments is novel and has not been considered in depth. The employed simulation method makes enables this analysis thanks to the advantages it exhibits over other methods.

Thus and once the basic dosimetric theory has been presented, the work has been developed as follows:

Two original contributions are presented directly related with the use of the ray launching code in two complex environments and capable to contain an acceptable volume of people. The selected environments are a car and an aircraft, demonstrating in the former the accuracy of the simulation tool when they are compared with real measurements and in the latter, its application in a more complex scenario since the airplane is bigger and is composed by much more objects. Likewise basic results from which they can perform dosimetry studies are shown. WBAN and WLAN technologies are studied considering the necessity of this work is supported by them since their rise is behind the necessity of controlling the emissions of the wireless communication systems based on electromagnetic waves.

After a comprehensive study of the different human body models proposed in the bibliography, a simplified human body model is chosen taking under consideration both its features and its suitability with the simulation tool. Two original contributions where this human body model is tested are proposed. On the one hand, a study centered in the human body is carried out; analyzing waves propagation inside it and over the skin. Comparing simulation results with measurement results, the good performance of the simplified model is supported. On the other hand, the human body model as well as its environment is considered, introducing it in a complex scenario surrounded by objects with different dielectric properties. Thus, the influence of the human body (a very absorptive object) on the power distribution obtained all over the scenario is verified. Moreover, all the study is based on the behavior of the patient monitoring system known as HOLTIN and therefore the potential of the simulation tool and human body model to determine the correct implementation of a WBAN is corroborated.

Three original publications, where dosimetric estimations are obtained from simulator, are presented to demonstrate its potential application in this area. In the first contribution a commercial aircraft is considered and estimations of electric field are compared with the principal electromagnetic exposure recommendations (ICNIRP and IEEE C95.1). Three frequencies are considered not only to check their behavior, but also taking into account that these are the frequencies where mobile networks, WBAN and WLAN operate. The second publication considers a car as the scenario and, with the aid of an spectrum analyzer and a dosimeter, it is corroborated that the simulation code works correctly. In the third paper SAR estimations in human body are carried out and electric field estimations are obtained in far and near field. Once these three cases have been shown, not only the potential of the simulation tool is demonstrated, but also it is shown that with usual emissions the different maximum thresholds are not exceeded.

Finally, the developed human body model is exported to another simulation tool, based in full wave technique, where the interaction between human and precursors is studied. Precursors can be counterproductive when dosimetry is studied, since precursors are capable of propagating more efficiently through dispersive medium and therefore the absorption rate of the tissues inside human body is raised.

Hence, the results extracted from this thesis can be summarized as follows:

- The need to use simulation techniques when different kinds of dosimetric estimations are carried out is corroborated.
- Not only the effectiveness of the ray launching code when dealing with the electromagnetic estimation into different complex environments is proved, but also its potential as dosimetric estimation tool is corroborated.
- Once the simplified human body has been developed and tested, its proper functioning as well as its suitability for certain dosimetric studies is shown.
- The potential of the human body model is demonstrated since it is exported to other simulation technique.

- With regard to the study of dosimetry, it is proved that when communication systems are working normally they do not generate values higher than the thresholds recommended by different regulation entities.

Work in progress and future lines

One of the lines that has been defined, deals with vehicular communications and two cases are studied, private transport and massive transport. In addition to wireless technologies that nowadays are operating jointly in these transports, new technologies that must be studied are being developed. In relation to motor vehicles as cars, buses or motorbikes, new MANET technologies known as VANET, which will be implemented in the future, are being developed. They will be implemented in vehicles and roads to increase the security of drivers and passengers. Nevertheless, massive transportation means shows other necessities as Internet connectivity especially in commercial flights where passengers are inside aircrafts for a long time.

Dosimetric study of these environments, as well as the influence of the human body when wireless systems are implemented is essential. Thus, we are working in this direction, the influence of the human body inside an urban bus supposing a wireless network has been studied and besides, dosimetry measurements have been carried out in a regular bus line. The next step is the study of radioelectric propagation depending on the density of people inside the vehicles, especially in big public transport services as airplanes or buses.

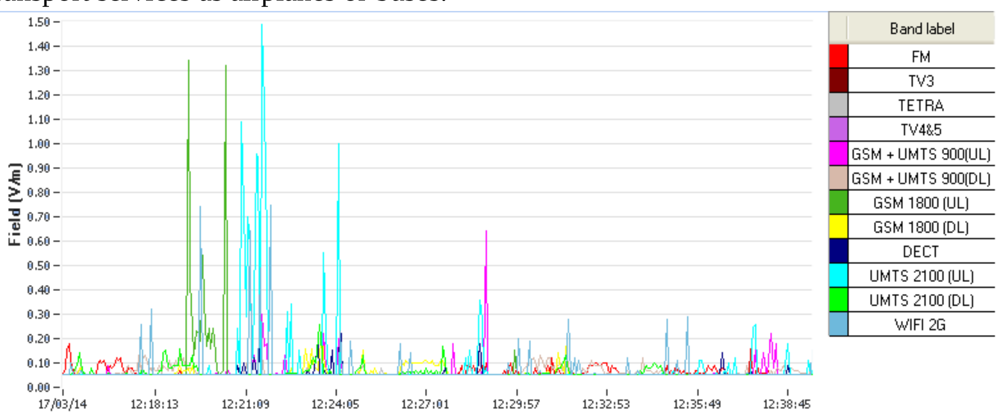

E-field strength measurement results in a regular bus line.

The consideration of other vehicles has been also taken into account, starting from two wheeled vehicles. In fact, a motorbike has been implemented in simulation code including a person over it. In this sense, sea vehicles as boats or canoes could be implemented as well as new aerial vehicles as light aircrafts or canopies.

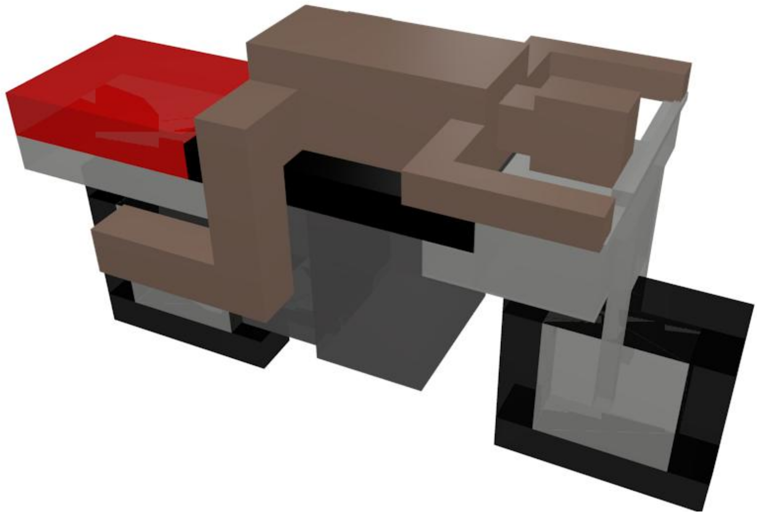

Implementation of the human body riding a motorbike.

Another line of work that is being developed is related to monitoring persons in different sport disciplines. Nowadays we are studying three sports, surfing, judo and running. These lines are especially interesting since the utilized devices must work wirelessly and must be suitable for the environment where the sport takes place, e.g. a sensor adhered to a surfer must be waterproof. Therefore, the use of the simulation tool presented in this thesis can aid to determine if the system is able to work under adverse conditions taking into account the way that it emits.

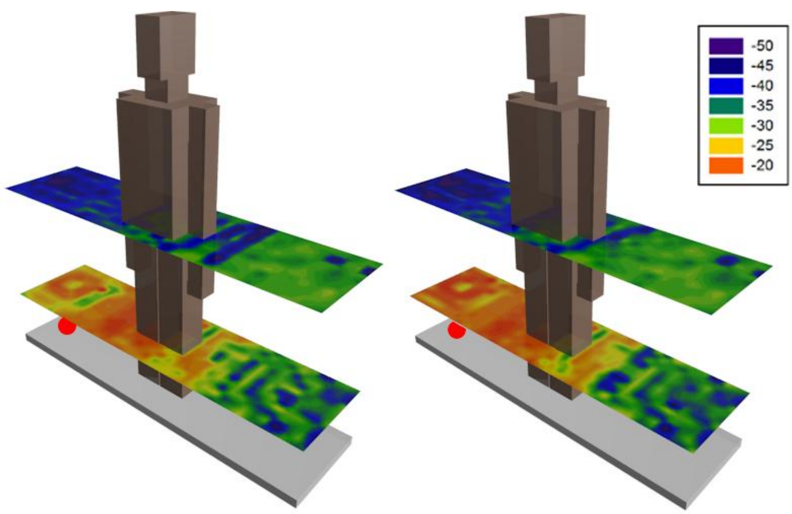

Received power level when the human body is situated over a surfboard.

Finally, an evident line of work can be found in the study of dosimetry in different kinds of scenarios, taking under consideration not only indicators as previously utilized SAR and electric field, but also SA or bioheat equation. In fact, a work related with SAR calculation when a microwave oven is emitting has been written and is under review.

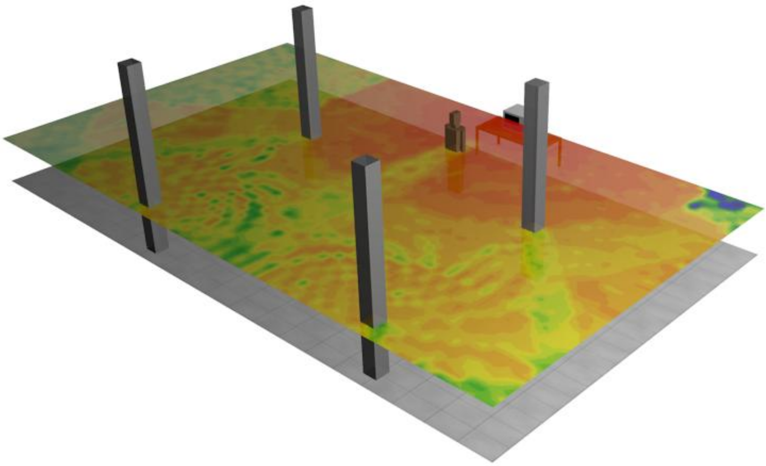

Received power level when a microwave oven is working and the human body is placed in front of it.

Besides, SA values have been calculated in a work related with precursors that is under review. From here, new SA calculations will be considered not only for an only point, but also for the entire human body as has been done previously with SAR. On the other hand, the implementation of bioheat equation is also a clear objective since it describes the mechanism by which electromagnetic energy turns into heat.

Related to this line of work, the possibility of hybridizing 3D Ray Launching technique is raised considering that this method is unsuitable for near field. Thus, FDTD technique could be used in the vicinity of the antenna and ray launching in the rest of the scenario, achieving good results in the vicinity of the antenna without compromising the efficiency of the simulation method.

Therefore the future lines can be summarized as follows:

- Undertake studies of the influence of people on EM wave propagation in different scenarios, with particular emphasis on mean of transport where new wireless technologies are being developed and the density of individuals may influence its functioning. It is also interesting to vary the density of people per square meter to check this effect.

- The consideration of new scenarios, both, vehicular environments and other environments where the influence of people is unavoidable, as sport disciplines in which the incursion of certain sensors may help in the development of competition.
- The performance of dosimetric estimations in more environments such as places where a large number of people will be confined or places where people will be exposed to radioelectric waves inevitably, as well as in areas considered "sensitive" such as schools.
- The implementation of bioheat equation to estimate the heat generated due to the exposure of people to electromagnetic waves. Moreover, to continue the study of different dosimetric indicators, especially the estimation of SA when precursors are considered.
- The hybridization of the code with the most suitable complete wave simulation technique to consider the near field, as well as a more exhaustive study of the interaction between radioelectric waves and the human body

Discusión general de los resultados, trabajo en desarrollo y líneas de futuro

A partir del trabajo presentado en esta tesis se cubren varios aspectos del calculo dosimétrico a través de métodos de simulación, centrado en concreto en el método de simulación determinista de trazado de rayos en 3D. Si bien tanto el modelado del cuerpo humano como su implementación en determinadas técnicas de simulación de onda completa son algo habitual en la bibliografía, con las que se obtiene un cálculo dosimétrico preciso de zonas localizadas del cuerpo humano, el estudio tanto de la influencia del cuerpo humano, así como de la evaluación dosimétrica de diferentes entornos es algo novedoso y en lo que se ha profundizado mínimamente. El método de simulación utilizado, hace posible el desarrollo de este trabajo, gracias a las ventajas que muestra frente a otros métodos

De esta manera y una vez presentada la teoría básica referente a dosimetría el trabajo se ha desarrollado de la siguiente manera.

Se proponen dos contribuciones originales relacionadas directamente con el uso del código de trazado de rayos en dos entornos complejos y susceptibles de albergar un volumen aceptable de personas. Los entornos seleccionado son un coche y un avión, demostrando en el primer caso la fiabilidad del método de simulación al comparar los resultados obtenidos con medidas reales y en el segundo caso su aplicación a un entorno considerablemente más complejo por su tamaño y número de objetos de que lo componen. Se presentan los resultados básicos a partir de los cuales se pueden llevar a cabo estudios dosimétricos. Se estudian tecnologías WBAN y WLAN, en las cuales se sustenta la necesidad de este trabajo, ya que su auge es el responsable de la necesidad de controlar las emisiones de los sistemas de comunicación inalámbricos por radiofrecuencia.

A partir de un estudio exhaustivo de los diferentes modelos de cuerpo humano utilizados en la bibliografía se escoge un modelo simplificado teniendo en cuenta sus características e idoneidad para con las herramienta de simulación. Se proponen dos contribuciones originales donde este es testado. En la primera de ellas un estudio centrado exclusivamente en el cuerpo humano es llevado a cabo, comprobando la propagación de las ondas en su interior así como encima de la piel. Comparando estos últimos resultados con medidas reales se determina el correcto funcionamiento del modelo simplificado. En el segundo artículo son considerados tanto el modelo cuerpo humano como su entrono introduciéndolo en una escenario complejo rodeado de numerosos objetos con diferentes características dieléctricas. De esta manera se comprueba la influencia del cuerpo humano, un objeto muy absorbente, en la distribución de potencia obtenida en el escenario. Además, todo el estudio se basa en el comportamiento del dispositivo de monitorización de pacientes HOLTIN, con lo que el potencial del modelo de cuerpo humano, así como de la herramienta de simulación para determinar la correcta implementación de una red WBAN es demostrado.

Tres publicaciones originales son tenidas en cuenta utilizando el simulador como herramienta para el cálculo dosimétrico y con el fin de demostrar su potencial en este campo. En la primera de ellas se tiene en cuenta un avión comercial donde se hacen estimaciones de campo eléctrico que son comparadas con las principales recomendaciones de exposición electromagnética (ICNIRP, IEEE C95.1). Además, tres frecuencias son consideradas con el fin de comprobar cómo se comportan estas, así como de tener en cuenta las frecuencias en las que trabajan las principales redes móviles, WBAN y WLAN. El segundo trabajo considera el coche como escenario donde gracias al uso de un analizador de espectros y un dosímetro se demuestra que el código de simulación funciona correctamente. En la tercera publicación, se llevan a cabo estimaciones de SAR sobre el cuerpo humano, además de llevar a cabo estimaciones de campo eléctrico en campo cercano y lejano. Después de presentar estos tres casos, no solo se demuestra el potencial de la herramienta de simulación, además se comprueba que emitiendo normalmente raramente se superan las recomendaciones impuestas por los diferentes organismos.

Finalmente el modelo de cuerpo humano es exportado a otra herramienta de simulación donde se estudia su interacción con los precursores. Resulta un estudio interesante ya que los precursores tienen la capacidad de propagarse más efectivamente por los entornos dispersivos, algo que puede ser contraproducente en el estudio de la dosimetría, ya que puede elevar el ratio de absorción de los órganos que componen el cuerpo. Por otro lado se demuestra la posibilidad de exportar el modelo simplificado de cuerpo humano desarrollado a otros métodos de simulación.

Por lo tanto los resultados obtenidos en esta tesis se pueden resumir en los siguientes puntos:

- Se demuestra la necesidad de usar técnicas de simulación para llevar a cabo estimaciones dosimétricas de distintos tipos.
- Se demuestra la eficacia del código de trazado de rayos a la hora de resolver el cálculo electromagnético en entornos complejos de distinta índole así como su potencial a la hora de llevar a cabo estimaciones dosimétricas.
- Después del desarrollo y la utilización del modelo de cuerpo humano simplificado, el buen funcionamiento de este es demostrado, así como su idoneidad para desempeñas determinados estudios dosimétricos.
- El potencial del modelo de cuerpo humano es probado al exportarlo a una técnica de simulación diferente.
- En lo que concierne al estudio dosimétrico como tal, se comprueba que trabajando en condiciones normales, los sistemas de comunicación estudiados no generan valores por encima del límite recomendado por los diferentes organismos de regulación.

Trabajo en desarrollo y líneas futuras

Una vez que las líneas de trabajo principales han sido afianzadas se puede contemplar una fotografía general a partir de la cual se desarrollan las líneas futuras y en las que actualmente se está trabajando.

Una de líneas claras que se han definido es la vehicular, con dos vertientes, el transporte privado y el transporte masivo. Además de las tecnologías inalámbricas que conviven hoy en día dentro de estos medios de transporte, se están desarrollando nuevas tecnologías que deben ser estudiadas. En lo que respecta a los vehículos a motor como, coches, autobuses e incluso motos, se están desarrollando nuevas tecnologías MANET denominadas como VANET que acabaran implementándose en vehículos y carreteras con el objetivo de aumentar la seguridad. En los métodos de transporte masivos ofrecer conectividad a los pasajeros del vehículo es uno de los objetivos que se plantean en la actualidad, especialmente en los vuelos comerciales donde los pasajeros se encuentran durante más tiempo en el interior.

El estudio dosimétrico de estos entornos, así como la influencia del cuerpo humano a la hora de implementar los diferentes sistemas inalámbricos es algo fundamental. Es por eso que actualmente se estás desarrollado trabajos en esta dirección, se ha estudiado la influencia del cuerpo humano en el interior de un autobús urbano suponiendo una red en su interior y se han hecho medidas de dosimetría en una línea convencional. El siguiente paso en esta línea es hacer estudios de densidad de personas en los que se varía el número de estas en los diferentes vehículos, especialmente en transportes públicos grandes como son los aviones y autobuses.

La idea también es considerar otros vehículos, empezando por vehículos de dos ruedas, existiendo ya una implementación de una motocicleta con una persona encima. En ese sentido se pueden plantear además diferentes vehículos marítimos como lanchas o barcas así como otros vehículos aéreos como avionetas o parapentes.

Otra línea de trabajo que está siendo desarrollada es la relacionada con la sensorización de las personas en diferentes modalidades deportivas. Actualmente tres deportes están siendo estudiados, el surf, el judo y el running. Estas líneas de trabajo resultan especialmente interesantes porque evidentemente los dispositivos utilizados tienen que ser inalámbricos así como resistentes a las condiciones en las que se da el deporte, por ejemplo, un sensor adherido a un surfista ha de ser resistente al agua y uno utilizado por un judoca debe resistir los golpes y no influir en la movilidad del usuario. Por lo tanto utilizar la herramienta presentada en esta tesis puede ayudar a determinar si el sistema podrá comunicarse bajo condiciones adversas teniendo en cuenta la forma en la que emite el dispositivo.

Por último existe una línea de trabajo evidente dentro del estudio dosimétrico de diferentes tipos de escenarios, considerando tanto los diferentes indicadores como el campo eléctrico y SAR ya presentados en este trabajo, así como otros diferentes como el SA o la ecuación de biocalor. De hecho, existe un trabajo pendiente de revisión en el que se expone el modelo de cuerpo a un horno microondas en el que se han obtenido resultados de SAR

Además, ya se han llevado a cabo cálculos de SA relacionados con los precursores dando como resultado un trabajo ya en revisión. A partir de aquí se van a considerar cálculos no solo en puntos concretos sino que también en todo el cuerpo al igual que se ha hecho con el SAR. La implementación de la ecuación de biocalor también parece un objetivo claro teniendo en cuenta que describe el mecanismo por el cual la energía electromagnética se convierte en calor.

Relacionado con esta línea, se plantea la posibilidad de llevar a cabo una hibridación de código teniendo en cuenta que este método no funciona adecuadamente en campo cercano. De esta manera se podría utilizar técnicas como FDTD en las proximidades de la antena y trazado de rayos en el resto del escenario, consiguiendo resultados correctos cerca de la antena sin comprometer en exceso la eficacia del método de simulación.

Por lo tanto las líneas futuras se pueden resumir en los siguientes puntos:

- Llevar a cabo estudios de la influencia de las personas en la propagación de las ondas en diferentes escenarios, haciendo especial hincapié en medios de transporte donde existen nuevas tecnologías en desarrollo y la densidad de personas pueda influir en su buen funcionamiento. Siendo interesante variar la densidad de personas por metro cuadrado para comprobar este efecto.

- Considerar nuevos escenarios tanto en el entorno vehicular como en otros entornos donde la presencia de la persona es fundamental, siendo un claro ejemplo de estos las diferentes modalidades deportivas en las que la incursión de ciertos sensores puede ayudar al desarrollo de la competición.
- Llevar a cabo estimaciones dosimétricas en más entornos, tanto por ser espacios con gran afluencia de gente o donde inevitablemente las personas van a ser sometidas a ondas electromagnéticas, así como en espacios considerados "sensibles", como pueden ser colegios, guarderías o hospitales.
- Implementar la ecuación de biocalor para poder estimar el calor generado como consecuencia de la exposición de las personas a las ondas electromagnéticas. Continuar además con el estudio de los diferentes indicadores dosimétricos, especialmente la estimación SA cuando se consideran los precursores.
- Hibridar el código con la técnica de onda completa más conveniente con el fin de poder considerar el campo cercano así como un estudio más exhaustivo de la interactuación de las ondas radioeléctricas con el cuerpo humano.

References

#

[3GPP 00] 3rd Generation Partnership Project, "3GPP Release99" (2000).

[3GPP 02] 3rd Generation Partnership Project, "3GPP Release5" (2002).

[3GPP 05] 3rd Generation Partnership Project, "Technical Specification Group Radio Access Network; Measurements of Radio Performances for UMTS Terminals in Speech Mode," Release 6. (2005).

[3GPP 09] 3rd Generation Partnership Project, "3GPP Release9" (2009).

[3GPP 11] 3rd Generation Partnership Project, "3GPP Release10" (2011).

A

[ALAL 05] A.R. Al-Ali, Y.R. Aji, H.F. Othman, F.T. Fakhreddin, "Wireless Smart Sensors Networks Overview," Sec. IFIP Int. Conf. Wless Opt. Com. Net. pp:536-540 (2005).

[ALAM 12] M.A. Alamoud, W. Schutz, "Okumura-Hata Model Tuning for TETRA Mobile Radio Networks in Saudi Arabia," 2nd Int. Conf. Adv. Comp. Tools. Eng. App. pp:47-51. (2012).

[ALEM 07] A. Alemdar, M. Ibnkahla, "Wireless Sensor Networks: Applications and Challenges," 9th Int. Symp. Sign. Proc Its App. pp:1-6 (2007).

[ALFA 05] Y. Alfadhl, X. Chen, "Numerical dosimetry of anatomically inhomogeneous animal models using an improved FDTD boundary implementation," IEEE Ant. Porp. Soc. Int. Symp. 3A. pp:819-822. (2005).

[ALMO 10] S.I. Al-Mously, "Computation of the Temperature-Rise in the Human Head Due to Different Mobile Phone Models," Med. Microw. Symp. pp:370-373 (2010)

[ARCH 14] http://www.archiexpo.es/cat/software-arquitectura/programas-analisis-estructural-R-906.html

[ATZO 14] L. Atzori, A. Iera, G. Morabito, "From “Smart Objects” to “Social Objects”:The Next Evolutionary Step of the Internet of Things," IEEE Com. Mag. 52(1). pp:97-105 (2014).

[AZPI 12] L. Azpilicueta, F. Falcone , J.J. Astráin, J. Villadangos, I.J. García Zuazola, H. Landaluce, I. Angulo, A. Perallos, "Measurement and modeling of a UHF-RFID system in a metallic closed vehicle," Microwave Opt. Tech. Lett. 54(9). pp:2126-2130. (2012).

[AZPI 14] L. Azpilicueta, M. Rawat, K. Rawat, F. Ghannouchi and F. Falcone, “Convergence Analysis in Deterministic 3D Ray Launching Radio Channel Estimation in Complex Environments,” ACES Journ. 29(4). (2014).

B

[BARI 13] N. Bari, G. Mani, S. Berkovich, "Internet of Things as a Methodological Concept," 4th Int. Conf. Comp. Geospa. Res. App. pp:22-24 (2013).

[BARU 11] M. Barua, M.S. Alam, X. Liang, X. Shen, "Secure and Quality of Service Assurance Scheduling Scheme for WBAN with Application to eHealth," IEEE Wireless Comm. Net. Conf. pp:1102-1106. (2011).

[BASH 10] Q.M. Bashayreh, A.A. Omar, A.M. Alshamali, "The effect of RF radiation on human health using stratified human head model," IEEE Radar Conf. pp:178-182 (2010)

[BAZZ 11] A. Bazzi, B.M. Masini, "Taking Advantage of V2V Communications for Traffic Management," IEEE Int. Vehic. Symp. pp:504-509. (2011).

[BEDF 12] M.D. Bedford, G.A. Kennedy, "Evaluation of ZigBee (IEEE 802.15.4) Time-of-Flight-Based Distance Measurement for Application in Emergency Underground Navigation," IEEE Trans. on Ant. Prop. 60(5). pp:2502-2510. (2012).

[BELL 13] O. Bello, S. Zeadally, "Intelligent Device-to-Device Communication in the Internet of Things," IEEE Syst. Journ. pp:1-11 (2013).

[BENK 14] I. Benkhelifa, N. Nouali-Taboudjemat, S. Moussaoui, "Disaster Management Projects using Wireless Sensor Networks: An Overview," 28th Int. Conf. Adv. Inf. Net. App. Work. pp:605-610 (2014).

[BERZ 12] E.L. Berz, F.P. Hessel, M.C. de Azambuja, J.C. Ody, "Prediction of RFID Systems Coverage Applied to Smart Cards Scenario," IEEE 23rd Int. Symp. Pers. Ind. Mob. Rad. Comm. pp:1484-1490. (2012).

[BIOD 14] http://www.biodigitalhuman.com/

[BOBA 07] J. Bobadilla, P. Gomez, J.I. Godino, "Mapaci: A Real Time e-Health Application to Assist Throat Complaint Patients," Sec. Int. Conf. Int. Web App. Serv. pp:63. (2007).

[BORN 09] C. Bornkesse; M. Schubert, M. Wuschek, "Determination of General Public Exposure to WiMAX Base Stations," 20th Int. Zurich Symp. Electromag. Comp. pp:333-336, (2009).

[BOTT 12] O. Bottauscio, M. Chiampi, L. Zilberti, L. "Boundary Element Solution of Electromagnetic and Bioheat Equations for the Simulation of SAR and Temperature Increase in Biological Tissues," IEEE Trans. Magnet. 48(2) pp:691-694 (2012)

[BRAG 14] A.S. Braga, R.L.F. Lopes, S.G.C. Fraiha, J.P.L. Araujo, H.S. Gomes, J.C. Rodrigues, H.R.O. Ferreira, G.P.S. Cavalcante, "Coverage Area Simulation for Indoor 4G Networks in 2.6 GHz and 3.5 GHz," 8th Eur. Conf. Ant. Prop. pp:2126-2129 (2014).

[BUEN 06] Jornada “Buenas prácticas en telefonía móvil y desarrollo local”, Pamplona, 25 de mayos de 2006

C

[CANS 03] A. G. Canseven, N. Seyhan, “Ellipsoid Models for Human and Guinea Pigs Exposed to Magnetic Fields”, IEEE Int. Symp. Electromag. Comp. 2. pp:1227-1231 (2003)

[CARL 13] G. Carluccio, D. Erricolo, O. Sukhoon, C.M. Collins, "An Approach to Rapid Calculation of Temperature Change in Tissue Using Spatial Filters to Approximate Effects of Thermal Conduction," IEEE Trans. Biomed. Eng. 60(6). pp:1735-1741 (2013).

[CAST 13] P. Castillejo, J.-F. Martinez, J. Rodriguez-Molina, A. Cuerva, A., "Integration of Wearable Devices in a Wireless Sensor Network for an E-Health Application," IEEE Wless Com. 20(4). pp: 38-49 (2013).

[CHRY 10] A. Chrysostomou, I. Zorbas, E. Papkelis, P. Frangos, "Radio coverage simulation for three-dimensional urban environment using physical optics, physical theory of diffraction and the near-to-far-field transformation method," Days Diff. (2010).

[CHUA 97a] H. R. Chuang, W. T. Chen, "Computer Simulation of the Human-Body Effects on a Circular-Loop-Wire Antenna for Radio-Pager Communications at 152, 280, and 400 MHz," IEEE Trans. Vehic. Tech.46(3). pp:544-599 (1997)

[CHUA 97b] H. R. Chuang, "Numerical Computation of Fat Layer Effects on Microwave Near-Field Radiation to the Abdomen of a Full-Scale Human Body Model", IEEE Trans. Microw. Theory Tech. 45(1) pp:118-125 (1997)

[COET 11] L. Coetzee, J. Eksteen, "The Internet of Things – Promise for the Future? An Introduction," IST- Africa Conf. Proc. pp:1-9 (2011).

[CORR 09] L.M. Correia, "A View of the COST 231-Bertoni-Ikegami Model," 3rd Eur. Conf. Ant. Prop. pp:1681-1685. (2009).

[COVA 09] G. Cova, H. Xiong, Q. Gao, E. Guerrero, R. Ricardo, J. Estevez, "A Perspective of State-of-the-Art Wireless Technologies for E-Health Applications," IEEE Int. Symp. IT Med. Edu. pp:76-81. (2009).

[CST 13] https://www.cst.com/Applications/Article/HUGO-Human-Body-Model

[CTIA 13] CTIA Wireless Association"Test Plan for Wireless Device Over-the-Air Performance, Method of Measurement for Radiated RF Power and Receiver Performance," Revision 3.3. (2013).

D

[DAW 98] T. W. Dawson, M. A. Stuchly, "High-Resolution Organ Dosimetry for Human Exposure to Low-Frequency Magnetic Fields", IEEE Trans. Mag. 34(3) pp:708-718 (1998)

[DAWO 12a] M. Dawood, H.U.R. Mohammed, A.V. Alejos, "Breast Cancer Detection Utilizing Brillouin Precursors at Microwave Frequencies," IEEE Ant. Prop. Soc. Int. Symp. pp:1-2 (2012).

[DAWO 12b] M. Dawood, Z. Zeeshan, A.V. Alejos "Brillouin Precursors Through Concrete Walls for Through-the-wall imaging at Microwave frequencies," IEEE Ant. Prop. Soc. Int. Symp. pp:1-2 (2012).

[DEVA 90] D.M.J. Devasirvatham, C. Banerjee, M. Krain, D.A. Rappaport, "Multi-Frequency Radiowave Propagation Measurements in the Portable Radio Environment," IEEE Int. Conf. Comm. 4. pp:1334-1340. (1990).

[DIAO 10] Y. Diao, M. Fu, H. Zhang, "An Overview of Range Detection Techniques for Wireless Sensor Networks," 8th World Con. Int. Contr. Auto. pp:1150-1155 (2010).

[DILE 09] V. Di Lecce, A. Amato "Route planning and user interface for an advanced intelligent transport system," Int. Trans. Sys. 5(3). pp:149-158. (2009).

[DIMB 91] P.J. Dimbylow, "Finite-difference time-domain calculations of absorbed power in the ankle for 10-100 MHz plane wave exposure," IEEE Tran. Biomed. Eng. 38(5). pp:423-428 (1991)

[DOBI 11] A. Dobircau, S. Folea, H. Valean, D. Bordencea, "Indoor Localization System Based on Low Power Wi-Fi Technology," 19th Telecomm. Forum. pp:317-320. (2011).

[DOMI 12] F. Dominguez, A. Touhafi, J. Tiete, K. Steenhaut, "Coexistence with WiFi for a Home Automation ZigBee product," IEEE 19th Symp. Comm Vehic. Tech pp:1-6. (2012).

[DURN 75] C. H. Durney, C. C. Johnson, H. Massoudi, “Long-Wavelength Analysis of Plane Wave Irradiation of a Prolate Spheroid Model of Man”, IEEE Trans. Microw. Theory Tech. 23(2). pp:246-253 (1975)

[DURN 79] C. H. Durney, M. F. Iskander, H.Massoudi, C. C. Johnson, “An Empirical Formula for Broad-Band SAR Calculations of Prolate Spheroidal Models of Humans and Animal”, IEEE Trans. Microw. Theory Tech. 27 (8). pp:758-763 (1979).

E

[ERG 14] http://ergonomia2010.files.wordpress.com/2010/05/proporcionesrelativash.jpg

F

[FASH 11] H. Fash, A. Hadjem, S. Lanteri, S. Lanteri, J.Wiart, M. F. Wong, “Calculation of the SAR Induced in Head Tissues Using a High-Order DGTD Method and Triangulated Geometrical Models”, IEEE Trans. Ant. Prop. 59(12). pp:4669-4678 (2011)

[FIGU 14] http://figure-drawings.com/How-to-Draw-Proportions.html

[FLORE 08] G.H.P. Florentino, C.A. Paz de Araujo, H.U. Bezerra, H.B.A. Junior, M.A. Xavier, V.S.V. de Souza, R.A. de M.Valentim, A. Morais, A.M.G. Guerreiro, G.B. Brandao, "Hospital Automation System RFID-Based: Technology Embedded In Smart Devices (Cards, Tags and Bracelets)," 30th Ann. Int. Conf. IEEE Eng. Med. Bio. Soc. pp:1455-1458. (2008).

[FRUH 11] A.L. Fruhling, S. Raman, A.R. Sambol, "Strategies for Developing a Mobile e-Health Emergency Response Consultation System," 44th Hawaii Int. Conf. Sys. Sci. pp:1-10. (2011).

[FUJI 06] K. Fujii, M. Takahashi, K. Ito, N. Inagaki, “Study on the Electric Field Distributions Around Whole Body Model with a Wearable Device Using the Human Body as a Transmission Channel,” First Eur. Conf. Ant. Prop. pp:1-4 (2006)

G

[GABR 96] Gabriel, C., “Compilation of the dielectric properties of body tissues at RF and microwave frequencies,” Brooks Air Force, Brooks AFB, TX, Tech. Rep. AL/OE-TR-1996–0037, 1996.

[GAO 14] H. Gao, X. Fang., J. Li, Y. Li., "Data Collection in Multi-Application Sharing Wireless Sensor Networks," IEEE Trans. Par. Dist. Sys. pp:1-10 (2014).

[GHAD 04] M. Ghaddar, L. Talbi, T. A. Denidni, “Human body modelling for prediction of effect of people on indoor propagation channel”, Elect. Lett. 40(25) (2004)

[GOUZ 07] I.A. Gouzouasis, I.S. Karanasiou, N.K. Uzunoglu, "FDTD Study of the Focusing Properties of a Hybrid Hyperthermia and Radiometry Imaging System using a Realistic Human Head Model," 29th Ann. Int. Conf. of the IEEE Eng. Med. and Bio. Society, pp: 3552-3555 (2007)

[GRAS 12] F. Grassi, G. Spadacini, S.A. Pignari, "Human Exposure in Arc-Welding Processes: Current versus Previous ICNIRP Basic

Restrictions," IEEE Int. Symp. Electromag. Comp. pp:749:754, (2012).

[GROU 14] http://grouper.ieee.org/groups/scc34/sc2/

[GUO 10] J.-K. Guo, C.-J. Tsai, C.-Jen Wang, C.-L. Lu "A ZigBee Network Application in Emergency Exit Guiding," Int. Comp. Symp. pp:91-94 (2010).

H

[HAMB 03] L. Hamberg, N. Lovehagen, M. Siegbahn, C. Tornevik, "A Method for Determination of RF Exposure Compliance for Pico Cell Base Stations by SAR Measurements in a Flat Phantom," IEEE Ant. Prop. Soc. Int. Symp. 2. pp:1009-1012 (2003)

[HASS 13a] N.M. Hassan, O.M. Olaniyi, A. Ahmed, E.M. Dogo, "Wireless Sensor Networks for Remote Healthcare Monitoring in Nigeria: Challenges and Way Forward," IEEE Int. Conf. Emerg. Sust. Tech. Pow. ICT Dev. Soc. pp:182-187. (2013).

[HASS 13b] O. Hassan, I. Adly, K.A. Shehata, "Vehicle Localization System based on IR-UWB for V2I Applications," 8th Int. Conf. Comp. Eng. Sys. pp:133-137. (2013).

[HEHU 12] P. Hehuan, M. Zeyun, "Research on Bluetooth Based Vehicular Hand Free System," Int. Conf Ind. Ctrl. Electr Eng. pp:1099-1101. (2012).

[HERS 10] P.C. Hershey, J.M. Pitts, O.M. Shepherd, "Monitoring and Response for Real-Time Voice Messages Transmitted Using Wi-Fi Within Net-Centric Enterprise Systems," Mil. Comm. Conf. pp:2050-2055. (2010).

[HIRA 00] A. Hirata, S.i. Matsuyama, T. Shiozawa, "Temperature Rises in the Human Eye Exposed to EM Waves in the Frequency Range 0.6–6 GHz," Trans. Electromag. Comp. 42(4) (2000).

[HOU 11] Q. Hou, L. Gao, "The Simulation of WLAN Outdoor Coverage in Hot Spot Area for Wireless Digital City," 7th Int. Conf. Wireless Comm. Net. Mob. Comp. pp:1-4 (2011).

[HU 11] S. Hu, C. Fan, W. Kou, L. Yang, F. Sun, D. Deng, "Heating of Rat Skin by High Power Millimeter Waves," Hum. Health Biomed. Eng. pp:908-911 (2011)

[HUAN 10] Y. Huang, G. Li, "Descriptive Models for Internet of Things," Int. Conf. Int. Cont. Inf. Proc. pp:483-486 (2010).

[HUAN 13] W.L. Huang, Y. Zhongdong, F. Zhu, L. Yang, F.-Y. Wang "Applicability of Short Range Wireless Networks in V2I Applications," 16th Int. IEEE Conf. Int. Trans. Sys. pp:231-236. (2013).

[HUNG 14] C.-H. Hung, Y.-W. Bai, H.-J. Wu, K.-J. Chung, "Monitor and Remote Control of a Heating Cloth for the Aged," IEEE Int. Conf. Cons. Electr. pp:266-267. (2014).

[HYUN 11] S.-Y. Hyun, S.-Y. Kim, "3-D Thin-Wire FDTD Analysis of Coaxial Probe Fed in Asymmetric Microwave Components," IEEE Trans. Microw. Theo. Tech. 59(11). pp:2808-2815. (2011).

I

[ICNI 98] ICNIRP (1998) Guidelines for limiting exposure to protection time-varying electric, magnetic and electromagnetic fields (up to 300 GHz). International Commission on Non-Ionizing Radiation.). Health Phys 74:494–522.

[IDE 12] C. Ide, B. Dusza, M. Putzke, C. Wietfeld, "Channel Sensitive Transmission Scheme for V2I-based Floating Car Data Collection via LTE," IEEE Int. Conf.Comm. pp:7151-7156 (2012).

[IEEE 05] IEEE Computer society, "Part 15.1: Wireless medium access control (MAC) and physical layer (PHY) specifications for wireless personal area networks (WPANs)," IEEE Standard for Information technology-Telecommunications and information exchange between systems-Local and metropolitan area networks-Specific requirements. (2005).

[IEEE 11] IEEE Computer society, "Part 15.4: Low-Rate Wireless Personal AreaNetworks (LR-WPANs) - Amendment 6: TV White Space Between 54 MHz and 862 MHz Physical Layer," IEEE Standard for Local and metropolitan area networks. (2011).

[IEEE 12a] IEEE Computer society, " Part 15.6: Wireless Body Area Networks," IEEE Standard for Information technology-Telecommunications and information exchange between systems-Local and metropolitan area networks-Specific requirements. (2012).

[IEEE 12b] IEEE Computer society, " Specific requirements Part 11: Wireless LAN Medium Access Control (MAC) and Physical Layer (PHY) Specifications," IEEE Standard for Information technology--Telecommunications and information exchange between systems Local and metropolitan area network. (2012).

[IEEE 99] Institute of Electrical and Electronics Engineers (1999) IEEE Standard for safety levels with respect to human exposure to radiofrequency electromagnetic fields, 3 kHz to 300 GHz. Document IEEE C95-1. New York

[ITUR 12a] Recommendation ITU-R P.1238-7, "Propagation data and prediction methods for the planning of indoor radiocommunication systems and radio local area networks in the frequency range 900 MHz to 100 GHz," pp:373-377. (2012).

[ITUR 12b] P.L. Iturri, J.A. Nazábal, L. Azpilicueta, P. Rodriguez, M. Beruete, C. Fernández-Valdivielso, F. Falcone, "Impact of High Power Interference Sources in Planning and Deployment of Wireless Sensor Networks and Devices in the 2.4GHz frequency band in Heterogeneous Environments," Sensors 12(11), pp:15689-15708. (2012).

[IVAN 12] S. Ivanov, C. Foley; S. Balasubramaniam;D. Botvich, "Virtual Groups for Patient WBAN Monitoring in Medical Environments," IEEE Trans. Biomed. Eng. 59(11). pp:3238-3246. (2012).

J

[JANE 07] T. Janevski, A. Tudzarov, P. Stojanovski, D. Temkov, "Applicative Solution for Easy Introduction of WLAN as Value-added Service in Mobile Networks," IEEE Vehic. Tech. Conf. pp:1096-1100. (2007).

[JIAN 11] S. Jianxiong, A.V. Alejos, M. Dawood, "Under-Sea Remote Sensing Using Brillouin Precursors," Int. Workshop Ant. Tech. pp:222-226 (2011).

K

[KAVI 09] K.V.N. Kavitha, A. Bagubali, L. Shalini, "V2V Wireless Communication Protocol for Rear-End Collision Avoidance on

Highways with Stringent Propagation Delay," Int. Conf. Adv. Rec. Tech. Comm. Comp. pp:661-663. (2009).

[KEEN 90] J.M. Keenan, A.J. Motley, "Radio coverage in buildings," British Telecom Tech. Journal, 8(1) pp:19-24. (1990).

[KWON 06] K. Kwon, S. Lim, S. Cho, J. Yoon, J. Cho, C. Cheon, Y. Kwon. "Planar Type Probe With Multiple-Polarization Response for in-vivo Permittivity Measurements of Heterogeneous Biological Tissues.," IEEE Microw. Wireless Comp. Let. 16(1). pp: 1-3 (2006).

L

[LAZZ 97] G. Lazzi, O. P. Gandhi, “Realistically Tilted and Truncated Anatomically Based Models of the Human Head for Dosimetry of Mobile Telephones,” IEEE Trans. Electromag. Comp. 39(1). pp:55-61 (1997).

[LEE 07] A.K. Lee, H.D. Choi, J.I. Choi, "Study on SARs in Head Models With Different Shapes by Age Using SAM Model for Mobile Phone Exposure at 835 MHz," IEEE Tran. Electromag. Comp. 49(2) pp:302-312 (2007).

[LEE 11] A.K. Lee, "A Comparison of Specific Absorption Rates in SAM Phantom and Child Head Models at 835 and 1900 MHz," IEEE Trans. Electromag. Comp. 53(3). pp:619-627 (2011).

[LIU 13] W. Liu, E.K. Park, "e-Health AON (Application-Oriented Networks)," 22nd Int. Conf. Comp. Comm. Net. pp:1-7. (2013).

[LIU 14] S. Liu, Y. Jiang, A. Striegel, "Face-to-Face Proximity Estimation Using Bluetooth On Smartphones," IEEE Trans. Mob. Comp. 13(4). pp:811-823. (2014).

[LOPE 12] A.J. Lopez-Barrantes, O. Gutierrez, F.S.D Adana, R. Kronberger, "Comparison of Empirical Models and Deterministic Models for the Analysis of Interference in Indoor Environments," Asia-Pacific Symp. Electromag. Comp. pp:509-512 (2012).

[LQTA 14] http://www.lqtechnology.net/portal/?Section=Holtin

[LUKO 09] D. Lukofsky, J. Bessette, H. Jeong, E- Garmire, U. Österberg "Can precursors improve the transmission of energy at optical frequencies?," Jour. Mod. Opt. 56(9). pp:1083-1090 (2009).

M

[MA 12] X. Ma; J. Martensson, "Optimal Controls of Vehicle Trajectories in Fleet Management using V2I Information," Int. Conf. Conn. Vehic. Expo. pp:1-6. (2012).

[MACH 06] Y, Machii, H. Aoki, K. Koshiji, "Fat Thickness Estimation Method Using Bio Electrical Property Examination by Gel Phantom Model Test," Int. Symp. Micro-NanoMech. Human Sci. pp:1-6 (2006)

[MARTI 09] M. Martínez-Espronceda, I. Martínez, S. Led, J.D. Trigo, I. Oses, J. Escayola; L. Serrano, J. García, A. Garcia, "INTENSA: Heart Failure Patient's Follow-up System Using the ISOlIEEEl1073 Standard," 9th Int. Conf. Inf. Tech. App. Biomed. pp:1-4, (2009).

[MASS 77] H. Massoudi , C. H. Durney, C. C. Johson, “Long-Wavelength Electromagnetic Absorption in Ellipsoidal Model Man and Animals”, IEEE Trans. On Microw. Theory and Tech. 25(1). pp:47-52 (1977)

[MEDE 00] A. Medeisis, A. Kajackas, "On the Use of the Universal Okumura-Hata Propagation Prediction Model in Rural Areas," IEEE 51st Vehic. Tech. Conf. Proc. 3. pp:1815-1818. (2000).

[MILA 12] V. Milanes, J. Villagra, J. Godoy, J. Simo, J. Perez, E. Onieva, E. "An Intelligent V2I-Based Traffic Management System," IEEE Trans. Int. Trans. Sys. 13(1). pp:49-58. (2012).

[MOHA 12] H.U.R. Mohammed, M. Dawood, A.V. Alejos, "Experimental Detection and Characterization of Brillouin Precursor Through Loamy Soil at Microwave Frequencies," IEEE Trans. Geosci. Remote Sens. pp:436-445 (2012).

[MONE 10] V. Monebhurrun, "Conservativeness of the SAM Phantom for the SAR Evaluation in the Child’s Head," IEEE Trans. Magn. 46(8). pp:3477-3480 (2010)

[MORE 12] A. Moreno, I. Angulo, A. Perallos, H. Landaluce, I.J. García Zuazola, L. Azpilicueta, J.J Astrain, F. Falcone, J. Villadangos, "IVAN: Intelligent Van for the Distribution of Pharmaceutical Drugs," Sensors. 12. pp:6587-6609. (2012).

[MOTR 06] V.C. Motrescu, U. van Rienen, "Simulation of Slowly Varying Electromagnetic Fields in the Human Body Considering the

Anisotropy of Muscle Tissues," IEEE Trans. Magn. 42(4). pp:747-750 (2006).

[MWES 13] C. Mwesigwa, "An e-Health Tele-Media Application for Patient Management," IST-Africa Conf. Exh. pp:1-7. (2013).

N

[NAGA 08] T. Nagaoka, S. Watanabe, “Development of Anatomically Realistic Whole-Body Models of Children and Their Use in Electromagnetic Dosimetry”, Cairo Int. Bio. Eng. Conf. pp:1-4 (2008)

[NAGA 09] T. Nagaoka, S. Watanabe, " Voxel-Based Variable Posture Models of Human Anatomy", Proc. IEEE 97(12). pp:2015-2025 (2009

[NAGA 11a] T. Nagaoka, S. Watanabe, "GPU-Based 3D-FDTD Computation for Electromagnetic Field Dosimetry," IEEE Africon pp:1-3. (2011).

[NAGA 11b] T. Nagaoka, S. Watanabe, “Japanese Voxel-based Computational Models and Their Applications for Electromagnetic Dosimetry”, XXXth URSI Gen. Assem. Sci. Symp. pp:1-4 (2011)

[NAJA 10] B.M. Najafabadi, R. Safian, "Heat Distribution Pattern of Double Brillouin Pulse Inside Water," IEEE. Int. Microw. Symp. pp:185-188 (2010).

[NAZA 12] J.A. Nazábal, P. Iturri López, L. Azpilicueta, F. Falcone, C. Fernández-Valdivielso, "Performance Analysis of IEEE 802.15.4 Compliant Wireless Devices for Heterogeneous Indoor Home Automation Environments," Int. Jour. Ant. Prop., Hindawi Publishing Corporation 2012,

[NEDE 09] A.-V. Nedelcu, F. Sandu, M. Machedon Pisu, M. Alexandru, P. Ogrutan, "Wireless-based Remote Monitoring and Control of Intelligent Buildings," IEEE Int. Workshop Rob. Sens. Env. pp:47-53. (2009).

[NLM 13] http://www.nlm.nih.gov/research/visible/visible_human.html

[NOIM 11] K. Noimanee, S. Noimanee, S. Wattanasirichaigoon, N. La-oopugsin, V. Mahasitthiwat, K. Thongbunjob, S. Tungjitkusolmun, P. Ratleadkarn, "Development of e-Health Application for Medical

Center in National Broadband Project," Biomed. Eng. Int. Conf. pp:262-265. (2011).

O

[OCW 14] http://ocw.unican.es/ciencias-de-la-salud/fisiologia-general/materiales-de-clase-1/bloque-ii/Tema%2011-Bloque%20II-La%20Piel.%20Estructura%20y%20Funciones.pdf

[OKUM 68] Y. Okumura, E. Ohmuri, T. Kawano, K. Fukuda, "Field Strength and its Viability in VHF and UHF land mobile service," Rev Elec. Comm Lab. 16(9-10), pp:825-873. (1968).

[OLSO 11] T.E. Olson, "Everything is a precursor: The asymptotic singular value decomposition for transmission through absorbing media," Int. Conf. Electromag. Adv. App. pp:335-338. (2011).

[ONG 03] K.G. Ong, W.R. Dreschel, C.A. Grimes, "Detection of Human Respiration Using Square-Wave Modulated Electromagnetic Impulses," Microw. Opt. Lett. 36(5). pp:339-343 (2003).

[ORTE 12] R. Ortega-Palacios, L. Leija, A. Vera, "Tumor Breast Phantom vs Breast Phantom Microwave Ablation: Thermal Experimentation and Electric Property Measurements," 9th Int. Conf. Elect. Eng. Comp. Sci. Auto. Contr. pp:1-4 (2012).

[OUGH 05] K.E. Oughstun, "Dynamical Evolution of the Brillouin Precursor in Rocard–Powles–Debye Model Dielectrics," IEEE Trans. Ant. Prop. 53(5). pp:1582-1590 (2005).

[OZEN 01] S. Özen, S. Çömlekçi, O. Çerezci', “An Evaluation for Coupling of Human to Magnetic Fields in Human Ellipsoidal Models with Frequency up to l00kHz” , Proc. 23rd Ann. IEEE EMBS Int. Conf. 4. pp:3997-4000 (2001).

P

[PAPA 13] A. Papalambrou, J. Gialelis, S. Serpanos, "Increasing security in wireless e-health systems," IEEE Int. Symp. Sign. Proces. Inf. Tech. pp:-15-20. (2013).

[PAPK 08] E.G. Papkelis, H.T. Anastassiu, P.V. Frangos, "A Time-Efficient Near-Field Scattering Method Applied to Radio-Coverage Simulation in Urban Microcellular Environments," IEEE Trans. Ant. Prop. 56(10). pp:3359-3363 (2008).

[PENN 48] H.H. Pennes, “Analysis of Tissue and Arterial Blood Temperature in the Resting Human Forearm,” J. of Appl. Phys. 1. pp:93-102 (1948).

[PETR 14] L. Petrillo, T. Mavridis, J. Sarrazin, D. Lautru, A. Benlarbi-Delaï, P. De Doncker, "Analytical Creeping Wave Model and Measurements for 60 GHz Body Area Networks," IEEE Trans. Ant. Prop. 62(8). pp: (2014).

[PODZ 12] A. Podziewski, K. Litwiniuk, J. Legierski, "Emergency Button – a Telco 2.0 application in the e-health environment," Fed. Conf. Comp. Sci. Inf. Sys. pp:663-677. (2012).

[POLJ 03] K. Poljak, N. Kovac, “The electromagnetic-thermal analysis of human exposure to radio base station antennas”, 17 lnt. Conf. App. Electromag. Comm. pp:1 - 3 (2003).

Q

[QABA 07] A.M. Qabazard, "Survey of Electromagnetic Field Radiation Associated with Power Transmission Lines in the State of Kuwait," Int. Conf. Electromag. Adv. App. pp:795-797, (2007).

R

[RAAD 13] H.R. Raad, A.I. Abbosh; H.M. Al-Rizzo, D.G. Rucker, "Flexible and Compact AMC Based Antenna for Telemedicine Applications," IEEE Trans. Ant. Prop. 61(2). pp:524-531 (2013).

[REIV 99] S. Reivomen, T. Keikko, J. Isokorpi, L. Korpinen, “Internal Currents in a Human Body with Spheroidal Model in 400 kv Switching Substation”, Int. Symp. High Volt. Eng. 2 pp:31-34 (1999).

[RUAN 09] F. Ruan, T. Duglosz, D. Shi, Y. Gao, “Cylinder Model of Human Body Impedance Based on Proximity Effect”, 3rd IEEE International Symp. Microw. Ant. Prop. EMC Tech. Wireless Comm. pp:27-29 (2009).

S

[SAFI 09] R. Safian, H. Mirzaei, H. Elhami, "Detection of Objects Inside Water Exploiting the Brillious Precursors," Eur. Rad. Conf. pp:517-520 (2009).

[SANC 09] David A.Sánchez-Hernández “High Frequency Electromagnetic Dosimetry” 2009 ARTECH HOUSE ,INC.

[SANG 14] K. Sangan, "Vice Versa," Eng. Tech 9(5). pp:50-53. (2014).

[SCHN 96] I. Schneider, F. Lambrecht, A, Baier, "Enhancement of the Okumura-Hata propagation model using detailed morphological and building data," 7th IEEE Int. Symp. Pers. Indoor. Mob Rad. Comm. 1. pp:34-38. (1996).

[SELV 08] K. Selvarajah, A. Tully, P.T. Blythe, "Zigbee for Intelligent Transport System Applications," IET Road Trans. Inf. Ctrl. & ITS UK Memb. Conf. pp:1-7 (2008).

[SHAG 09] H. Shagoshtaasbi, "A Forth Order Finite Difference Scheme for Pennes' Bioheat Equation in a Three Dimensional Triple-Layered Skin Structure With Multilevel Blood Vessel," IEEE EUROCON pp:146-151 (2009)

[SHIN 04] S.C. Shin, C.Y. Ryu, J.H. Kang, S.H. Nam, Y.S. Song, T.G. Lim, J.W. Lee, D.G. Park, S.H. Kim, Y.T. Kim, "Realization of an e-Health System to Perceive Emergency Situations," 26th Ann. Int. Conf. IEEE Eng. Med. Bio. Soc. 2.pp:3309-3312. (2004).

[SHIN 07] S. Nishizawa; F.M. Landstorfer; Y. Kamimura, "Low-Frequency Dosimetry of Inhomogeneous MagneticFields Using the Coil Source Model and the Household Appliance," IEEE Trans. Boimed. Eng. 54(3) pp:497-502 (2007)

[SHIY 14] C. Shiyao, X. Yunyang, L. Baihui,W. Hui, "The Application of ZigBee Technology to the Intelligent Bus Query System," 6th Int. Conf. Meas. Tech. Mecha. Auto. pp:672-674. (2014).

[SHOS 06] L. Shoshiashvili, A. Razmadze, N. Jejelava, R. Zaridze, L.G. Bit-Babik, A. Faraone, "Validation Of Numerical Bioheat Fdtd Model," Proc. XIth Int. Seminar/Workshop Dir. Inv. Probl. Electromag. Acouts. Wave Theo. pp:201-204 (2006)

[SKID 96] R.R. Skidmore, T.S. Rappaport, A.L. Abbott, "Interactive Coverage Region and System Design Simulation for Wireless Communication Systems in Multifloored Indoor Environments: SMT Plus," 5th IEEE Int. Conf. Univ. Perso. Comm. 2. pp:646-650 (1996).

[SPEA 13a] http://www.speag.com/]

[SPEA 13b] http://www.speag.com/products/em-phantom/whole-body/posable-phantom-popeye/

[STAK 03] S.W. Staker, C.L. Holloway, A.U. Bhobe, M. Piket-May, "Alternating-Direction Implicit (ADI) Formulation of the Finite-Difference Time-Domain (FDTD) Method: Algorithm and Material Dispersion Implementation," IEEE Trans. Electromag. Comp. 45(2). pp:156-166. (2003).

[STAM 11] R. Stam, "Comparison of International Policies on Electromagnetic Fields (Power Frequency and Radiofrequency Fields)," National Institute for Public Health and the Environment. (2011).

[SUJA 05] B. Sujak, D. Kumar Ghodgaonkar, B.M. Ali, S.Khatun, "Indoor Propagation Channel Models for WLAN 802.1lb at 2.4GHz ISM Band," Asia-Pacific App. Electromag. (2005).

[SURD 08] J. Surda, E. Cocherova, O. Ondracek, “Tissue Parameters Influence on the Microwave Energy Absorption in Biological Objects”, 14th Conf. Microw. Tech. pp:1-4 (2008).

T

[TAYL 95] H.C. Taylor, J.W. Hand, R.W. Lau, "FDTD Modelling for Microwave Dosimetry fnd Thermography," IEEE Colloq. App. Microw. pp:11/1-11/6. (1995).

[TOYO 08] K. Toyoda, T. Uno, T. Arima, "Comparison of FT-FDTD and Spectral Domain FDTD for Periodic Structures," Int. Workshop Ant. Tech Small Ant. Nov. Mmetamat. pp:191-194. (2008).

U

[UZUN 87] N. K. Uzunoglu, E. A. Angelikas, “Field Distributions in a Three-Layer Prolate Spheroidal Human Body Model for a Loop Antenna Irradiation”, IEEE Tran. Ant. Prop. 35(10) pp: 1180-1185 (1987).

V

[VUCH 13] M. Vuchkovikj, I. Munteanu, T. Weiland, "Numerical Approach for Separation and Movement of the Fingers of the HUGO Model for

Analysis of SAR Distribution," 21st Int. Conf. Soft., Telecomm. Comp. Net. pp:1-5 (2013).

W

[WANG 00] Y. Wang; S. Safavi-Naeini, S.K. Chaudhuri, "A Hybrid Technique Based on Combining Ray Tracing and FDTD Methods for Site-Specific Modeling of Indoor Radio Wave Propagation," IEEE Trans. Ant. Prop. 48(5). pp:743-754. (2000).

[WANG 08] Q. Wang, J. Wang, "SA/SAR analysis for multiple UWB pulse exposure," Asia-Pacific Symp. Electromag. Comp. pp:212-215 (2008)

[WANG 11] M. Wang, L. Lin, J. Chen; D. Jackson, W. Kainz, Y. Qi, P. Jarmuszewski, "Evaluation and Optimization of the Specific Absorption Rate for Multiantenna Systems," IEEE Trans. on Electromag. Comp. 53(3). pp:628-637 (2011)

[WANG 13a] S. Wang, A. Huang, T. Zhang, "Performance Evaluation of IEEE 802.15.4 for V2V Communication in VANET," 5th Int. Conf. Comp. Inf. Sci. pp:1603-1606. (2013).

[WANG 13b] J. Wang, Q. Wang, "Body Area Communications Channel Modeling, Communication Systems, and EMC," 2013 John Wiley & Son Singapore Pte. Ltd.

[WARS 74] "Biologic Effects and Health Hazards of Microwave Radiation", Warsaw, Polish Medical Publication (1974).

[WATA 10] T. Watanabe, N. Michishita, Y. Yamada, "Surface Electric Field Distributions of Lightweight Phantom Composed of Wave Absorber for Simplified SAR Measurement," Proc. Asia-Pacific Microw. Conf. pp:1352-1355 (2010).

[WHO 14] http://www.who.int/es/index.html

X

[XIE 10] Z. Xie, G. Liu, S. Wu, Z. Fang, Y. Gan, "Pennes Equation Based Blood Perfusion Model and its Application in Face Recognition," IEEE Int. Conf. Inf. Auto. pp:2443-2446 (2010).

Y

[YAMA 13] T. Yamamoto, K. Sano, K. Koshiji, X. Chen, S. Yang, M. Abe, and A. Fukuda, "Development of electromagnetic phantom at low-frequency band," 35th Ann. Int. Conf. IEEE Eng. Med. Bio. Sci. pp:1887-1890 (2013).

[YANG 07] D. Yang, M.C. Converse, D.M. Mahvi, J.G. Webster, "Expanding the Bioheat Equation to Include Tissue Internal Water Evaporation During Heating," IEEE Trans. Biomed. Eng. 54(8). pp:1382-1388 (2007).

[YOON 12] S. Yoon, S.T. Park, H. Park, H.S. Yoo "Security Analysis of Vulnerable Wi-Fi Direct," 8th Comp. Net. Tech. pp:340-343. (2012).

Z

[ZEEB 10] E. Zeeb, G. Moritz, W. Thronicke, M. Lipprandt, A. Hein, F. Müller, J. Krüger, O. Dohndorf, A. Litvina, C. Fiehe, I. Lück, F. Golatowski, D. Timmermann, "Generic Platform for Advanced E-Health Applications," 12th IEEE Int. Conf. e-Health Net. App. Serv. pp:201-208. (2010).

[ZENG 10] N. Zeng, K-J Qin, J. Li, "Intelligent Transport Management System for Urban Traffic Hubs Based on an Integration of Multiple technologies," IEEE 17th Int. Conf. Ind. Eng. Eng, Manag. pp:1178-1183. (2010).

[ZHAN 12] L.-J. Zhang, B. Zhang; Z.-H. Xue, W.-M. Li; W. Ren, "Analysing Periodic Structures using FDTD Algorithm," Int. Conf. Microw. Mili. Wave Tech. pp:1-4. (2012).

[ZHAO 11] H. Zhao, Z. Shen, "Efficient Modeling of Three-Dimensional Reverberation Chambers Using Hybrid Discrete Singular Convolution-Method of Moments," IEEE Trans. Ant. Prop. 59(8). 2943-2953. (2011).

[ZHOU 09] M. Zhou, Q. Chen, "Estimation of Temperature Distribution in Biological Tissue by Analytic Solutions of Pennes' Equation," 2nd Int. Conf. Biomed. Eng. Inf. pp:1-4 (2009).

Author's merits

Journal Papers

[PAPER A] P. López Iturri, E. Aguirre, L. Azpilicueta, U. Gárate, F. Falcone, “ZigBee Radio Channel Analysis in a Complex Vehicular Environment”, *IEEE Antennas and Propagation Magazine*, Vol. 56, Issue 4, pp:232-245. 2014.

[PAPER B] E. Aguirre, P. López Iturri, L. Azpilicueta, J. Arpón, F. Falcone, "Characterization and Consideration of Topological Impact of Wireless Propagation in a Commercial Aircraft Environment", *IEEE Antennas and Propagation Magazine*, Vol. 55, Issue 6, pp:240-258. 2013.

[PAPER C] E. Aguirre, J. Arpon, L. Azpilicueta, S. De Miguel Bilbao, V. Ramos, and F. J. Falcone, "Evaluation of electromagnetic dosimetry of wireless systems in complex indoor scenarios with human body interaction," *Progress In Electromagnetics Research B*, Vol. 43, 189-209. 2012.

[PAPER D] S. Led, L. Azpilicueta, E. Aguirre, M. Martínez de Espronceda, L. Serrano, F. Falcone, “Analysis and Description of HOLTIN Service Provision for AECG monitoring in Complex Indoor Environments,” *Sensors*, vol. 13, Issue 4, pp. 4947-4960. 2013.

[PAPER E] E. Aguirre, J. Arpón, L. Azpilicueta1, P. López Iturri, S. de Miguel, V. Ramos and F. Falcone, “Estimation of Electromagnetic Dosimetric Values from Non-Ionizing Radiofrequency Fields in an Indoor

Commercial Airplane Environment”, *Electromagnetic Biology and Medicine*, Published online 24 July 2013.

[PAPER F] Erik Aguirre, Peio Lopez Iturri, Leire Azpilicueta, Silvia de Miguel-Bilbao, Victoria Ramos and Francisco Falcone, “Analysis of Estimation of Electromagnetic Dosimetric Values from Non-Ionizing Radiofrequency Fields in Conventional Road Vehicle Environments”,*Electromagnetic Biology and Medicine*, Published online 21 January 2014.

[PAPER G] S. de Miguel-Bilbao, E. Aguirre, P. Lopez Iturri, L. Azpilicueta, J. Roldan, V. Ramos, F. Falcone, "Evaluation of Electromagnetic Interference and Exposure Assessment from s-Health Solutions based on Wi-Fi Devices," *BioMed Research International*.

[PAPER H] A.V. Alejos, F. Falcone, M. Dawood, E. Aguirre, L. Azpilicueta Evaluation of the Brillouin precursor performance for ultra wide band intra-body technologies, *Journal of Electromagnetic Waves and Applications*, Vol. 27, Issue 17, 1, pp 2213-2220. 2013.

[PAPER 9] L. Azpilicueta, P. Lopez Iturri, E. Aguirre, F. Falcone, “Radio Channel Characterization for Bluetooth Communication Systems Onboard Commercial Aircrafts*,” Microwave and Optical Technology Letters*, vol 56, Issue 11, pp:2660-2664. 2014.

Conferences

[Conf 1] E. Aguirre, J. Salaberri, J. Becerra, V. Torres, D. Chávarri, F. Falcone, “Análisis de Detectabilidad de Señales RFID e Implicaciones de Seguridad en entornos Interiores”, in *XXV Simposium Nacional de la Unión Científica Internacional de Radio, URSI 2010*, (Bilbao), 2010.

[Conf 2] J. Arpón, E. Aguirre, L. Azpilicueta, V. Ramos, F. Falcone, “Analysis of Dosimetry Estimation in Large Enclosed Vehicles”, in *IEEE International Symposium on Antennas and Propagation and USNC/URSI National Radio Science Meeting* (Chicago), 2012.

[Conf 3] E. Aguirre, J. Arpón, L. Azpilicueta, V. Ramos, F. Falcone, “Evaluation of Dosimetry of Wireless Systems in Complex Indoor Scenarios with Human Body Interaction”, in *IEEE International Symposium on Antennas and Propagation and USNC/URSI National Radio Science Meeting* (Chicago), 2012.

[Conf 4] J. Arpón, E. Aguirre, L. Azpilicueta, S. de Miguel, V. Ramos, F. Falcone, “Assesment on Electromagnetic Spectrum within Large Enclosed Vehicles”, in *Progress in Electromagnetics Research Symposium, PIERS 2012*, (Moscow), 2012.

[Conf 5] E. Aguirre, J. Arpón, L. Azpilicueta, S. de Miguel, V. Ramos, F. Falcone, “Impact of Realistic Human Body Interaction in Indoor Wireless System Evaluation”, in *Progress in Electromagnetics Research Symposium, PIERS 2012*, (Moscow), 2012.

[Conf 6] J. Arpón, E. Aguirre, L. Azpilicueta, S. de Miguel, V. Ramos, F. Falcone, “Evaluación Dosimétrica en el Entorno Interior de un Avión”, in *XXVII Simposium Nacional de la Unión Científica Internacional de Radio, URSI 2012*, (Elche), 2012.

[Conf 7] E. Aguirre, J. Arpón, L. Azpilicueta, S. de Miguel, V. Ramos, F. Falcone, “Evaluación Dosimétrica de Sistemas Inalámbricos en Entornos Interiores con Interacción del Cuerpo Humano”, in *XXVII Simposium Nacional de la Unión Científica Internacional de Radio, URSI 2012*, (Elche), 2012.

[Conf 8] S. Led, L. Azpilicueta, E. Aguirre, M. M. de Espronceda, L. Serrano, F. Falcone, “Analysis of AECG Monitoring Wireless Channel Performance in Indoor Environments”, in *2013 IEEE International Symposium on Antennas and Propagation and USNC-URSI National Radio Science Meeting*, (Florida), 2013

[Conf 9] A. Vazquez Alejos, F. Falcone Lanas, E. Aguirre Gallego, Muhammad Dawood, “Performance evaluation of medium-matched waveforms and pulse shaping for application in ultrawideband intra-body technologies”, in *2013 IEEE International Symposium on Antennas and Propagation and USNC-URSI National Radio Science Meeting*, (Florida), 2013

[Conf 10] E. Aguirre, L. Azpilicueta, S. de Miguel, V. Ramos, F. Falcone, "Role of Material Changes and Topological Influence in Deterministic Estimation of Dosimetric Values in Complex Indoor Scenarios", in *2013 IEEE International Symposium on Antennas and Propagation and USNC-URSI National Radio Science Meeting*, (Florida), 2013

[Conf 11] S de Miguel-Bilbao, J García, E Aguirre, L Azpilicueta, F Falcone, V Ramos, "Assessment of Statistical Distribution of Exposure to Electromagnetic Fields From Social Alarm Devices," in *13th*

Mediterranean Conference on Medical and Biological Engineering (MEDICON 2013), (Seville), 2013.

[Conf 12] L. Azpilicueta, P. Lopez Iturri, E. Aguirre, U. Garate, F. Falcone, "Análisis del Canal Radioeléctrico en un Entorno Vehicular Complejo", in *XXVIII Simposium Nacional de la Unión Científica Internacional de Radio, URSI,* (Santiago de Compostela), 2013.

[Conf 13] P. López, L. Azpilicueta, E. Aguirre, S. de Miguel Bilbao, V. Ramos, F. Falcone, "Análisis Dosimétrico de las Fugas de Hornos Microondas", in *XXVIII Simposium Nacional de la Unión Científica Internacional de Radio, URSI*, (Santiago de Compostela), 2013.

[Conf 14] E. Aguirre, L. Azpilicueta, P. Lopez Iturri, C. Zubiri, J.J. Astráin, J. Villadangos, F. Falcone, "Caracterización Radioeléctrica de Sistemas Inalámbricos Embarcados en Autobuses Urbanos", in *XXVIII Simposium Nacional de la Unión Científica Internacional de Radio, URSI,* (Santiago de Compostela), 2013.

[Conf 15] E. Aguirre, P. Lopez Iturri, L. Azpilicueta, S. de Miguel-Bilbao, V. Ramos, F. Falcone,"Dosimetric Assessment for Non-Ionizing ISM 2.4 GHz Wireless Systems in a Commercial Passenger Aircraft" in *8th European Conference on Antennas and Propagation EuCAP 2014*, (The Hague), 2014.

[Conf 16] A. Alejos, M. Dawood, F. Falcone, E. Aguirre, “Radio Channel Characterization of Intra-body Propagation Under Frequency Dispersive Perspective”, in *8th European Conference on Antennas and Propagation EuCAP 2014*, (The Hague), 2014.

[Conf 17] P. Lopez-Iturri, E. Aguirre, L. Azpilicueta, J.J. Astrain, J. Villadangos, F. Falcone, "Radio Characterization for ISM 2.4 GHz Wireless Sensor Networks for Judo Applications" in *1st Int. Elec. Conf. on Sens. and App., Sciforum Electronic Conference Series*; 2014.

[Conf 18] L. Azpilicueta, P. López Iturri, E. Aguirre, I. Mateo, J.J. Astráin, J. Villadangos, F. Falcone, "Analysis of Radio Wave Propagation for ISM 2.4GHz Wireless Sensor Networks in Inhomogeneous Vegetation Environments" in *1st Int. Elec. Conf. on Sens. and App., Sciforum Electronic Conference Series*; 2014.

[Conf 19] E. Aguirre, P. Lopez-Iturri, L. Azpilicueta, J.J. Astrain, Jesús Villadangos, F. Falcone, "Analysis of Wireless Sensor Network Topology and Estimation of Optimal Network Deployment by

Deterministic Radio Channel Characterization" in *1st Int. Elec. Conf. on Sens. and App., Sciforum Electronic Conference Series*; 2014.

[Conf 20] A. Vazquez Alejos, M. Dawood, E. Aguirre, F. Falcone Lanas, "Review of Specific Absorption definition considering the evolution of the Brillouin precursors" in *2014 IEEE International Symposium on Antennas and Propagation and USNC-URSI National Radio Science Meeting*, (Memphis), 2014

[Conf 21] A. Leon, L. Azpilicueta, E. Aguirre, P. Lopez-Iturri, F. Falcone, "Topological Dependence in the Performance of Deterministic Wireless Channel Estimation" in *2014 IEEE International Symposium on Antennas and Propagation and USNC-URSI National Radio Science Meeting*, (Memphis), 2014

[Conf 22] E. Aguirre, M. Flores, L. Azpilicueta, P. Lopez Iturri, F. Falcone, V. Ramos, A. Solanas, "Implementing Context Aware Scenarios to Enable Smart Health in Complex Urban Environments", in *2014 IEEE International Symposium on Medical and Measurements and Applications MeMeA*, (Lisbon), 2014.

[Conf 23] E. Salinero, L. Azpilicueta, E. Aguirre, P. Lopez-Iturri, J.J. Astrain, J. Villadangos, F. Falcone, "Channel Characterization in Indoor Wireless Sensor Network Deployment in Commercial Environment" in *2014 IEEE International Symposium on Antennas and Propagation and USNC-URSI National Radio Science Meeting*, (Memphis), 2014

[Conf 24] T. Laborra, L. Azpilicueta, P. Lopez-Iturri, E. Aguirre, F. Falcone, "Estimation of Wireless Coverage in Complex Cave Environments for Speleology Applications" in *2014 IEEE International Symposium on Antennas and Propagation and USNC-URSI National Radio Science Meeting*, (Memphis), 2014.

[Conf 25] P. Lopez-Iturri, E. Aguirre, L. Azpilicueta, S. De Miguel-Bilbao, V. Ramos, F. Falcone, "Assessment of Electromagnetic Dosimetric values from Non-Ionizing Radiofrequency Sources in a Conventional Road Vehicle" in *2014 IEEE International Symposium on Antennas and Propagation and USNC-URSI National Radio Science Meeting*, (Memphis), 2014.

[Conf 26] H. Baghdadi, E. Aguirre, P. Lopez-Iturri, L. Azpilicueta, J.J. Astrain, J. Villadangos, F. Falcone, "Analysis of Radiopropagation of Wireless Transceivers in Surfboards" in *2014 IEEE International Symposium* *on Antennas and Propagation and USNC-URSI National Radio Science Meeting*, (Memphis), 2014.

[Conf 27] H. Baghdadi, E. Aguirre, P. Lopez, L. Azpilicueta, J.J. Astráin, J. Villadangos, F. Falcone, " Caracterización Radioeléctrica en Entorno Acuático para Sistemas Inalámbricos Embebidos en Tablas de Surf" in *XXIX Simposium Nacional de la Unión Científica Internacional de Radio. URSI 2014*, (Valencia), 2014.

[Conf 28] E. Salinero, L. Azpilicueta, P. Lopez, E. Aguirre, Francisco Falcone, "Caracterización del Canal Radioeléctrico en Grandes Superficies Comerciales" in *XXIX Simposium Nacional de la Unión Científica Internacional de Radio. URSI 2014*, (Valencia), 2014.

[Conf 29] T. Laborra, E. Aguirre, P. Lopez, L. Azpilicueta, J.J. Astráin, J. Villadangos, F. Falcone, "Sistema de Comunicación en Tiempo Real Basado en WSN para Aplicaciones Espeleológicas" in *XXIX Simposium Nacional de la Unión Científica Internacional de Radio. URSI 2014*, (Valencia), 2014.

[Conf 30] Erik Aguirre, Peio Lopez-Iturri, Leire Azpilicueta, Francisco Falcone, "Characterization of Wireless Channel Response in In-Vehicle Environments" in *14th Mediterranean Microwave Symposium*, (Marrakech), 2014.

[Conf 31] Peio López-Iturri, Erik Aguirre, Leire Azpilicueta, Carlos Fernández-Valdivielso, Ignacio Matías, Francisco Falcone, "Analysis of Efficient Dense Wireless Sensor Network Deployment in Smart City Environments" in *IEEE Sensors*, (Valencia), 2014.